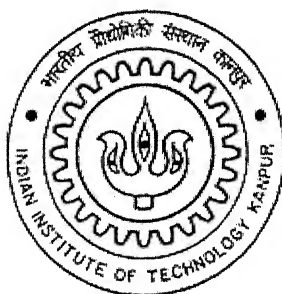


# ULTIMATE LATERAL LOAD CAPACITY AND DISPLACEMENTS AT WORKING LOADS OF UNDER-READED PILE

by  
Vanta Sreedhar

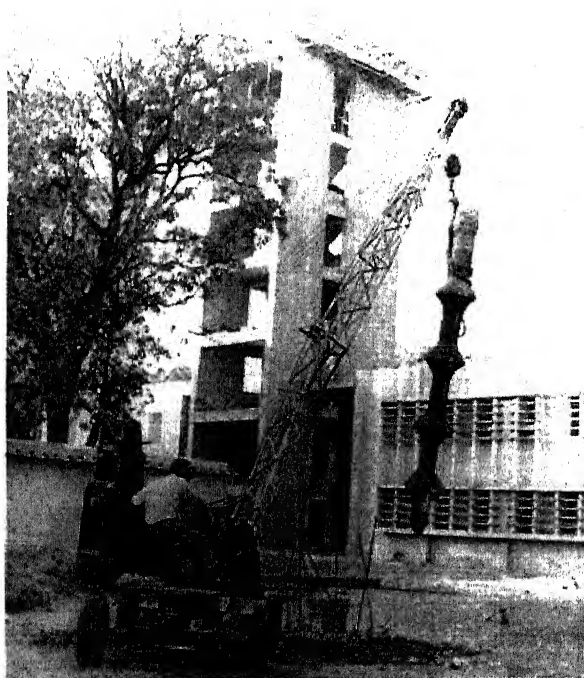


DEPARTMENT OF CIVIL ENGINEERING  
INDIAN INSTITUTE OF TECHNOLOGY KANPUR  
July 2001

# ULTIMATE LATERAL LOAD CAPACITY AND DISPLACEMENTS AT WORKING LOADS OF UNDER-READED PILE

*A Thesis Submitted  
in Partial Fulfillment of the Requirements  
for the Degree of*  
**MASTER OF TECHNOLOGY**

by  
**Vanta Sreedhar**



to the

**DEPARTMENT OF CIVIL ENGINEERING  
INDIAN INSTITUTE OF TECHNOLOGY KANPUR**

July 2001

E-3 OCT 2001/CE

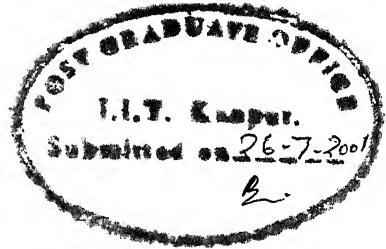
पुस्तकालय केन्द्र पुस्तकालय

भारतीय प्रौद्योगिकी संस्थान कानपुर

अवधि क्र० A.....134987.....



A134987



## CERTIFICATE

Certified that the work contained in this thesis entitled “ *Ultimate Capacity and Displacements at Working Loads of Laterally Loaded Under-reamed Pile*” has been carried out by Sri Vanta.Sreedhar under our supervision and the same has not been submitted elsewhere for a degree.

A handwritten signature in cursive script, likely belonging to V.V.G.S.T. Ramakrishna.

(V.V.G.S.T.Ramakrishna)  
Scientist  
Central Building Research Institute  
Roorkee

A handwritten signature in cursive script, likely belonging to M.R. Madhav.

(M.R.Madhav)  
Professor  
Department of Civil Engineering  
I I T Kanpur



## **Acknowledgement**

I am pleased to acknowledge to, with profound gratitude and indebtedness, Dr.M.R.Madhav, for his valuable, untiring guidance and constant encouragement that enabled me to undertake the studies covered in this thesis.

I owe a great deal of gratitude to Dr.V.V.G.S.T.Ramakrishna and Dr.Chandra Prakash, Scientists, CBRI Roorkee, for their valuable suggestions during this thesis.

And finally, my sincere thanks to all my beloved friends and colleagues who played a pivotal role in my IITK life. Special thanks to Murthy, Raja Sekhar and Dhanunjay.

**Sreedhar.V**

## Abstract

Under-reamed piles originally developed to counteract swelling pressures in expansive soils, are frequently used in alluvial soils in the Gangatic plains to transmit mostly compressive and tensile and occasionally lateral loads. Prediction of ultimate capacity and displacements of under-reamed piles subjected to lateral loads is one of the complex problems for the design of structures subjected to lateral loads, e.g. wind loads, etc. The ultimate lateral resistance and the ground line lateral displacements under working loads of free and fixed head single and double bulb under-reamed piles in different soil conditions, have been investigated by Broms (1964), extended Broms and Winkler subgrade reaction approaches respectively. The effects of size and location of the bulb, length to diameter ratio of the pile and eccentricity of application of load from the ground on ultimate capacity and ground line lateral displacements are quantified. Results are presented by normalising the ultimate lateral load capacity and lateral displacements at ground level of under-reamed piles, with the corresponding values of cylindrical piles. The effects of single and double bulbs have also been quantified.

The results from the proposed design methods have been compared with available test data. Satisfactory agreement has been found between the measured and the calculated ultimate lateral resistances and between calculated and measured deflections at working loads. It is desirable that few more in situ tests be carried out to validate the proposed analyses.

# Contents

<b>1</b>	<b>Introduction</b>	<b>1</b>
<b>2</b>	<b>Literature Review</b>	<b>8</b>
2.1	General . . . . .	8
2.2	Analytical Investigations . . . . .	8
2.3	Experimental Investigations . . . . .	14
2.4	Concluding Remarks . . . . .	15
<b>3</b>	<b>Ultimate Lateral Load Capacity</b>	<b>16</b>
3.1	General . . . . .	16
3.2	Homogeneous Soils . . . . .	18
3.2.1	Rigid Free Head Single Bulb Under-reamed Pile . . . . .	18
3.2.1.1	Statement of the Problem . . . . .	18
3.2.1.2	Analysis Based on Broms's Theory . . . . .	19
3.2.1.3	Analysis Based on Modified Broms's Theory . . . . .	21
3.2.1.4	Results and Discussion . . . . .	22
3.2.2	Rigid Free Head Double Bulb Under-reamed Pile . . . . .	26
3.2.2.1	Analysis Based on Broms's Theory . . . . .	27
3.2.2.2	Results and Discussion . . . . .	29
3.2.3	Rigid Fixed Head Under-reamed Pile . . . . .	34
3.2.3.1	Fixed Head Short Single Bulb Under-reamed Pile . . . . .	34
3.2.3.2	Rigid Fixed Head Intermediate Length Single Bulb Under-reamed Pile . . . . .	38
3.3	Non-homogeneous Soils . . . . .	42
3.3.1	Rigid Free Head Single Bulb Under-reamed Pile . . . . .	42
3.3.1.1	Analysis Based on Broms's Theory . . . . .	42
3.3.1.2	Results and Discussion . . . . .	44
3.3.2	Rigid Free Head Double Bulb Under-reamed Pile . . . . .	50
3.3.2.1	Analysis Based on Broms's Theory . . . . .	50
3.3.2.2	Results and Discussion . . . . .	54

3.3.3	Rigid Fixed Head Short Single Bulb Under-reamed Pile . . . . .	59
3.3.3.1	Analysis Based on Broms's Theory . . . . .	59
3.3.3.2	Results and Discussion . . . . .	60
3.3.4	Rigid Fixed Head Intermediate Length Single Bulb Under-reamed Pile . . . . .	62
3.3.4.1	Analysis Based on Broms's Theory . . . . .	62
3.3.4.2	Results and Discussion . . . . .	63
4	Deformation at Working Loads . . . . .	67
4.1	General . . . . .	67
4.2	Homogeneous Soils . . . . .	70
4.2.1	Rigid Free Head Single Bulb Under-reamed Pile . . . . .	71
4.2.1.1	Analysis . . . . .	71
4.2.1.2	Results and Discussion . . . . .	72
4.2.2	Rigid Free Head Double Bulb Under-reamed Pile . . . . .	74
4.2.2.1	Analysis . . . . .	74
4.2.2.2	Results and Discussion . . . . .	75
4.3	Non-homogeneous Soils . . . . .	77
4.3.1	Rigid Free Head Single Bulb Under-reamed Pile . . . . .	78
4.3.1.1	Analysis . . . . .	78
4.3.1.2	Results and Discussion . . . . .	79
4.3.2	Rigid Free Head Double Bulb Under-reamed Pile . . . . .	81
4.3.2.1	Analysis . . . . .	81
4.3.2.2	Results and Discussion . . . . .	82
4.3.3	Validation . . . . .	85
4.3.4	Verification from the Test Results . . . . .	85
5	Conclusions . . . . .	90
6	References . . . . .	94

# List of Figures

1.1	Structures Subjected to Active Lateral Loads (a) Transmission Line Tower and (b) Overhead Tank. . . . .	1
1.2	Piles Subjected to Passive Lateral Loads (a) Pile Adjacent to Tunnel and (b) an Embankment. . . . .	2
1.3	Failure Modes for Free and Fixed Head Piles. . . . .	3
1.4	Methods of Increasing Lateral Resistance of Piles. . . . .	4
1.5	Under-reamed Piles (a) Single and (b) Double Bulb Under-reams. . . . .	5
1.6	Flow Chart for the Analyses. . . . .	7
2.1	Distribution of Lateral Earth Pressures (a ) Deflections, (b) Probable and (c) Assumed Distribution of Soil Reactions. . . . .	9
2.2	Distribution of Soil Reactions on Horizontal and Vertical Members. . . . .	10
2.3	Pile Subjected to Soil Movement. . . . .	14
3.1	Ultimate Lateral Resistances for Different Slip Field Patterns. . . . .	17
3.2	Undrained Shear Strength in Homogeneous and Non-homogeneous Cohesive Soils. . . . .	18
3.3	Actual and Assumed Shape and Loading of an Under-reamed Pile. . . . .	18
3.4	Distribution of Soil Reaction - Broms's Theory (a ) Kinematics of Under-reamed Pile (Single Bulb), (b) Probable Distribution of Soil Reactions and (c) Simplified Soil Reaction. . . . .	19
3.5	Kinematics of Single Bulb Under-reamed Pile - Point of Rotation Within the Bulb. . . . .	21
3.6	Kinematics of Single Bulb Under-reamed Pile- Modified Broms's Theory. . . . .	22
3.7	Effect of Length of Bulb on Ultimate Capacity for Free Head Single Bulb Under-reamed Pile - Homogeneous Soils. . . . .	23
3.8	Effect of Diameter of Bulb on Ultimate Capacity for Free Head Single Bulb Under-reamed Pile in Homogeneous Soils --Broms's Theory. . . . .	23
3.9	Effect of L/d Ratio on Ultimate Capacity for Free Head Single Bulb Under-reamed Pile in Homogeneous Soils - Broms's Theory. . . . .	24

3.10	Effect of Eccentricity on Ultimate Capacity for Free Head Single Bulb Under-reamed Pile in Homogeneous Soils - Broms's Theory. . . . .	24
3.11	Effect of Length of Bulb on Ultimate Capacity for Free Head Single Bulb Under-reamed Pile in Homogeneous Soils - Modified Broms's Theory. . . . .	25
3.12	Effect of Diameter of Bulb on Ultimate Capacity for Free Head Single Bulb Under-reamed Pile in Homogeneous Soils - Modified Broms's Theory. . . . .	25
3.13	Effect of $D^*$ on Ultimate Capacity for Free Head Single Bulb Under-reamed Pile in Homogeneous Soils - Modified Broms's Theory. . . . .	26
3.14	Distribution of Soil Reaction-Broms's Theory (a) Kinematics of Double Bulb Under-reamed Pile, (b) Probable Distribution of Soil Reactions and (c) Simplified Soil Reaction. . . . .	27
3.15	Definition Sketch-Broms's Theory (a) Kinematics of Double Bulb Under-reamed Pile and (b) Distribution of Forces along the Pile. . . . .	28
3.16	Effect of Length of Bulb on Ultimate Capacity for Free Head Double Bulb Under-reamed Pile in Homogeneous Soils - Broms's Theory. . . . .	30
3.17	Effect of Diameter of Bulb on Ultimate Capacity for Free Head Double Bulb Under-reamed Pile in Homogeneous Soils - Broms's Theory. . . . .	30
3.18	Effect of Spacing on Ultimate Capacity for Free Head Double Bulb Under-reamed Pile in Homogeneous Soils - Broms's Theory. . . . .	31
3.19	Effect of Length of Bulb on Ultimate Capacity for Free Head Double Bulb Under-reamed Pile in Homogeneous Soils - Modified Broms's Theory. . . . .	32
3.20	Effect of Diameter of Bulb on Ultimate Capacity for Free Head Double Bulb Under-reamed Pile in Homogeneous Soils - Modified Broms's Theory. . . . .	32
3.21	Effect of Spacing on Ultimate Capacity for Free Head Double Bulb Under-reamed Pile in Homogeneous Soils - Modified Broms's Theory. . . . .	33
3.22	Effect of $D^*$ on Ultimate Capacity for Free Head Double Bulb Under-reamed Pile in Homogeneous Soils - Modified Broms's Theory. . . . .	34
3.23	Failure Mode of Short Fixed Head Under-reamed Pile: (a) Deflection and (b) Distribution of Forces. . . . .	35
3.24	Ultimate Capacity of Fixed Head Short Cylindrical Pile. . . . .	36
3.25	Effect of Length of the Bulb on Ultimate Capacity for Fixed Head Short Single Bulb Under-reamed Pile in Homogeneous Soils - Broms's Approach. . . . .	36
3.26	Effect of Diameter of the Bulb on Ultimate Capacity for Fixed Head Short Single Bulb Under-reamed Pile in Homogeneous Soils - Broms's Theory. . . . .	37
3.27	Effect of Length of Bulb on Ultimate Capacity for Fixed Head Short Single Bulb Under-reamed Pile in Homogeneous Soils-Modified Broms's Approach. . . . .	37

3.28 Effect of Diameter of Bulb on Ultimate Capacity for Fixed Head Short Single Bulb Under-reamed Pile in Homogeneous Soils-Modified Broms's Approach. . . . .	38
3.29 Failure Mode of Fixed Head Intermediate Length Under-reamed Pile (a) Kinematics and (b) Distribution of Soil Reaction. . . . .	39
3.30 Effect of Length of Bulb on Ultimate Capacity for Fixed Head Intermediate Length Under-reamed Pile in Homogeneous Soils-Broms's Approach. . . . .	40
3.31 Effect of Diameter of Bulb on Ultimate Capacity for Fixed Head Intermediate Length Under-reamed Pile in Homogeneous Soils - Broms's Approach. . . . .	40
3.32 Effect of Length of Bulb on Ultimate Capacity for Fixed Head Intermediate Length Under-reamed Pile in Homogeneous Soils - Modified Broms's Approach. . . . .	41
3.33 Effect of Diameter of Bulb on Ultimate Capacity for Fixed Head Intermediate Length Under-reamed Pile in Homogeneous Soils - Modified Broms's Approach. . . . .	41
3.34 Pile Embedded in a Non-homogeneous Soil Stratum. . . . .	42
3.35 Failure Mode of Free Head Single Bulb Under-reamed Pile in Non-Homogeneous Soils (a) Kinematics and (b) Distribution of Forces along the Length of the Pile. . . . .	43
3.36 Effect of Length of Bulb on Ultimate Capacity for Free Head Single Bulb Under-reamed Pile in Non-homogeneous Soils - Broms's Theory. . . . .	45
3.37 Effect of Diameter of Bulb on Ultimate Capacity for Free Head Single Bulb Under-reamed Pile in Non-homogeneous Soils - Broms's Theory. . . . .	46
3.38 Effect of $L/d$ Ratio on Ultimate Capacity for Free Head Single Bulb Under-reamed Pile in Non-homogeneous Soils - Broms's Theory. . . . .	46
3.39 Effect of $\alpha$ on Ultimate Capacity for Free Head Single Bulb Under-reamed Pile in Non-homogeneous Soils - Broms's Theory. . . . .	47
3.40 Effect of Length of Bulb on Ultimate Capacity for Free Head Single Bulb Under-reamed Pile in Non-homogeneous Soils - Modified Broms's Theory. . . . .	48
3.41 Effect of Diameter of Bulb on Ultimate Capacity for Free Head Single Bulb Under-reamed Pile in Non-homogeneous Soils - Modified Broms's Theory. . . . .	48
3.42 Effect of $D^*$ on Ultimate Capacity for Free Head Single Bulb Under-reamed Pile in Non-homogeneous Soils - Modified Broms's Theory. . . . .	49
3.43 Effect of $\alpha$ on Ultimate Capacity for Free Head Single Bulb Under-reamed Pile in Non-homogeneous Soils - Modified Broms's Theory. . . . .	49
3.44 Distribution of Soil Reaction in Non-homogeneous Soils - Broms's Theory (a) Kinematics, (b) Probable Distribution and (c) Simplified Soil Reaction. . . . .	50

3.45	Failure Mode of Double Bulb Under-reamed Pile in Non-homogeneous Soils (a ) Kinematics and (b) Distribution of Forces along the Pile Length.	52
3.46	Effect of Length of Bulb on Ultimate Capacity for Free Head Double Bulb Under-reamed Pile in Non-homogeneous Soils - Broms's Theory. . . . .	54
3.47	Effect of Diameter of Bulb on Ultimate Capacity for Free Head Double Bulb Under-reamed Pile in Non-homogeneous Soils - Broms's Theory. . .	55
3.48	Effect of L/d Ratio on Ultimate Capacity for Free Head Double Bulb Under-reamed Pile in Non-homogeneous Soils - Broms's Theory. . . . .	55
3.49	Effect of Spacing on Ultimate Capacity for Free Head Double Bulb Under-reamed Pile in Non-homogeneous Soils - Broms's Theory. . . . .	56
3.50	Effect of $\alpha$ on Ultimate Capacity for Free Head Double Bulb Under-reamed Pile in Non-homogeneous Soils - Broms's Theory. . . . .	56
3.51	Effect of Length of Bulb on Ultimate Capacity for Free Head Double Bulb Under-reamed Pile in Non-homogeneous Soils - Modified Broms's Theory.	57
3.52	Effect of Diameter of Bulb on Ultimate Capacity for Free Head Double Bulb Under-reamed Pile in Non-homogeneous Soils - Modified Broms's Theory. . . . .	57
3.53	Effect of Spacing on Ultimate Capacity for Free Head Double Bulb Under-reamed Pile in Non-homogeneous Soils - Modified Broms's Theory. . . . .	58
3.54	Effect of $D^*$ on Ultimate Capacity for Free Head Double Bulb Under-reamed Pile in Non-homogeneous Soils - Modified Broms's Theory. . . . .	58
3.55	Failure Mode of Short Fixed Head Under-reamed Pile in Non-homogeneous Soils (a) Deflection and (b) Forces along the Pile Length. . . . .	59
3.56	Effect of Length of Bulb on Ultimate Capacity for Fixed Head Short Single Bulb Under-reamed Pile in Non-homogeneous Soils-Broms's Approach. .	60
3.57	Effect of Diameter of Bulb on Ultimate Capacity for Fixed Head Short Single Bulb Under-reamed Pile in Non-homogeneous Soils-Broms's Approach. . . . .	61
3.58	Effect of $\alpha$ on Ultimate Capacity for Fixed Head Short Single Bulb Under-reamed Pile in Non-homogeneous Soils - Broms's Approach. . . . .	61
3.59	Failure Mode of Fixed Head Intermediate Length Under-reamed Pile in Non-homogeneous Soils. . . . .	62
3.60	Effect of Length of Bulb on Ultimate Capacity for Fixed Head Intermediate Length Under-reamed Pile in Non-homogeneous Soils - Broms's Approach. . . . .	64
3.61	Effect of Diameter of Bulb on Ultimate Capacity for Fixed Head Intermediate Length Under-reamed Pile in Non-homogeneous Soils - Broms's Approach. . . . .	64



3.62	Effect of $\alpha$ on Ultimate Capacity for Fixed Head Intermediate Length Under-reamed Pile in Non-homogeneous Soils - Broms's Approach. . . . .	65
3.63	Effect of Length of Bulb on Ultimate Capacity for Fixed Head Intermediate Length Under-reamed Pile in Non-homogeneous Soils - Modified Broms's Theory. . . . .	65
3.64	Effect of Diameter of Bulb on Ultimate Capacity for Fixed Head Intermediate Length Under-reamed Pile in Non-homogeneous Soils - Modified Broms's Theory. . . . .	66
3.65	Effect of $\alpha$ on Ultimate Capacity for Fixed Head Intermediate Length Under-reamed Pile in Non-homogeneous Soils - Modified Broms's Theory. . . . .	66
3.66	Normalised Ultimate Lateral Capacity of Cylindrical Pile for Homogeneous Soils-Broms's Theory. . . . .	67
3.67	Normalised Ultimate Lateral Capacity of Cylindrical Pile in Non-homogeneous Soils-Broms's Theory. . . . .	67
4.1	Pile in Winkler Foundation. . . . .	69
4.2	Stress - Displacement Relation . . . . .	71
4.3	Modulus of Subgrade Reaction in Homogeneous and Non-homogeneous Soils. . . . .	71
4.4	Definition Sketch (a) Kinematics of Under-reamed Pile and (b) Distribution of Forces along the Pile. . . . .	72
4.5	Effect of Length of Bulb on Normalised Deformation Coefficient for Rigid Free Head Single Bulb Under-reamed Pile in Homogeneous Soils. . . . .	73
4.6	Effect of Diameter of Bulb on Normalised Deformation Coefficient for Rigid Free Head Single Bulb Under-reamed Pile in Homogeneous Soils. . . . .	74
4.7	Effect of Eccentricity on Normalised Deformation Coefficient for Rigid Free Head Single Bulb Under-reamed Pile in Homogeneous Soils. . . . .	75
4.8	Definition Sketch for Double Bulb Under-reamed Pile in Homogeneous Soils (a) Kinematics and (b) Distribution of Forces. . . . .	75
4.9	Effect of Length of Bulb on Normalised Deformation Coefficient for Rigid Free Head Double Bulb Under-reamed Pile in Homogeneous Soils. . . . .	77
4.10	Effect of Diameter of Bulb on Normalised Deformation Coefficient for Rigid Free Head Double Bulb Under-reamed Pile in Homogeneous Soils. . . . .	78
4.11	Effect of Spacing on Normalised Deformation Coefficient for Rigid Free Head Double Bulb Under-reamed Pile in Homogeneous Soils. . . . .	78
4.12	Variation of Coefficient of Subgrade Reaction in Non-homogeneous Soils. . . . .	79
4.13	Definition Sketch of Rigid Free Head Single Bulb Under-reamed Pile in Non-homogeneous Soil (a) Kinematics and (b) Distribution of Forces. . . . .	80

4.14	Effect of Length of Bulb on Normalised Deformation Coefficient for Rigid Free Head Single Bulb Under-reamed Pile in Non-homogeneous Soils. . .	82
4.15	Effect of Diameter of Bulb on Normalised Deformation Coefficient for Rigid Free Head Single Bulb Under-reamed Pile in Non-homogeneous Soils. . .	82
4.16	Effect of $\alpha$ on Normalised Deformation Coefficient for Rigid Free Head Single Bulb Under-reamed Pile in Non-homogeneous Soils. . . . .	83
4.17	Definition Sketch of Rigid Free Head Double Bulb Under-reamed Pile - Non-homogeneous Soils (a) Kinematics and (b) Distribution of Forces. . .	84
4.18	Effect of Length of Bulb on Normalised Deformation Coefficient for Rigid Free Head Double Bulb Under-reamed Pile in Non-homogeneous Soils. . .	85
4.19	Effect of Diameter of Bulb on Normalised Deformation Coefficient for Rigid Free Head Double Bulb Under-reamed Pile in Non-homogeneous Soils. . . . .	85
4.20	Effect of Spacing on Normalised Deformation Coefficient for Rigid Free Head Double Bulb Under-reamed Pile in Non-homogeneous Soils. . . . .	86
4.21	Effect of $\alpha$ on Normalised Deformation Coefficient for Rigid Free Head Double Bulb Under-reamed Pile in Non-homogeneous Soils. . . . .	87
4.22	Effect of Depth in Straight Shaft Piles Under Lateral Loads. . . . .	88
4.23	Effect of Depth in (a) Single and (b) Double Bulb Under-reamed Pile. . .	88
4.24	Comparison of Test Results for Ultimate Capacity of Single Bulb Under-reamed Pile in Non-homogeneous Soils. . . . .	90
4.25	Comparison of Test Results for Ultimate Capacity of Double Bulb Under-reamed Pile in Non-homogeneous Soils. . . . .	90
4.26	Comparison of Test Results for Deformation of Single Bulb Under-reamed Pile of $L/d=10$ in Non-homogeneous Soils. . . . .	93
4.27	Comparison of Test Results for Deformation of Single Bulb Under-reamed Pile of $L/d=15$ in Non-homogeneous Soils. . . . .	93
4.28	Comparison of Test Results for Deformation of Single Bulb Under-reamed Pile of $L/d=20$ in Non-homogeneous Soils. . . . .	94
4.29	Comparison of Test Results for Deformation of Double Bulb Under-reamed Pile of $L/d=10$ in Non-homogeneous Soils. . . . .	94
4.30	Comparison of Test Results for Deformation of Double Bulb Under-reamed Pile of $L/d=15$ in Non-homogeneous Soils. . . . .	95
4.31	Comparison of Test Results for Deformation of Double Bulb Under-reamed Pile of $L/d=20$ in Non-homogeneous Soils. . . . .	95

# List of Tables

4.1	Variation of Initial Undrained Shear Strength of the Soil for Different L/d Ratios of the Cylindrical Pile. . . . .	86
4.2	Comparison of Test Results for Ultimate Capacity of Single Bulb Under-reamed Pile in Non-homogeneous Soils. . . . .	87
4.3	Comparison of Test Results for Ultimate Capacity of Double Bulb Under-reamed Pile in Non-homogeneous Soils. . . . .	87
4.4	Variation of Initial Subgrade Modulus with Non-homogeneity Factor for Cylindrical Pile of L/d =10. . . . .	87
4.5	Variation of Initial Subgrade Modulus with Non-homogeneity Factor for Cylindrical Pile of L/d=15. . . . .	88
4.6	Variation of Initial Subgrade Modulus with Non-homogeneity Factor for Cylindrical Pile of L/d=20. . . . .	88
4.7	Comparison of Test Results for Deformation of Single Bulb Under-reamed Pile of L/d=10 in Non-homogeneous Soils. . . . .	88
4.8	Comparison of Test Results for Deformation of Single Bulb Under-reamed Pile of L/d=15 in Non-homogeneous Soils. . . . .	88
4.9	Comparison of Test Results for Deformation of Single Bulb Under-reamed Pile of L/d=20 in Non-homogeneous Soils. . . . .	89
4.10	Comparison of Test Results for Deformation of Double Bulb Under-reamed Pile of L/d=10 in Non-homogeneous Soils. . . . .	89
4.11	Comparison of Test Results for Deformation of Double Bulb Under-reamed Pile of L/d=15 in Non-homogeneous Soils. . . . .	89
4.12	Comparison of Test Results for Deformation of Double Bulb Under-reamed Pile of L/d=20 in Non-homogeneous Soils. . . . .	89

# Chapter 1

## Introduction

Single piles and pile groups are frequently subjected to large lateral forces in addition to compressive and tensile forces. These forces may be caused by earthquakes, by wave or wind forces or by lateral earth pressures. Structures subjected to lateral loads can be classified into two types: (1) structures such as bridge abutments, piers, waterfront structures, transmission line towers, overhead water tanks, etc., (Figure. 1.1) are often subjected to lateral forces caused by wind in case of on shore and waves and currents in case of coastal structures

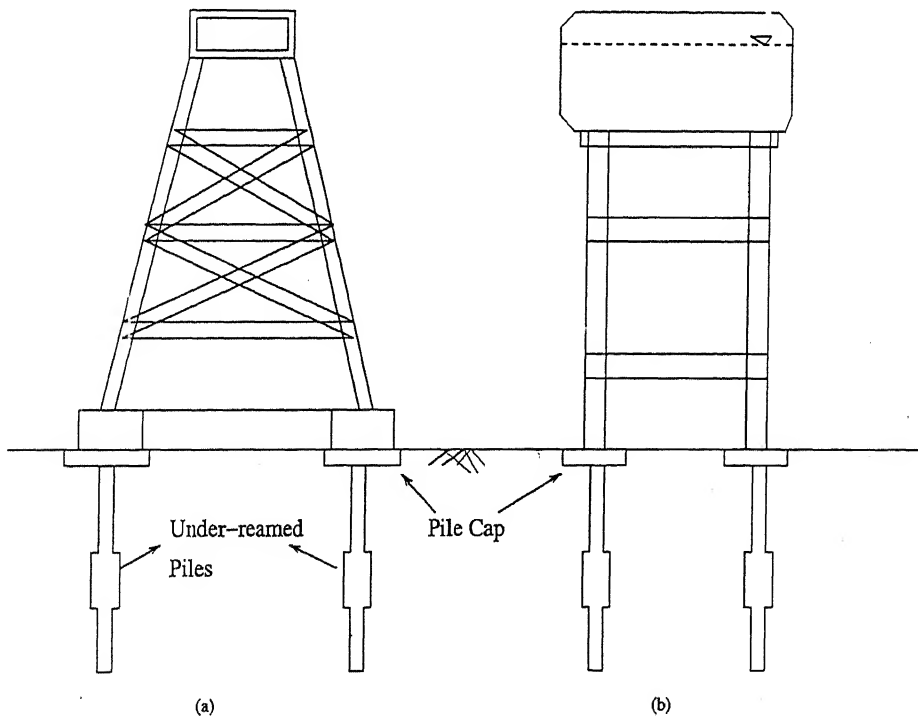


Figure 1.1: Structures Subjected to Active Lateral Loads (a) Transmission Line Tower and (b) Overhead Tank.

and (2) the structures such as piles adjacent to tunnels and piles adjacent to embank-

ments (Figure. 1.2) are subjected to passive lateral forces. The safety of these structures depends on the ability of the supporting piles to resist the resulting lateral forces.

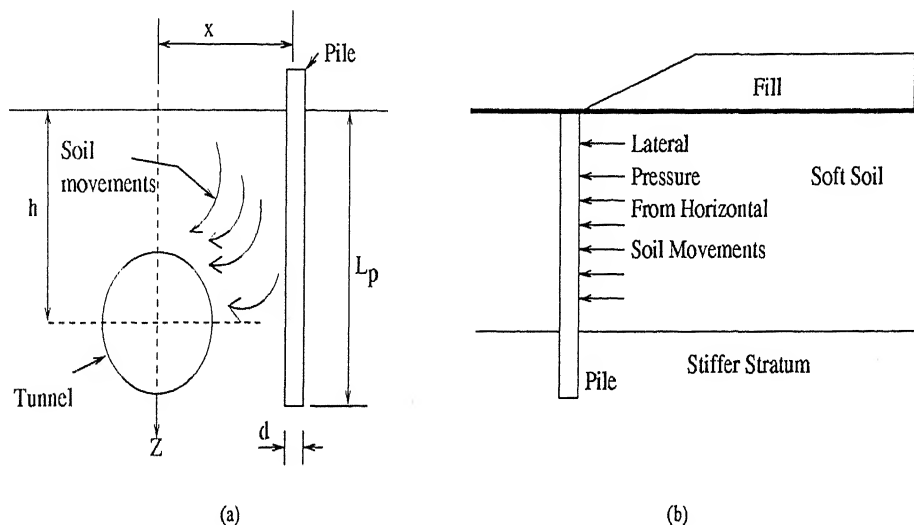


Figure 1.2: Piles Subjected to Passive Lateral Loads (a) Pile Adjacent to Tunnel and (b) an Embankment.

The lateral load capacity of pile foundations is critically important for the design of structures in case of soft alluvial or marine soil deposits characterized by low shear strength and high compressibility. The building codes governing the design of structures in these areas specify frequently that the ability to resist a lateral force should equal to 10% of the applied axial load.

Pile supported retaining walls, abutments or lock structures frequently have to resist high lateral forces. These lateral forces may be caused by lateral earth pressures acting on the retaining walls or rigid frame bridges, by differential fluid pressures acting on lock structures or by horizontal thrust loads acting on abutments of fixed or hinged arch bridges.

The design of piles subjected to lateral loads and moments involves two phases. The first is the estimation of ultimate load carrying capacity and second phase involves the design for working loads of the pile. The criteria adopted in the two cases are respectively: (1) maximum load the pile is subjected to in its life time, is less than the ultimate load carrying capacity of pile, and (2) the deflections of a laterally loaded pile at normal working loads are within specified limits. For the former, a specified soil pressure distribution is assumed to act on the pile and its load carrying capacity estimated while for the later case a simple elastic approach is used.

The allowable lateral load on piles is generally governed by considerations of allowable deflections. However, in cases where deflections may not be critical, the allowable load is often determined by applying an appropriate safety factor to the computed ultimate

lateral load. The ultimate lateral load capacity of piles is usually assessed from the theories of Hansen (1961) or Broms (1964 a).

The load-deflection relationships of laterally loaded piles driven into cohesive soils are similar to the stress-strain relationships as obtained from consolidated-undrained tests (McClelland & Focht 1958). At loads less than one-half to one-third the ultimate lateral resistance of the pile, the deflections increase approximately linearly with the applied load. At higher load levels, the load-deflection relationships become non-linear and the maximum resistance is in general reached when the deflection at the ground surface is approximately equal to 20% of the diameter or the width of the pile.

The ultimate lateral resistance of a pile is governed by either the yield strength of the pile section or by the ultimate lateral resistance of the supporting soil. In the former case it will be assumed that failure takes place through the formation of a plastic hinge. The possible modes of failure of laterally loaded floating piles are illustrated in figure 1.3.

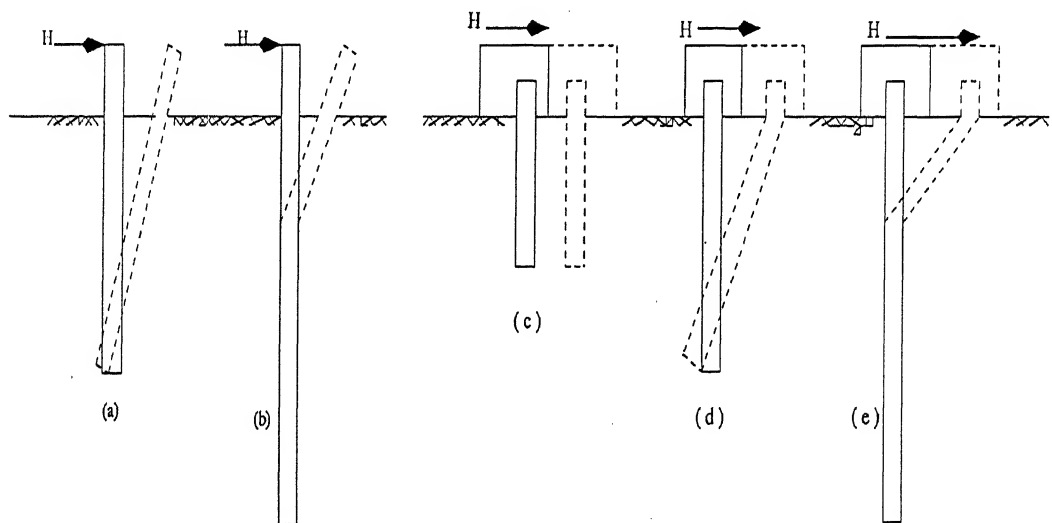


Figure 1.3: Failure Modes for Free and Fixed Head Piles.

An unrestrained pile, which is free to rotate about a certain point at depth, is defined herein as a free-headed pile. Failure of a free-head pile takes place when (a) the maximum bending moment in the pile attains the moment causing yielding or failure of the pile section or (b) the mobilised lateral earth pressures attain the maximum lateral resistance of the supporting soil along the full length of the pile as it rotates as a unit about a point located at some distance below the ground surface. The mode of failure depends on the pile length, the stiffness of the pile section, and on the load-deformation characteristics of the soil. Failure caused by attaining the maximum bearing capacity of the surrounding soil (Figure 1.3 a) takes place when the length of the pile and its penetration depth are small whereas the failure caused by the formation of a plastic hinge at the section

of maximum bending moment (Figure 1.3 b) takes place when the pile penetration is relatively large.

At working loads, lateral deflections and the distributions of bending moments and shear forces are calculated by the theory of subgrade reaction. The deflection of a pile is considered to increase approximately linearly with the applied load. Lateral deformations of the pile is partly caused by the shear deformation of the soil at the time of loading and partly by consolidation and creep subsequent to loading.

The unit soil reaction,  $p$ , acting on a laterally loaded pile increases in proportion to the lateral deflection,  $y$ , expressed by the equation,  $p=ky$ , where the coefficient,  $k$ , defined as the coefficient of subgrade reaction for cohesive soils is approximately proportional to the unconfined compressive strength of the soil. As undrained strengths of normally consolidated clays and silts increase approximately linearly with depth, the coefficient of subgrade reaction also is expected to be in a similar manner. The undrained strength of overconsolidated clays is approximately constant with depth if the overconsolidation of the soil has been caused by glaciation. In such cases, the coefficient of subgrade reaction for overconsolidated clays is considered to be approximately constant with depth.

Broms (1972) has discussed some methods of increasing the lateral resistance of piles as shown in figure 1.4. Most of these methods rely on increasing the dimensions and/or stiffness of the piles near the ground surface. The use of a sand or gravel fill placed around a pile (Figure 1.4 a) is very effective for soft clays when the piles are subjected to cyclic loads.

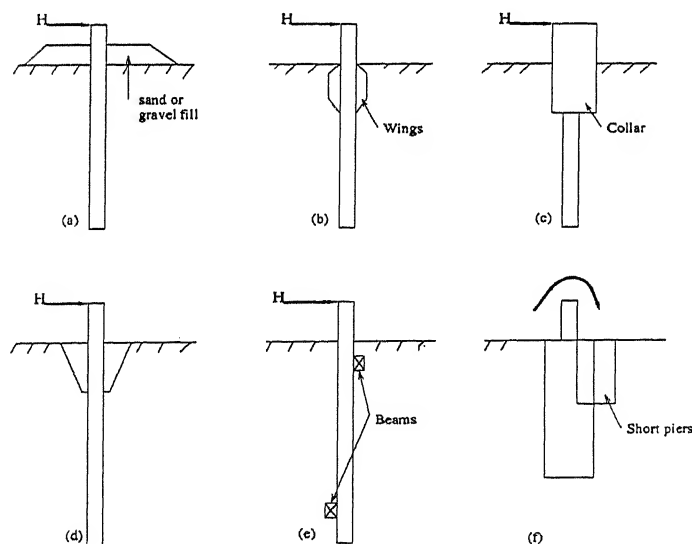


Figure 1.4: Methods of Increasing Lateral Resistance of Piles.

Under-reamed piles were first introduced for expansive soil ( black cotton soils ) areas in mid fifties. But due to their better performance and economy they have found a much wider use in almost all types of soil strata. Under-reamed piles (Figure 1.5) have been

extensively used in India, both as load-bearing and anchor piles in expansive soils. For anchor piles, a single enlarged bulb is often used, while for load-bearing, one or more bulbs may be used. A single bulb under-reamed pile can be treated in a similar manner to a pile with an enlarged base, except that the bulb may be situated above the base of the pile.

In India, large tracts, mainly south of Vindhya range covering almost the entire Deccan plateau, are covered by black cotton soils. These expansive soils are clays with montmorillonite as the predominant clay mineral, exhibiting excessive swelling and shrinkage resulting in high volume changes. The range of liquid limit for these soils is 40 to 100, plasticity index 20 to 60 and shrinkage limit 9 to 14. Volumetric shrinkage is reported to be 40 to 50 percent. During shrinkage there is a formation of hexagonal columnar structure with vertical cracks upto 10 cm wide at ground level and extending upto about 3 m depth. Cracking of buildings, mostly provided with conventional type of strip footings on these expansive soils, has been a common occurrence.

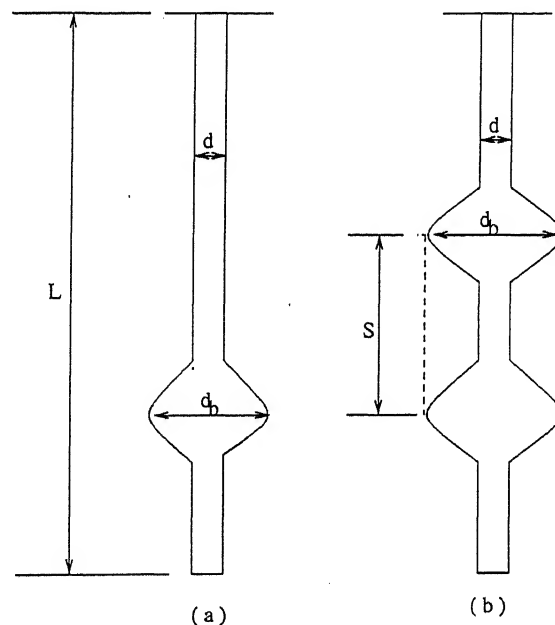


Figure 1.5: Under-reamed Piles (a) Single and (b) Double Bulb Under-reams.

If the footings are anchored down to a depth of inappreciable ground movement near constant water content, the foundation can be expected to remain stable and in turn the superstructure will not be subjected to differential movements and consequent cracking. Under-reamed piles are usually adopted for foundations in expansive soils. This is similar to 'pier and beam' construction which has been extensively used in Texas and several other countries. The provision of the bulbs in an under-reamed pile are useful in two ways; (1) it provides larger bearing area at greater depths which are more firm and stable and (2) it serves as an anchor and keeps the foundation stable in the event of any upward



drag of pile stem. The provision of more than one bulb along the stem further improves the performance of the pile and the latter is then called multi under-reamed pile.

Mohan et al. (1967) suggest that the base and shaft resistances be added to give the ultimate load carrying capacity. From the model tests carried it is confirmed that for double or multiple under-reamed piles with the bulbs suitably placed, the soil between the bulbs tends to act as part of the pile, so that the full resistance of the soil can be developed on the surface of cylinder with a diameter equal to that of the bulbs and height equal to their spacing. The optimum spacing of the bulbs in a multiple under-reamed pile lies between 1.25 and 1.5 times the bulb diameter of the under-reamed pile for maximum efficiency.

Although fairly reliable methods have been developed for predicting the lateral load capacity and displacements for straight-shafted piles, to date, very little information is available to guide engineers in the design of under-reamed piles subjected to lateral loads. Under-reamed piles having one or more bulbs can have considerable uplift resistance and can resist lateral loads more effectively than cylindrical piles. Depending on the magnitude of loads acting on the structure, single or multiple bulbs can be used.

In the analysis developed herein, the following precepts have been assumed; (a) the deflections at working loads of a laterally loaded pile should not be so excessive as to impair the proper function of the member and that (b) its ultimate strength of the pile is sufficiently high as to prevent complete collapse even under the most unfortunate combination of factors. The emphasis has been placed on behavior at working loads and at failure. The behavior at failure has been analysed assuming that the ultimate strength of the pile section or the ultimate strength of the supporting soil has been attained.

The main objectives of the present research are four fold:

- to develop a theoretical procedure for analysing the ultimate lateral capacity and ground line deformation of an under-reamed pile,
- to investigate the effect of the pile geometry, position of the bulbs, fixidity and soil type on both capacity and deformation,
- to generate design charts for assessing the pile response which can be used readily in practice, and
- to validate the applicability of the present methods via the study of published field test data.

Methods of computing the deflections and distributions of soil reactions at working loads and methods for calculation of the ultimate lateral resistance and deformations of free and fixed head under-reamed short rigid piles are presented in succeeding sections as indicated in the flow chart given below (Figure 1.6).

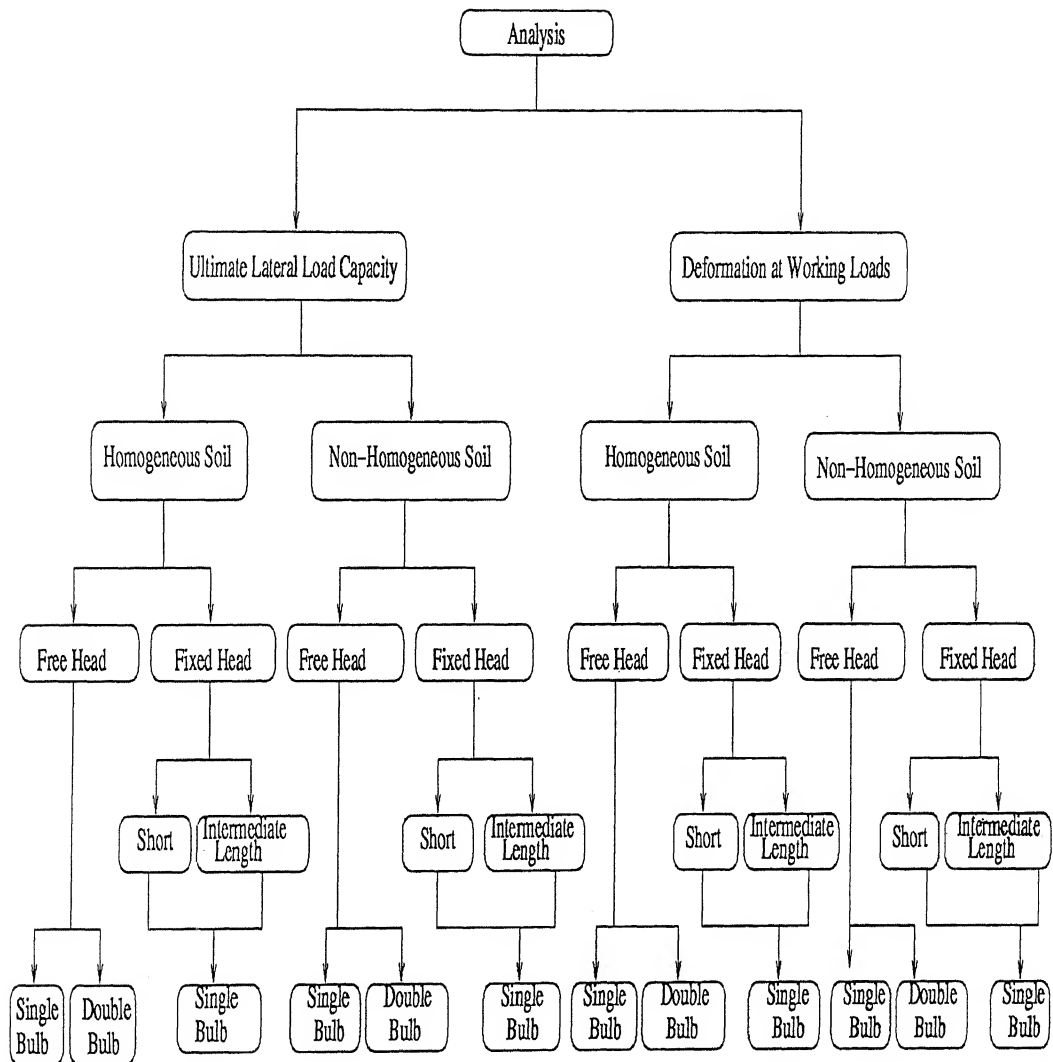


Figure 1.6: Flow Chart for the Analyses.

# Chapter 2

## Literature Review

### 2.1 General

This chapter reviews the analytical investigations on straight shafted piles and experimental studies on behavior of under-reamed piles under the action of lateral loads. In the review of the analytical investigations, attention is focussed mainly to recent studies on cylindrical piles under lateral loads, which have added to the clear understanding of the problem. Experimental investigation on under-reamed piles subjected to lateral loads were mainly carried out CBRI, Roorkee. Generalized conclusions drawn, which form the basis for the assumptions made in the subsequent chapters on the analyses of under-reamed piles are given at the end of the chapter.

### 2.2 Analytical Investigations

A comprehensive review of the analytical studies is presented in this section. Most of the analytical studies reported in the literature treat the problem of flexural behavior of pile as a beam or beam-column on or in elastic foundation.

Barber (1953) presented probably for the first time numerical solutions using the finite-difference approach, for horizontal displacement and rotation of vertical pile subjected to lateral load considering both constant and linearly varying soil moduli with depth.

Broms (1964 a) presented theories for the estimation of ultimate resistances and deflections at working loads of laterally loaded single piles in both cohesive and cohesionless soils. Both free and fixed head piles are considered. It is assumed that the ultimate soil resistance develops all along the length of the pile for rigid pile, whereas for the case of flexible pile, the ultimate load carrying capacity is arrived at from the consideration of

failure of the pile because of the development of a plastic hinge in the pile. Lateral deflections at working loads are evaluated using the concept of subgrade reaction considering the boundary conditions both at the ground surface and at the bottom of each individual pile. The behavior at working loads were analysed by assuming the laterally loaded pile to behave as an elastic member and the supporting soil as a linearly deforming material.

The considered failure mechanism and the resulting distribution of mobilised soil reaction at failure along a laterally loaded free-head cylindrical pile driven into a cohesive soil in the estimation of ultimate lateral capacity of cylindrical pile is shown in figure 2.1. The soil located in front of the loaded pile close to the ground surface heaves upwards in the direction of least resistance, while the soil located at some depth below the ground surface moves laterally. The pile separates from the soil on its rear down to a certain depth below the ground surface.

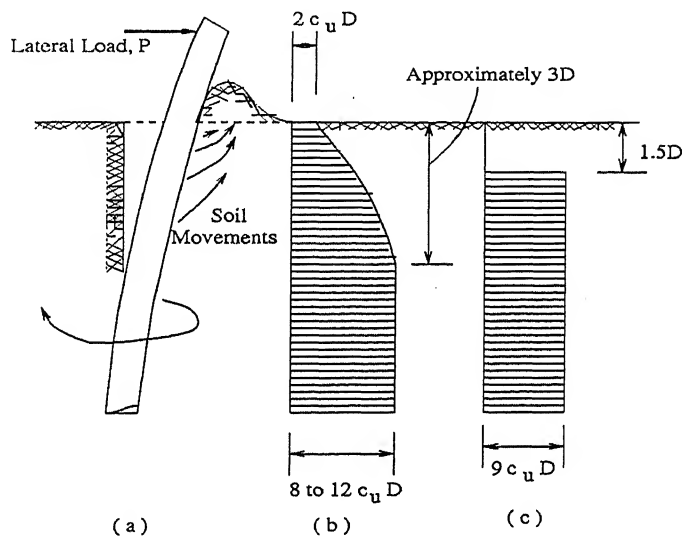


Figure 2.1: Distribution of Lateral Earth Pressures (a ) Deflections, (b) Probable and (c) Assumed Distribution of Soil Reactions.

At working loads, deflections of a single and group of piles are considered to increase approximately linearly with the applied load. Part of lateral deflection is caused by shear deformation of the soil at the time of loading and part by consolidation and creep subsequent to loading. It is assumed that, the unit soil reaction,  $p$ , acting on a laterally loaded pile increases in proportion to the lateral deflection,  $y$ , expressed by the equation,  $p = ky$ , where  $k$  is the coefficient of subgrade reaction. In the estimation of lateral deflections of a pile, coefficient of subgrade reaction computed by assuming that it is equal to that of a strip founded on the surface of a semi-infinite, ideal elastic medium. The distribution of bending moments, shear forces, soil reactions, and deflections are considered to be the same for horizontal and the vertical members as shown in figure 2.2. Increase of deflections of laterally loaded pile caused by consolidation is considered

to be the same as the increase of deflections which take place with time for spread and raft footings founded at or some depth below the ground surface.

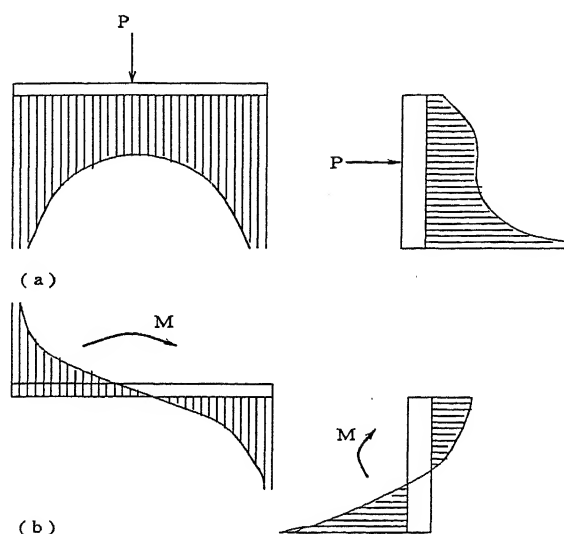


Figure 2.2: Distribution of Soil Reactions on Horizontal and Vertical Members.

Apparent coefficient of subgrade reaction for stiff to very stiff clays which governs the long term lateral deflections and the distributions of lateral earth pressures should be taken as  $(1/2 \text{ to } 1/4)$  the initial coefficient of subgrade reaction, and for the normally consolidated clays, as  $(1/3 \text{ to } 1/6)$  the initial value.

Poulos (1971 a) presented the solution for horizontal displacement and rotation of a vertical pile subjected to lateral load and moment. The soil is idealised as a homogeneous, isotropic and semi-infinite elastic mass and Mindlin's theory is used for calculating displacements. Comparisons between the elastic solutions and the corresponding solutions from Winkler's subgrade modulus approach show that, the latter considerably overestimates the displacements and rotation of the pile, but give a very reasonable estimate of the moments in the pile. Poulos (1971 b) extended the analysis for group of piles.

Madhav et al. (1971) present the results for laterally loaded piles based on elastoplastic Winkler model. The response of a vertical pile to a lateral load is analysed. The two soil parameters, the coefficient of subgrade reaction and the strength or the yield stress of the soil are treated as constants. Effects of the parameters like the stiffness, and the yield stress of the soil, length of the pile, and the depth of the plastic zone, load-deflection relation, deflection at the top of the pile, and the moment along the length of the pile are studied. The non-linear nature of the deflection curve is considered in the analysis.

Basudhar (1971) obtained solutions for the axially and laterally loaded pile problem and presented the results in dimensionless form. The effects of variation of axial force and soil modulus with depth are considered and exhaustive numerical results presented for layered soil, elasto-plastic soil and for a pile driven through a compressible strata.

Banerjee and Davies (1978) present an approximate elastic analysis of single piles embedded in a soil of linearly increasing modulus with depth. The solution for point loads acting at the interface of a two-layer elastic half space had been formulated. Comprehensive plots of the results are presented in non-dimensional form. Analysis predicts higher bending moments due to lateral loads than the predicted values by a homogeneous soil model, for both free and fixed head piles. Results show that the lateral stiffnesses are influenced by the non-homogeneity index with the maximum reduction in the axial stiffness of the pile-soil system to be about 30%.

Randolph (1981) presents an analysis of the behavior of flexible piles under lateral load embedded in elastic soil with stiffness varying linearly with depth. The concept of a characteristic soil stiffness representing the average soil stiffness over the active length of the pile is introduced. The ground level deformations of the pile are calculated from a pair of expressions covering the range of soil conditions from constant soil stiffness to soil stiffness proportional to depth. Charts for deformed shape of the pile, for ground level loading by a lateral force or moment are presented.

Georgiadis and Butterfield (1982) present an analysis of laterally loaded piles in which the pile is treated as an elastic beam supported on non-linear, shear coupled, horizontal springs. The edge forces which act along the pile length are considered and proven to be of significant importance to the pile behavior. The characteristics of the axial springs and the shear coupling are determined from the interpretation of horizontal plate bearing tests. The results obtained from laterally loaded pile tests are compared with the analytically predicted pile behavior.

Krishnan et al. (1983) present the results of systematic parametric investigations of static and dynamic responses of single free-head piles embedded in a soil stratum, the modulus of which increases linearly with depth. Study is conducted by means of finite-element formulation which accounts for three dimensionality of soil deformation. The soil is modeled as a linear hysteretic continuum and the excitation consists of a sinusoidally time-varying horizontal force or moment, applied at the pile head. Comprehensive plots of results are presented in non-dimensional form.

Randolph and Houlsby (1984) present classical plasticity theory to derive exact solutions for the limiting lateral resistance of a circular pile in cohesive soil. Two approaches are used to estimate collapse loads. In the lower bound approach, a stress distribution is assumed which is in equilibrium with the given applied load, and does not contravene the failure criterion. In the second approach, failure mechanism is postulated and the collapse load estimated by equating the rate of dissipation of energy within the deforming soil mass to the work done by the external load. The solutions developed are based on a rigid, perfectly plastic response of the soil, with shear strength independent of the total stress level. The soil deforms at constant volume. The limiting soil pressure of  $10.5c_u$  is suggested for cohesive soil for flow around the pile and  $3c_u$  at the ground surface.

Poulos (1985) presented the expressions for ultimate lateral load capacity of a cylindrical pile in a two-layer cohesive soil profile. Both free and fixed head piles are considered and dimensionless solutions given for failure of the supporting soil or of the pile itself. The analysis is based on statics. Equilibrium relationships of lateral forces and moments are used to derive the ultimate lateral load capacity for short piles. For long piles, the point of maximum moment is determined and equated to the yield moment of the pile.

Verruijt and Kooijman (1989) present a numerical model for a laterally loaded pile in a horizontally layered elastic continuum, which combines advantages of both subgrade reaction and elastic continuum approaches. The model is verified for homogeneous elastic material and a medium having a modulus of elasticity proportional to depth.

Loy et al. (1994) derive a closed form solution for the lateral load capacity of single vertical piles in saturated non-homogeneous cohesive soils whose undrained shear strength increases linearly with depth. Both restrained and unrestrained short and long piles are considered. The principles used for the analysis of a laterally loaded pile are the same as for a statically determinate member. It is assumed that the moment at a plastic hinge remains constant once the hinge forms. The soil reaction is considered to increase linearly with depth as undrained shear strength increases linearly with depth in non-homogeneous cohesive soils.

It is found that the non-homogeneity of cohesive soils has significant effect on the ultimate lateral resistance of short piles for both free and fixed head conditions but little effect for long piles. No additional benefit accrues by increasing the pile length, to increase the lateral resistance for long piles for both free and fixed head conditions because the plastic hinge forms at shallower depth. To increase the lateral resistance of long piles, it is preferable to increase the pile section yield moment.

Stewart et al.(1994) present empirical design charts to estimate maximum pile bending moment and pile head deflection based on the relative soil-pile stiffness and current loading level. The analytical approach is developed on the basis of a simple deformation mechanism which relates the lateral pressure acting on a pile to the approximate relative soil-pile displacement.

Goh et al. (1997) present a simplified numerical procedure based on the finite-element method for analyzing the response of single piles to lateral soil movements caused by the construction of embankments (Figure 1.2 b). The bending of the pile is modeled by beam elements. The complex phenomenon of the soil-pile interaction is modeled by hyperbolic soil springs. Only the immediate short-term response of the pile to the imposed total stress from the embankment load is considered.

Hsiung and Chen (1997) present a simplified method for the analysis and design of long cylindrical piles under lateral load in uniform clays. The method is based on the concept of the coefficient of subgrade reaction with consideration of the soil properties being extended to include elasto-plastic behavior. Maximum deflections and moments under lateral load were evaluated using the finite-element method.

In the calculation, four controlling factors such as coefficient of subgrade reaction, yielding displacement of the soil, diameter of the pile and the elastic modulus of pile stiffness are considered. It has been assumed in the analysis that the coefficient of subgrade reaction increases linearly with depth for normally consolidated clay and stays constant with depth for an overconsolidated clay.

Chen and Poulos (1997) present a theoretical procedure for analyzing the lateral response of vertical piles subjected to lateral soil moments. The lateral pile response is computed via a simplified boundary-element analysis, using a specified free-field soil movement profile.

Chen et al. (1999) present a two-stage approach for analysing the lateral response of piles caused by tunneling (Figure 1.2 a). Free-field soil movements induced by tunneling, i.e., the soil movements without the presence of pile, are estimated based on an analytical method and these soil movements are imposed on the pile in simplified boundary element analysis to compute the pile responses. In the analysis, pile is modeled as a simple elastic beam, and the surrounding soil as an elastic continuum. Through a parametric study, it is investigated that the influence of tunneling on pile response depends on a number of factors, including tunnel geometry, ground loss ratio, soil strength, pile diameter, and ratio of pile length to tunnel cover depth. Simple design charts are presented for



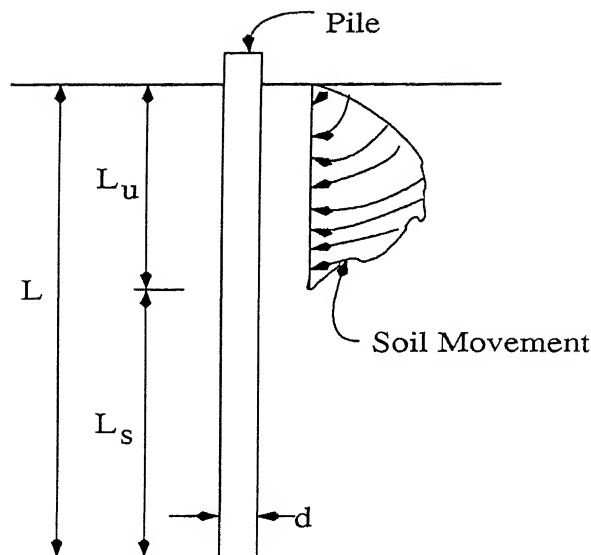


Figure 2.3: Pile Subjected to Soil Movement.

estimating maximum pile responses adjacent to tunneling operations.

## 2.3 Experimental Investigations

In the literature, the experimental studies on under-reamed piles appear to have been conducted only at C.B.R.I. Roorkee.

Meyerhof et al. (1980) investigated the ultimate lateral resistance and the lateral deflection at working loads of rigid vertical walls and piles with free head and embedded in two-layered sand and clay.

Soneja and Garg (1980) conducted field and model tests on under-reamed piles in silty sand. Model tests were conducted on timber piles and the bulb diameter was kept 2.5 times the shaft diameter of the pile. The vertical spacing between the two bulbs was 1.5 times the bulb diameter in case of two bulb under-reamed piles. Effects of various parameters like depth and diameter of pile shaft, number and position of bulbs of an under-reamed pile are presented and concluded that the lateral load capacity of piles increases with increase in depth and shaft diameter of pile. The provision of a bulb increases the lateral load capacity to a great extent.

Prakash and Chandra (1983) present the results of lateral load tests on bored cast-in-situ concrete single under-reamed piles in silty sand deposits.

Briaud et al.(1985) present a method to predict the behavior of piles subjected to

lateral loads on the basis of the results of pressuremeter tests performed in prebored holes. The method is used to predict the pile head response of 17 laterally loaded piles including driven and bored piles ranging from 0.32 m to 1.37 m in diameter and from 3 m to 21 m in length. The predictions are compared with the load test results.

Meyerhof et al. (1988) evaluate the ultimate lateral resistance and ground line lateral deflections of flexible cylindrical piles under working loads of free standing single model piles and small pile groups, of various materials and different embedded lengths, subjected to horizontal load. An extensive series of lateral load tests were conducted on model piles in loose and soft clay. The test results of piles of various stiffnesses in sand and clay were compared with theoretical analyses based on the concept of an effective embedded depth in terms of the behavior of equivalent rigid piles. It was found that in the absence of structural pile failure the ultimate lateral load capacity of flexible piles can be expressed in terms of an equivalent rigid pile by using effective embedded depth which depends on the relative pile stiffness.

Dongqing et al.(1998) present the results of series of tests on laterally loaded single piles in medium stiff clay. The piles (0.09 m to 0.6 m diameter) were instrumented with strain gauges to determine the moment distribution along the piles and lateral deflections. Test results from static load tests have been analysed assuming that the load-displacement relationship of the soil is hyperbolic.

## 2.4 Concluding Remarks

Based on the review of experimental and analytical investigations, certain generalised conclusions are drawn:

- Coefficient of subgrade reaction and plastic resistance are considerably influenced by different factors, viz: stiffness of the soil, remolding, repetition of lateral load, vibrations during driving and size of loaded area.
- Broms's approach can be used for estimating the ultimate capacity and the Winkler's subgrade reaction approach for determining deflection and slope of cylindrical piles at working loads;
- Non-homogeneity of cohesive soils has significant effect on the ultimate lateral resistance of short vertical cylindrical piles for both free and fixed head conditions but little effect on long piles; and
- Fixed head condition provides higher lateral resistance than free head condition for both short and long cylindrical piles.

# Chapter 3

## Ultimate Lateral Load Capacity

### 3.1 General

The necessity of analysis of laterally loaded piles arises from the use of piles as foundations for retaining walls, bridge abutments, piers, fenders, dolphins, anchors for bulkheads, waterfront structures, and unbalanced machines subjected to lateral loads. There are two approaches in calculation of the ultimate load capacity of piles: (1) the "static" approach, which uses the normal soil-mechanics method to calculate the load capacity from measured soil parameters; and (2) the "dynamic" approach, which estimates the load capacity of driven piles from analysis of pile-driving data. Presently, former approach is adopted in estimating the ultimate lateral load capacity of under-reamed piles in cohesive soils.

Several theoretical methods have been published which predict the behavior of short rigid cylindrical piles under lateral loads (Hansen, 1961; Broms, 1964; Meyerhof et al., 1981). These methods assume some form of lateral soil pressure distribution along the length of the pile, which is considered to be uniform along the width of the pile. Hansen (1948) has shown that the ultimate soil reaction against a laterally loaded pile driven into a cohesive soil varies between  $8.3c_u$  and  $11.4c_u$ , where cohesive strength,  $c_u$ , is equal to half the unconfined compressive strength of the soil. McKenzie (1955) has found from experiments that the maximum lateral resistance is equal to approximately  $8c_u$ , while Dastidar (1956) used a value of  $8.5c_u$  for calculating the restraining effects of piles driven into cohesive soil. On the other hand, Reese (1958) has indicated that the ultimate soil reaction at failure increases from approximately  $2c_u$  at the ground surface to  $12c_u$  at a depth of approximately three pile diameters below the ground surface. The ultimate lateral resistance is a function of the shape at the cross-sectional area and the roughness of the pile surface. The ultimate lateral resistance calculated by Broms (1964 a) varied between  $8.28c_u$  and  $12.56c_u$  as shown in figure 3.1. The calculated ultimate lateral resistance does not vary significantly and is not affected appreciably by the roughness

appreciably by the roughness or by the shape at the pile section. A value of  $9c_u$  has been used in the calculations of the ultimate lateral resistance of piles in cohesive soil.

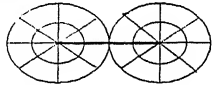
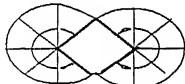
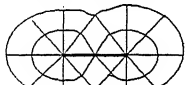
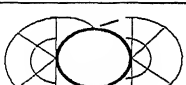

Slip Field Pattern	Surface	Ultimate Lateral Resistance $q_{ult}/c_u$
	Rough	12.56
	Rough	11.42
	Smooth	11.42
	Smooth	9.14
	Smooth	8.28

Figure 3.1: Ultimate Lateral Resistances for Different Slip Field Patterns.

Even though there are well established elasto-plastic solutions available at present for the analysis of laterally loaded cylindrical piles, many engineers still use the simple rigid pile theories. From soil-pile interaction point of view, the bottom portion of the pile buried in the soil behaves like a short rigid pile. Therefore there is a necessity to derive simple methods which give very quick and accurate estimates of rigid pile capacities. In the present research, for the analysis and computation of the ultimate lateral capacity of rigid under-reamed piles, a comprehensive method which is an extension of Broms's approach for cylindrical piles based on a simplified soil pressure distribution along the pile length is adopted. The lateral soil reaction is neglected upto a depth of  $1\frac{1}{2}$  pile diameters and is equated to  $9.0c_u$  below this depth.

In the analysis of laterally loaded piles, evaluation of the average undrained shear strengths of medium to stiff clays is difficult since it is affected by cracks and fissures in the clay. Penetration and pressuremeter tests should preferably be used to evaluate the shear strength and the deformation properties of both cohesive and cohesionless soils. The disturbance caused by the drilling of the boreholes for the pressuremeter tests can be reduced by using self boring pressuremeter.

Analysis of an under-reamed pile for both ultimate capacity and deformation, is carried out based on simple statics (equilibrium of lateral forces and moments).

## 3.2 Homogeneous Soils

In homogeneous soils, undrained shear strength,  $c_u$ , of the soil is considered to be constant with depth.

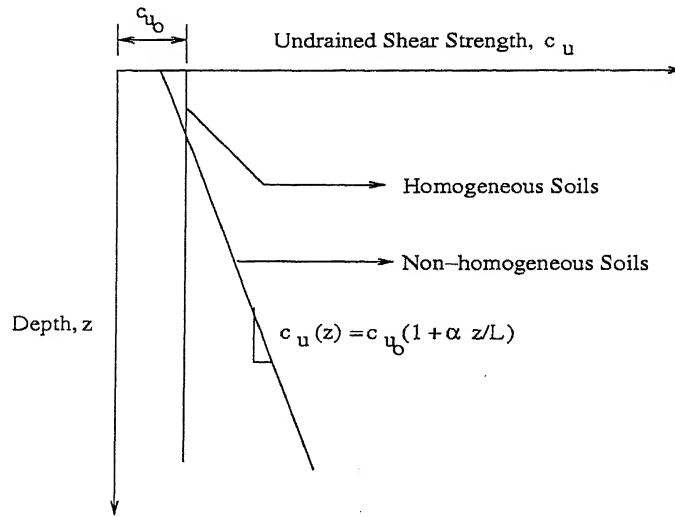


Figure 3.2: Undrained Shear Strength in Homogeneous and Non-homogeneous Cohesive Soils.

### 3.2.1 Rigid Free Head Single Bulb Under-reamed Pile

#### 3.2.1.1 Statement of the Problem

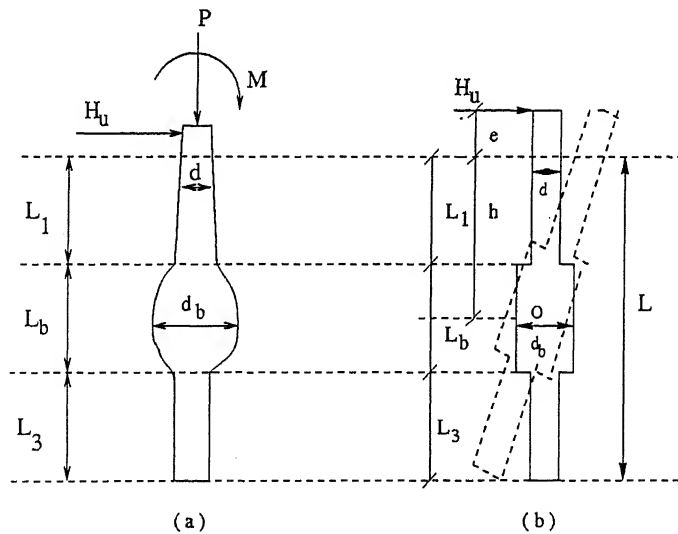


Figure 3.3: Actual and Assumed Shape and Loading of an Under-reamed Pile.

In the actual field, pile is subjected to a combination of axial and lateral loads and moments (Figure 3.3). In the present research, pile subjected to lateral load alone is

considered. In the analysis of an under-reamed pile, the actual shape of the bulb is replaced by an equivalent cylinder having identical projected surface and plan areas. The actual shape of bulb in the field is as shown in figure 3.3a. To simplify the analysis the shape of the bulb is assumed to be cylindrical as shown in figure 3.3b for both ultimate capacity and deformation of an under-reamed pile.

The diameter and length of the pile are  $d$  and  $L$  respectively. The bulb diameter is  $d_b$ . Depth of the top of bulb from the ground surface, length of the bulb and length of pile from the bottom of bulb to tip of the pile are  $L_1$ ,  $L_b$  and  $L_3$  respectively. The pile rotates as a rigid body about a point,  $O$ , at a depth,  $h$ , from the ground surface due to a load,  $H_u$ , applied with an eccentricity,  $e$ , above the ground surface.

### 3.2.1.2 Analysis Based on Broms's Theory

The failure mechanism and the resulting distribution of mobilized soil reaction at failure along a laterally loaded free-head under-reamed pile driven into a homogeneous cohesive soil is shown in figure 3.4. The ultimate lateral resistances for different shapes and roughnesses of the pile section vary between  $8.28c_u$  and  $12.58c_u$  (Figure 3.1). A value of  $9c_u$  is adopted from a depth of  $1\frac{1}{2}$  pile diameters (Figure 3.4 c) in the calculations of the ultimate lateral resistance of the under-reamed piles in homogeneous cohesive soils.

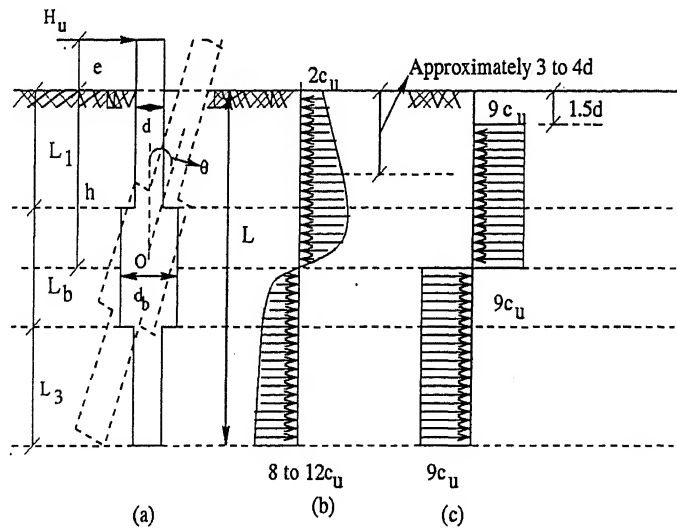


Figure 3.4: Distribution of Soil Reaction - Broms's Theory (a ) Kinematics of Under-reamed Pile (Single Bulb), (b) Probable Distribution of Soil Reactions and (c) Simplified Soil Reaction.

When the pile is subjected to lateral load at its tip, failure takes place when the soil attains its maximum resistance along the total length of the pile and the pile rotates as a rigid body about a point,  $O$ , located at depth,  $h$ , below the ground surface. Three different possible locations of the point of rotation along the length of the pile, (1) above,

(2) within and (3) below the bulb are considered. The maximum bending moment occurs at the level where the total shear force in the pile section is equal to zero. The kinematics and forces along the length of the pile for the depth of point of rotation located within the bulb of an under-reamed pile are shown in figure 3.5.

*a. Point of Rotation Above the Bulb:*

For equilibrium, the sum of the horizontal forces is equal to zero, that is

$$H_u + 9c_u d(L_1 - h) + 9c_u d_b L_b + 9c_u d L_3 - 9c_u d(h - 1.5d) = 0 \quad (3.1)$$

or in a normalized form:

$$H_u^* = \frac{H_u}{c_u d L} = 9(2h^* - D^* - d_r L_b^* - L_1^* - L_3^*) \quad (3.2)$$

where  $h^* = \frac{h}{L}$ ,  $L_1^* = \frac{L_1}{L}$ ,  $L_b^* = \frac{L_b}{L}$ ,  $L_3^* = \frac{L_3}{L}$ ,  $e^* = \frac{e}{L}$ ,  $d_r = \frac{d_b}{d}$ , and  $D^* = \frac{1.5}{(L/d)}$ .

Taking moments of all the forces about the point of application of the load, for equilibrium,

$$\begin{aligned} 9c_u d(h - 1.5d) \left[ \frac{h - 1.5d}{2} + 1.5d + e \right] - 9c_u d(L_1 - h) \left[ \frac{L_1 - h}{2} + h + e \right] - \\ 9c_u d_b L_b \left[ \frac{L_b}{2} + L_1 + e \right] - 9c_u d L_3 \left[ \frac{L_3}{2} + L_1 + L_b + e \right] = 0 \end{aligned} \quad (3.3)$$

or in a normalised form:

$$\begin{aligned} h^{*2} + 2e^* h^* - [d_r \{ \frac{1}{2} L_b^{*2} + L_1^* L_b^* + e^* L_b^* \} + \frac{1}{2} D^{*2} + e^* D^* + \\ \frac{1}{2} (L_1^{*2} + L_3^{*2}) + e^* L_1^* + L_1^* L_3^* + L_b^* L_3^* + e^* L_3^*] = 0 \end{aligned} \quad (3.4)$$

Equation 3.4 is solved for  $h^*$  for known values of  $L_1^*$ ,  $L_b^*$ ,  $L_3^*$ ,  $d_r$  and  $e^*$ .

The dimensionless ultimate lateral resistance,  $H_u^* = \frac{H_u}{c_u d L}$  is then calculated from equation 3.2.

Equations 3.2 and 3.4 for other two cases are obtained as

*b. Point of Rotation Within the Bulb:*

$$H_u^* = \frac{H_u}{c_u d L} = 9[L_1^* - L_3^* - D^* + d_r(2h^* - 2L_1^* - L_b^*)] \quad (3.5)$$

and

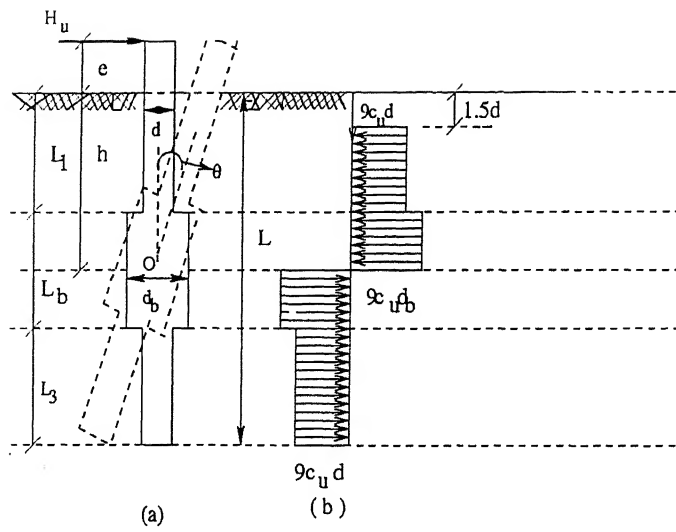


Figure 3.5: Kinematics of Single Bulb Under-reamed Pile - Point of Rotation Within the Bulb.

$$2d_r h^{*2} + 4e^* d_r h^* - d_r [2L_1^* (L_1^* + L_b^*) + L_b^{*2} + 2e^* (2L_1^* + L_b^*)] + L_1^{*2} + D^{*2} + 2e^* (L_1^* - D^*) - L_3^{*2} - 2L_3^* (1 - L_3^*) = 0 \quad (3.6)$$

c. *Point of Rotation Below the Bulb:*

$$H_u^* = \frac{H_u}{c_u d L} = 9[2h^* + d_r L_b^* - D^* - L_b^* - 1] \quad (3.7)$$

and

$$h^{*2} + 2e^* h^* + d_r \left[ \frac{1}{2} L_b^{*2} + L_1^* L_b^* + e^* L_b^* \right] - L_1^* L_b^* - \frac{1}{2} D^{*2} - e^* D^* - \frac{1}{2} L_b^{*2} - e^* L_b^* - e^* - \frac{1}{2} = 0 \quad (3.8)$$

### 3.2.1.3 Analysis Based on Modified Broms's Theory

In Broms's method, the lateral soil reaction is assumed to be zero upto a depth of  $1\frac{1}{2}$  pile diameters and  $9c_u$  below this depth. The soil resistance upto a depth of 1.5 times the diameter of the pile is ignored to allow for disturbance and softening of soft marine clays. For alluvial soil, the soil resistance ignored in Broms's analysis, is taken into account in estimating the lateral capacity of under-reamed pile (modified Broms's theory) (Figure 3.6).

Expressions for the evaluation of both the depth of point of rotation and the nor-



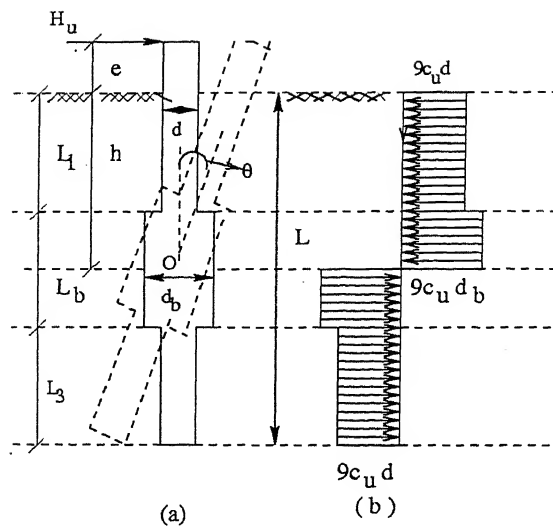


Figure 3.6: Kinematics of Single Bulb Under-reamed Pile- Modified Broms's Theory.

malised ultimate lateral load capacity of single bulb under-reamed pile according to modified Broms approach for the three possible cases of point of rotation are the same as the expressions evaluated based on Broms's theory but by neglecting the term  $D^*$ .

### 3.2.1.4 Results and Discussion

Ultimate lateral resistances of rigid free head single bulb under-reamed pile in homogeneous soil are quantified using both Broms's and modified Broms's approaches. If the diameter ratio,  $d_r$ , equals 1, the ultimate lateral resistance of the under-reamed pile estimated by the present method become identical to the values predicted by Broms for cylindrical piles. The ultimate capacity of under-reamed pile,  $H_{ur}^*$ , is normalised with respect to that of straight shafted pile,  $H_{st}^*$ . The normalised ultimate lateral resistance,  $H_u^* = H_{ur}^*/H_{st}^*$ , varies with depth of the bulb,  $L_1^* = L_1/L$ , from the ground surface. As the depth of the bulb from the ground surface increases, the normalised ultimate lateral resistance decreases upto a depth of 0.5 to 0.7 times the length of the pile and increases slightly for  $L_1^* > 0.7$ . No significant increase in the ultimate lateral resistance of under-reamed pile is discerned by providing the bulb in the region of 0.5 to 0.7 times the length of pile.

For diameter ratio,  $d_r = 2.5$ ,  $L/d = 10$ ,  $L_b^* = 0.2$  and eccentricity,  $e^* = 0.02$ , the ultimate lateral resistance of under-reamed pile is 1.92 times that of straight shafted pile for the bulb at ground surface (Figure 3.7). For the length of the bulb,  $L_b^*$ , increasing from 0.1 to 0.3, the normalised ultimate lateral resistance,  $H_{ur}^*/H_{st}^*$ , increases from 1.5 to 2.23, a 49% increase, for  $d_r = 2.5$ ,  $L/d = 10$  and  $e^* = 0.02$  (Figure 3.7). The percentage increase in the ultimate lateral resistance decreases with increase in length of the bulb. The rate of change of normalised ultimate lateral resistance with respect to depth of the

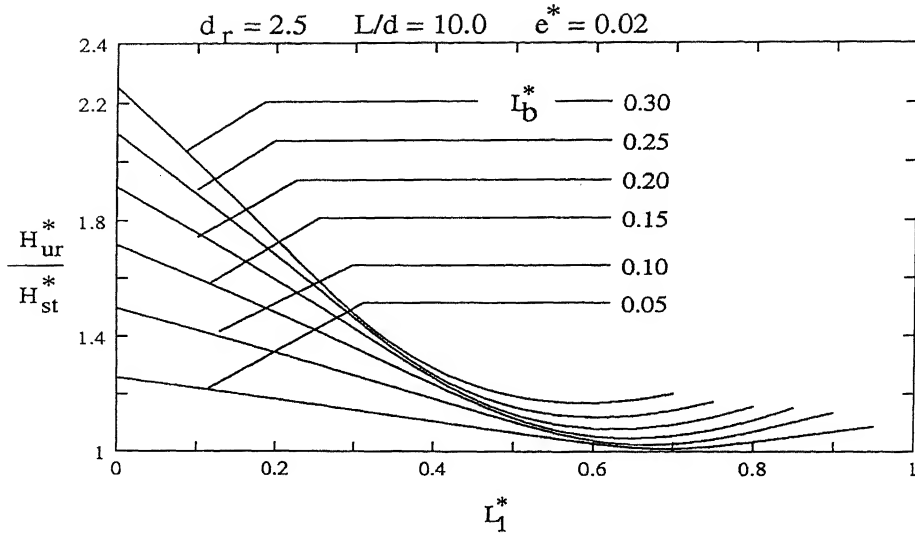


Figure 3.7: Effect of Length of Bulb on Ultimate Capacity for Free Head Single Bulb Under-reamed Pile - Homogeneous Soils.

bulb increases with increase in length of the bulb (Figure 3.7).

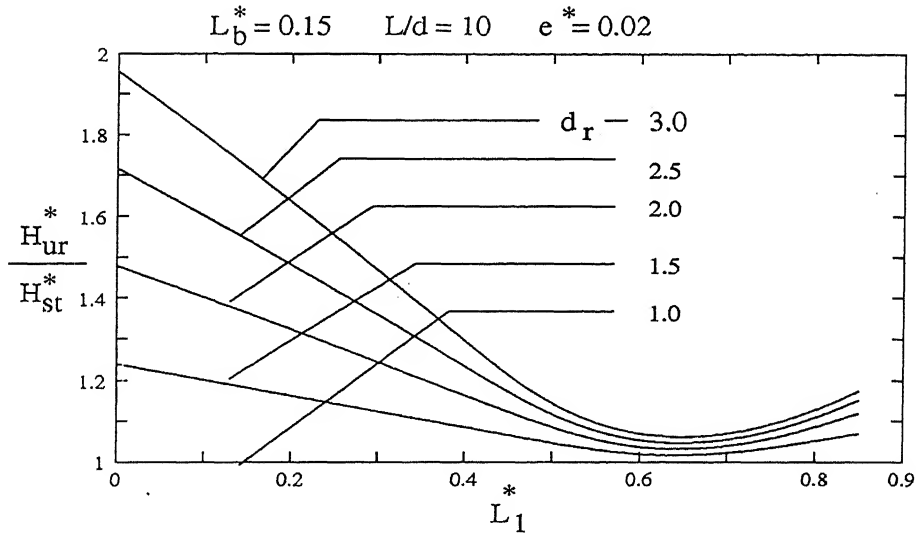


Figure 3.8: Effect of Diameter of Bulb on Ultimate Capacity for Free Head Single Bulb Under-reamed Pile in Homogeneous Soils - Broms's Theory.

The normalised ultimate lateral resistance increases from 1.24 to 1.96 for the diameter ratio,  $d_r$ , increasing from 1.5 to 3.0 for  $L_b^* = 0.15$ ,  $L/d=10$  and  $e^* = 0.02$ , a 58% increase (Figure. 3.8). Percentage increase in the ratio,  $H_{ur}^*/H_{st}^*$ , is almost constant with increase in the diameter ratio (Figure 3.8). The rate of change of the ratio,  $H_{ur}^*/H_{st}^*$ , with respect to the depth of the bulb increases with increase in diameter ratio of the single bulb under-reamed pile (Figure 3.8). No significant increase in the ultimate lateral resistance with increase in the diameter ratio for the bulb at or below the mid length of the pile.

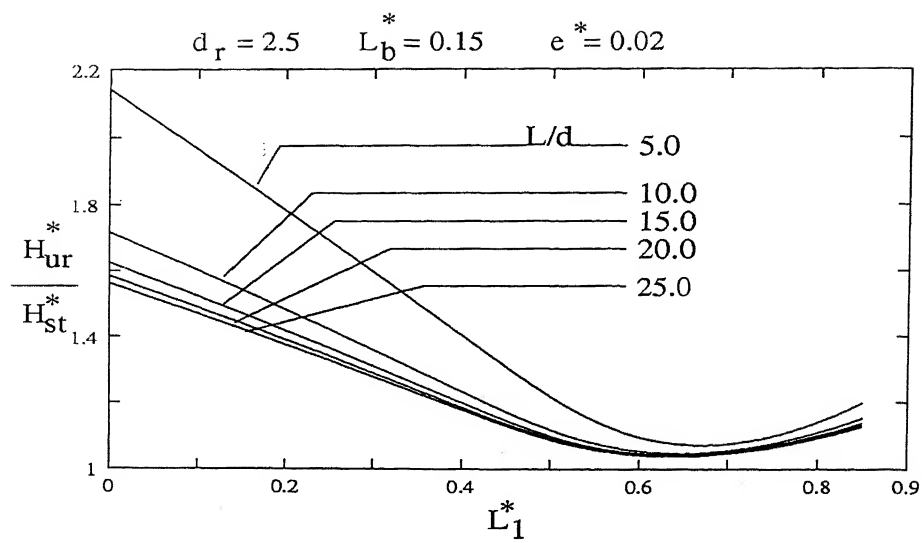


Figure 3.9: Effect of  $L/d$  Ratio on Ultimate Capacity for Free Head Single Bulb Under-reamed Pile in Homogeneous Soils - Broms's Theory.

The ultimate lateral resistance of under-reamed pile for  $d_r=2.5$ ,  $L_b^* = 0.15$  and  $e^* = 0.02$  is 2.15 and 1.72 times that of the cylindrical pile for  $L/d$  is 5.0 and 10.0 respectively (Figure 3.9). The ratio,  $H_{ur}^*/H_{st}^*$ , decreases with  $L/d$  ratio, since both the independent values of under-reamed and cylindrical pile capacities increase simultaneously with  $L/d$  ratio. The percentage decrease in the normalised ultimate lateral resistance is significant for increase in the  $L/d$  ratio from 5.0 to 10.0. No significant decrease in the ratio,  $H_{ur}^*/H_{st}^*$ , for greater values of  $L/d$  ( $L/d > 10.0$ ) (Figure 3.9).

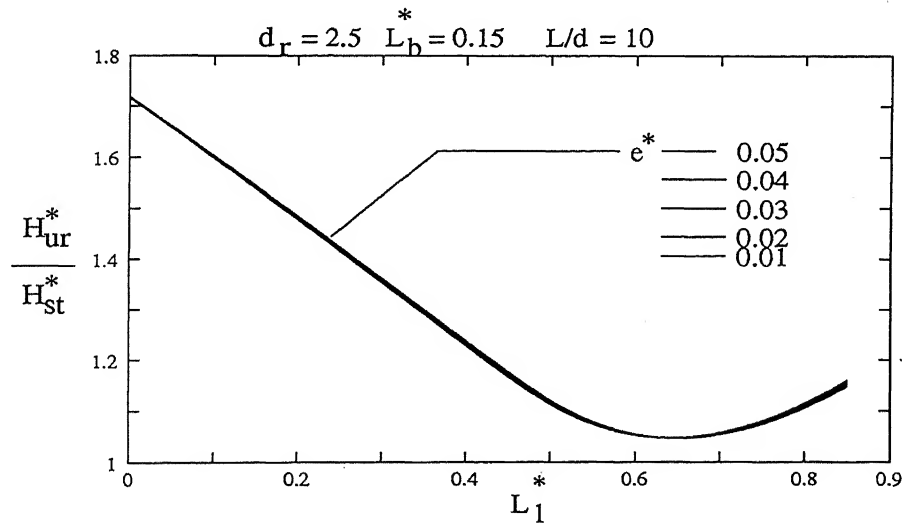


Figure 3.10: Effect of Eccentricity on Ultimate Capacity for Free Head Single Bulb Under-reamed Pile in Homogeneous Soils - Broms's Theory.

The normalised ultimate lateral resistance appears to be independent of eccentricity,

$e^*$ , (Figure 3.10).

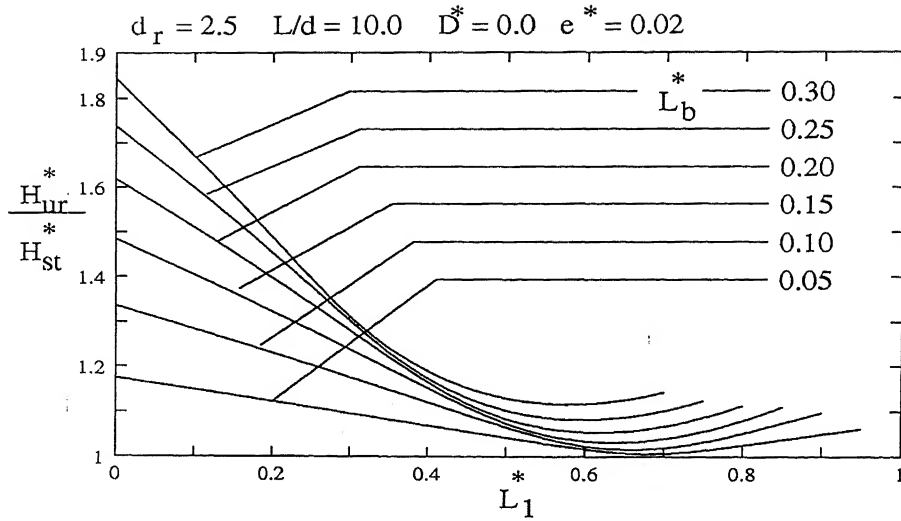


Figure 3.11: Effect of Length of Bulb on Ultimate Capacity for Free Head Single Bulb Under-reamed Pile in Homogeneous Soils - Modified Broms's Theory.

Figures 3.11 through 3.13 depict the effects of length and diameter of the bulb and  $D^*$  on the ultimate lateral resistance of single bulb under-reamed pile based on modified Broms's approach. The normalised ultimate lateral resistance increases with increase in length of the bulb (Figure 3.11). The normalised ultimate lateral resistance increases from 1.34 to 1.85 (Figure 3.11) for the length of the bulb,  $L_b^*$ , increasing from 0.1 to 0.3, a 38% increase, against 1.5 to 2.23 (Figure 3.7) based on Broms's theory.

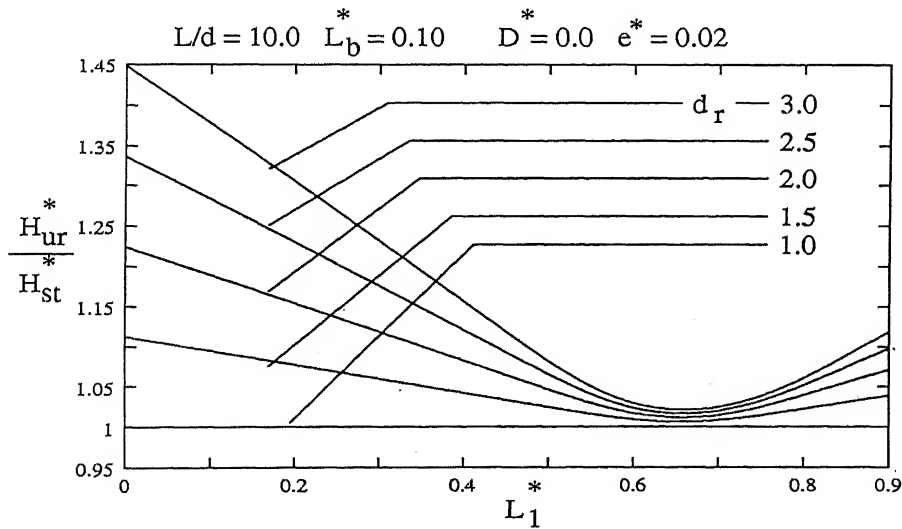


Figure 3.12: Effect of Diameter of Bulb on Ultimate Capacity for Free Head Single Bulb Under-reamed Pile in Homogeneous Soils - Modified Broms's Theory.

For the diameter ratio,  $d_r$ , increasing from 1.5 to 3.0 for  $L_b^* = 0.10$ ,  $L/d=10$  and

$e^* = 0.02$ , the normalised ultimate lateral resistance increases from 1.11 to 1.45, a 31% increase with 100% increase in the diameter ratio (Figure 3.12). The rate of change of the ratio,  $H_{ur}^*/H_{st}^*$ , with respect to the bulb increases with increase in the diameter ratio (Figure 3.12). No significant increase in the ultimate lateral capacity of the under-reamed pile with increase in the diameter ratio of the bulb for the bulb at  $(0.6 \text{ to } 0.7)L$  of the pile (Figure 3.12).

The curve ( $D^* = 0.15$ ) and ( $D^* = 0.0$ ) represents Broms's and modified Broms's approaches respectively (Figure 3.13). No significant increase in the ultimate lateral capacity of under-reamed pile with increase in  $D^*$  for the bulb at or below 0.5 times the length of the pile (Figure 3.13).

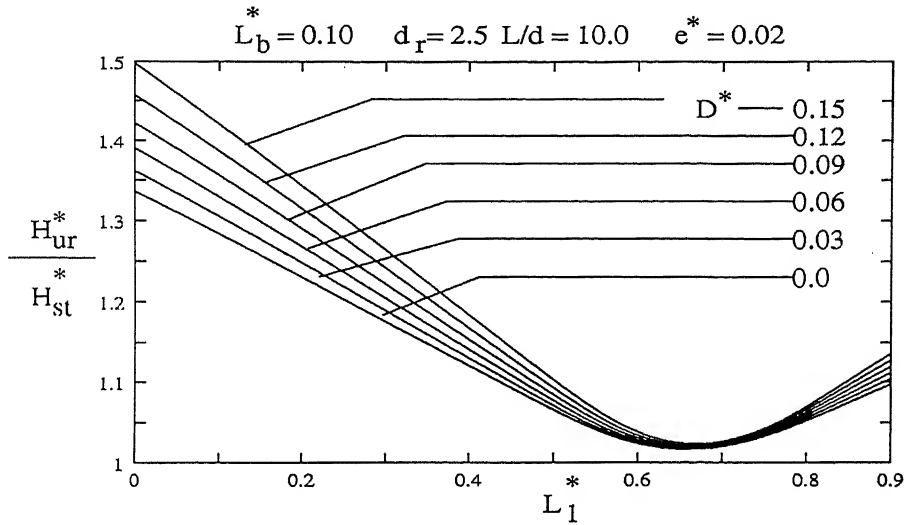


Figure 3.13: Effect of  $D^*$  on Ultimate Capacity for Free Head Single Bulb Under-reamed Pile in Homogeneous Soils - Modified Broms's Theory.

In both Broms's and modified Broms's approaches, the increase of normalised ultimate lateral resistance decreases with the length of the bulb (Figures 3.7 and 3.11). However, the rate of increase of the ratio,  $H_{ur}^*/H_{st}^*$ , is almost constant with increase in the diameter ratio of the bulb (Figures 3.8 and 3.12).

### 3.2.2 Rigid Free Head Double Bulb Under-reamed Pile

The failure mechanism and the resulting distribution of mobilised soil reaction at failure for double bulb under-reamed pile driven into a homogeneous cohesive soil as shown in figure 3.14.

Consider a double bulb under-reamed pile of diameter,  $d$ , length,  $L$ , and bulb diameter as  $d_b$ . Depth of top of the bulb from the ground surface, length of the bulbs and the length of pile below the bottom bulb are  $L_1$ ,  $L_{b1}$ ,  $L_{b2}$  and  $L_4$  respectively. Spacing between the two bulbs is  $S$ . Pile rotates as a rigid body about a point,  $O$ , at a depth,  $h$ , from

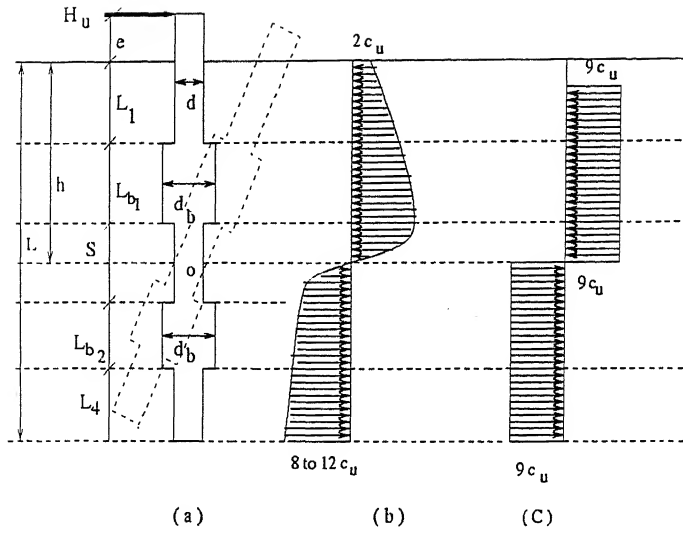


Figure 3.14: Distribution of Soil Reaction-Broms's Theory (a) Kinematics of Double Bulb Under-reamed Pile, (b) Probable Distribution of Soil Reactions and (c) Simplified Soil Reaction.

the ground surface against an applied lateral load,  $H_u$ , at an eccentricity,  $e$ , above the ground surface (Figure 3.14 a).

### 3.2.2.1 Analysis Based on Broms's Theory

In analysing the reaction of the double bulb under-reamed pile against the applied lateral load, possible positions of the point of rotation along the length of the pile are (1) above the top bulb (2) within the top bulb (3) in between the two bulbs (4) within the bottom bulb and (5) below the bottom bulb.

#### a. Point of Rotation Above the Two Bulbs:

From the force and moment equilibrium equations, once again

$$H_u^* = \frac{H_u}{c_u d L} = 9[2h^* - d_r(L_{b1}^* + L_{b2}^*) - L_1^* - L_4^* - S^* - D^*] \quad (3.9)$$

and

$$\begin{aligned} 2h^{*2} + 4e^*h^* - d_r[L_{b1}^{*2} + L_{b2}^{*2} + 2L_{b1}^*(L_1^* + e^*) + 2L_{b2}^*(L_1^* + L_{b1}^* + S^* \\ + e^*)] - [L_1^{*2} + 2e^*L_1^* + S^{*2} + 2S^*(L_1^* + L_{b1}^* + e^*) + L_4^{*2} + 2L_4^*(1 \\ - L_4^*) + D^{*2} + 2e^*D^*] = 0 \end{aligned} \quad (3.10)$$

where  $L_1^* = \frac{L_1}{L}$ ,  $L_{b1}^* = \frac{L_{b1}}{L}$ ,  $L_{b2}^* = \frac{L_{b2}}{L}$ ,  $L_4^* = \frac{L_4}{L}$  and  $S^* = \frac{S}{L}$ .

**b. Point of Rotation Within the First Bulb:**

$$II_u^* = \frac{H_u}{c_u d L} = 9[2d_r h^* - d_r[2L_1^* + L_{b_1}^* + L_{b_2}^*] + L_1^* - L_4^* - S^* - D^*] \quad (3.11)$$

and

$$\begin{aligned} 2d_r h^{*2} + 4e^* d_r h^* - [d_r\{2L_1^{*2} + L_{b_1}^{*2} + L_{b_2}^{*2} + 4e^* L_1^* + 2L_{b_1}^*(L_1^* \\ + e^*) + 2L_{b_2}^*(1 - L_{b_2}^* - L_4^*)\} + S^{*2} + 2S^*(L_1^* + L_{b_1}^* + e^*) + \\ L_4^{*2} + 2L_4^*(1 - L_4^*) + D^{*2} + 2e^* D^* - L_1^{*2} - 2e^* L_1^*] = 0 \end{aligned} \quad (3.12)$$

**c. Point of Rotation Between the Two Bulbs:**

Soil reaction and kinematics of double bulb under-reamed pile for the case of depth of point of rotation lying in between the two bulbs are shown in figure 3.15.

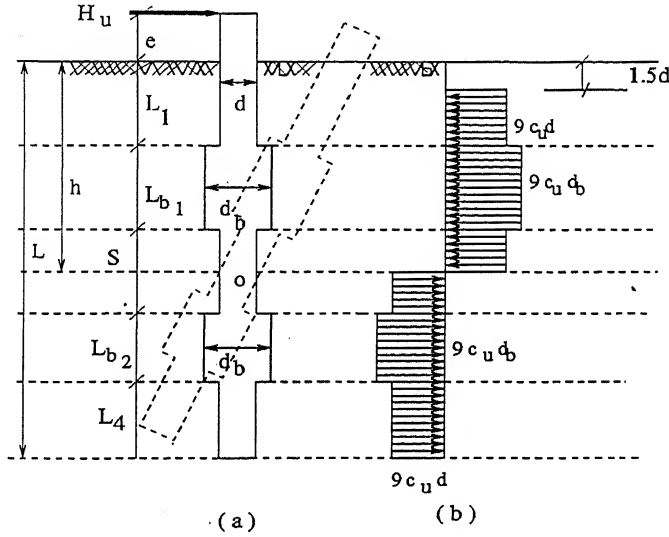


Figure 3.15: Definition Sketch-Broms's Theory (a) Kinematics of Double Bulb Under-reamed Pile and (b) Distribution of Forces along the Pile.

$$H_u^* = \frac{H_u}{c_u d L} = 9[2h^* + d_r(L_{b_1}^* - L_{b_2}^*) - D^* - L_1^* - 2L_{b_1}^* - S^* - L_4^*] \quad (3.13)$$

and

$$\begin{aligned} 2h^{*2} + 4e^* h^* + d_r[L_{b_1}^{*2} - L_{b_2}^{*2} + 2L_{b_1}^*(L_1^* + e^*) - 2L_{b_2}^*(L_1^* + L_{b_1}^* + S^* \\ + e^*)] - [L_1^{*2} + 2L_{b_1}^{*2} + L_4^{*2} + 4L_{b_1}^*(L_1^* + e^*) + S^{*2} + 2S^*(L_1^* + L_{b_1}^* \\ + e^*) + 2e^* L_1^* + 2L_4^*(1 - L_4^*) + D^{*2} + 2e^* D^*] = 0 \end{aligned} \quad (3.14)$$

*d. Point of Rotation Within the Bottom Bulb:*

$$H_u^* = \frac{H_u}{c_u dL} = 9[2d_r h^* - d_r(2L_1^* + L_{b_1}^* + 2S^* + L_{b_2}^*) + L_1^* + S^* - L_4^* - D^*] \quad (3.15)$$

and

$$\begin{aligned} 2d_r h^{*2} + 4e^* d_r h^* - d_r[2L_1^{*2} + L_{b_1}^{*2} + L_{b_2}^{*2} + 2S^{*2} + 2L_1^* L_{b_1}^* + 4S^*(L_1^* + \\ L_{b_1}^*) + 4e^*(L_1^* + S^*) + 2L_{b_2}^*(L_1^* + L_{b_1}^* + S^*) + 2e^*(L_{b_1}^* + L_{b_2}^*)] + L_1^{*2} + \\ 2e^* L_1^* - D^{*2} - 2e^* D^* + S^{*2} + 2S^*(L_1^* + L_b^* + e^*) - L_4^{*2} - 2L_4^*(1 - \\ L_4^*) = 0 \end{aligned} \quad (3.16)$$

*e. Point of Rotation Below the Two Bulbs:*

$$H_u^* = \frac{H_u}{c_u dL} = 9[2h^* + d_r(L_{b_1}^* + L_{b_2}^*) - L_{b_1}^* - L_{b_2}^* - 1 - D^*] \quad (3.17)$$

and

$$\begin{aligned} 2h^{*2} + 4e^* h^* + d_r[L_{b_1}^{*2} + L_{b_2}^{*2} + 2L_{b_1}^*(L_1^* + e^*) + 2L_{b_2}^*(1 - L_{b_2}^* - \\ L_4^*)] - [L_{b_1}^{*2} + L_{b_2}^{*2} + 2L_{b_1}^*(L_1^* + e^*) + 2L_{b_2}^*(1 - L_{b_2}^* - L_4^*) + 1 \\ + D^{*2} + 2e^*(1 + D^*)] = 0 \end{aligned} \quad (3.18)$$

### 3.2.2.2 Results and Discussion

Ultimate capacity of double bulb under-reamed piles in homogeneous soils are estimated and presented in the form of normalised ultimate lateral resistance,  $H_{ur}^*/H_{st}^*$ , as a function of the depth of the bulb from the ground surface,  $L_1^*$ . Length and diameters of the two bulbs are considered to be of the same size. If the diameter ratio,  $d_r$ , equals 1, the ultimate lateral resistance of double bulb under-reamed pile is identical to the value predicted by Broms for straight shafted pile. By providing one more bulb to a single bulb under-reamed pile, the normalised ultimate lateral resistance is 2.5 (Figure 3.16), a 31% increase, over the capacity of single bulb under-reamed pile (Figure 3.7), for  $d_r = 2.5$ ,  $L/d=10$ ,  $L_b^* = 0.2$  and  $e^* = 0.02$ , for the bulbs at and near the ground surface with zero spacing between them.

The normalised ultimate lateral resistance,  $H_u^*/H_{st}^*$ , increases from 1.9 to 2.48, a 30% increase, for the length of the bulbs increasing from 0.1 to 0.2 for  $d_r = 2.5$ ,  $L/d=10$ ,  $S^* = 0.0$  and  $e^* = 0.02$  (Figure 3.16). No significant increase in the ratio,  $H_u^*/H_{st}^*$ , occurs with increasing length of the bulb for  $L_1^* > \frac{1}{4}$  length of the pile (Figure 3.16). Percentage increase of the normalised ultimate lateral resistance decreases with increase in the length of the bulb,  $L_b^*$ . No increase in the normalised ultimate lateral resistance for the length



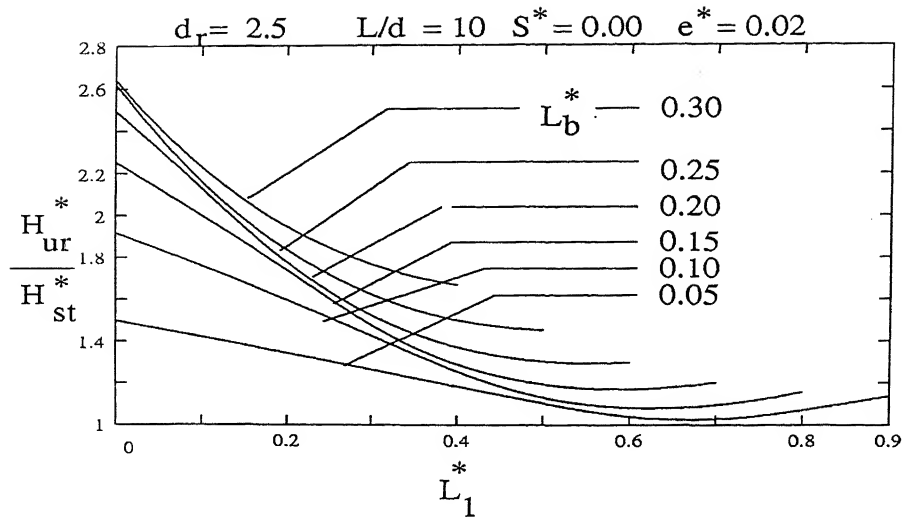


Figure 3.16: Effect of Length of Bulb on Ultimate Capacity for Free Head Double Bulb Under-reamed Pile in Homogeneous Soils - Broms's Theory.

of the bulb,  $L_b^* > 0.25$ , for  $L/d=10$ ,  $d_r = 2.5$ ,  $S^* = 0.0$  and  $e^* = 0.02$  (Figure 3.16). The rate of change of the ratio,  $H_u^*/H_{st}^*$ , with respect to depth of the bulb increases with increase in the length of the bulb.

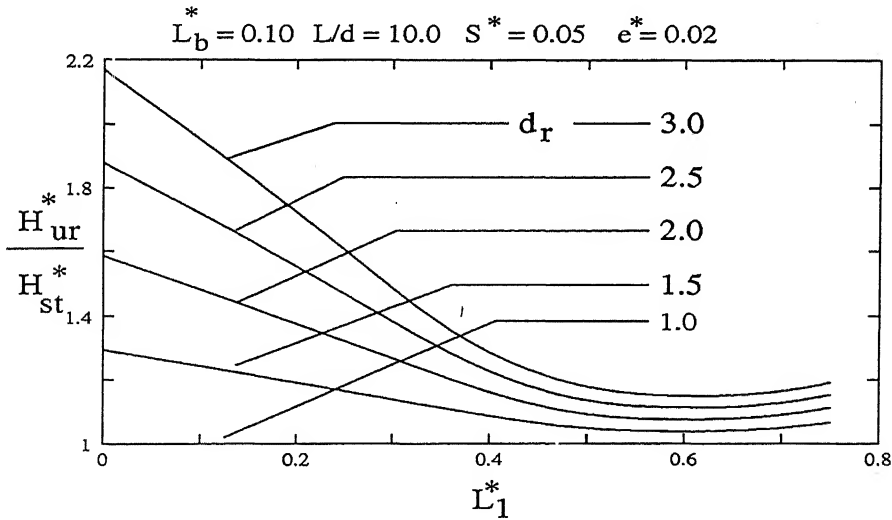


Figure 3.17: Effect of Diameter of Bulb on Ultimate Capacity for Free Head Double Bulb Under-reamed Pile in Homogeneous Soils - Broms's Theory.

For  $d_r = 2.0$ , the additional lateral capacity is about 60% to that of cylindrical pile (Figure 3.17) for  $L_b^* = 0.10$ ,  $L/d=10$ ,  $S^* = 0.05$  and  $e^* = 0.02$ . For the diameter ratio increasing from 1.5 to 3.0, the normalised ultimate lateral resistance increases from 1.3 to 2.18, a 68% increase in the capacity for  $L_b^* = 0.10$ ,  $L/d=10$ ,  $S^* = 0.05$  and  $e^* = 0.02$  (Figure 3.17). The same percentage increase in the ratio,  $H_u^*/H_{st}^*$ , occurs with increase

in the diameter ratio,  $d_r$ , for any position of the bulb through out the length of the pile (Figure 3.17).

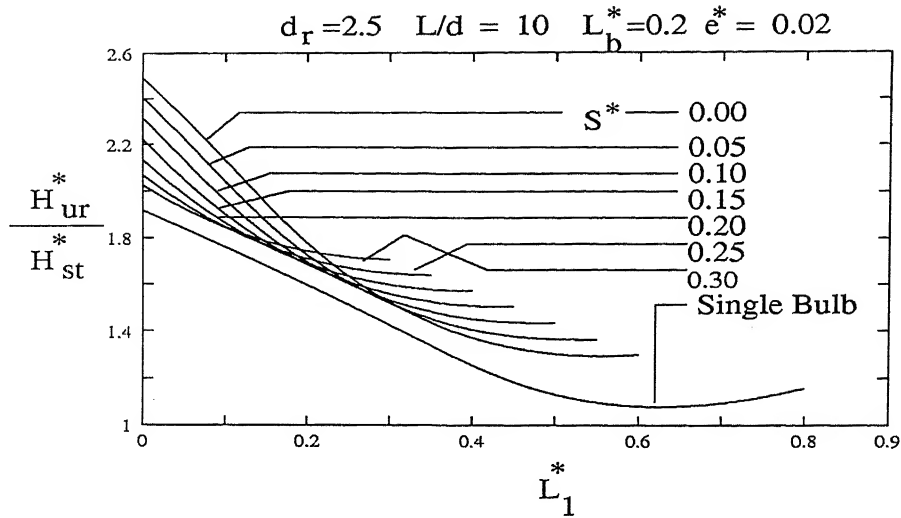


Figure 3.18: Effect of Spacing on Ultimate Capacity for Free Head Double Bulb Under-reamed Pile in Homogeneous Soils - Broms's Theory.

The effect of spacing between the bulbs in case of double bulb under-reamed pile is shown in figure 3.18. For the spacing between the bulbs,  $S^* = 0.0$ , the normalised ultimate lateral resistance is 2.48, whereas it is 1.9 for single bulb under-reamed pile (Figure 3.18). From figures 3.7 and 3.18, for  $L_b^* = 0.20$  and  $S^* = 0.30$ , the normalised ultimate lateral resistance is the same as that for single bulb under-reamed pile for  $L_b^* = 0.20$ , because the second bulb of the double under-reamed pile lies in the depth range of 0.5 to 0.7 times the length of the pile. This indicates that no additional benefit arises by providing the bulb in that region. In case of double bulb under-reamed pile, it is preferable to keep the second bulb either above or below the region of  $(0.5 \text{ to } 0.7)L$ .

The ultimate lateral resistance of double bulb under-reamed pile according to modified Broms's approach, increases with increase in both length and diameter ratio of the bulb as shown in figures 3.19 and 3.20 respectively. In all the cases (Figure 3.19 through 3.22), trends of the curves are similar to those by Broms's approach.

The normalised ultimate lateral resistance increases with increase in length of the bulb. For the length of the bulb,  $L_b^*$ , increasing from 0.1 to 0.2, the normalised ultimate lateral resistance increases from 1.61 to 2.00; a 24% increase, for  $d_r = 2.5$ ,  $L/d=10$ ,  $S^* = 0.0$  and  $e^* = 0.02$  (Figure 3.19). The rate of change of the ratio,  $H_{ur}^*/H_{st}^*$ , increases with increase in length of the bulb (Figure 3.19). No significant increase in the normalised ultimate lateral resistance for the length of the bulb,  $L_b^* > 0.25$  (Figure 3.19).

For the diameter ratio,  $d_r$ , increasing from 1.5 to 3.0 for  $L_b^* = 0.1$ ,  $L/d=10$ ,  $D^* = 0.0$ ,  $S^* = 0.1$  and  $e^* = 0.02$  (Figure 3.20), the normalised ultimate lateral resistance increases

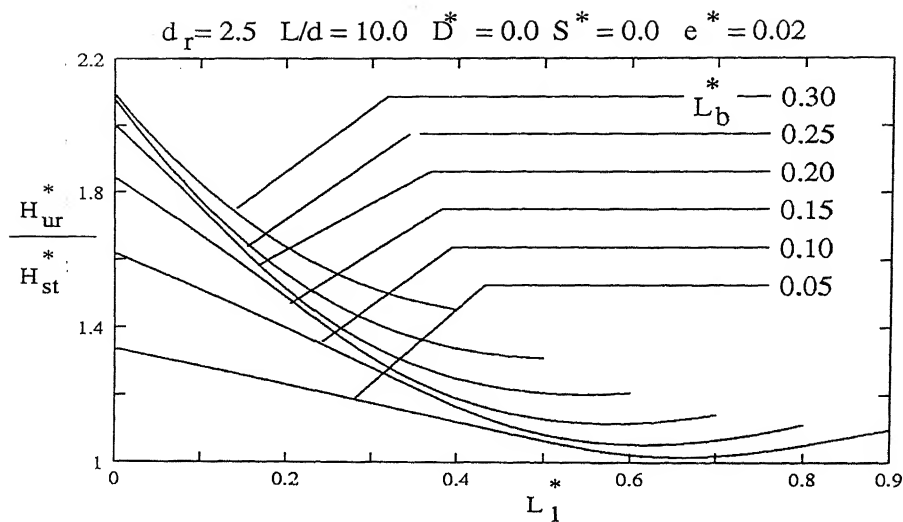


Figure 3.19: Effect of Length of Bulb on Ultimate Capacity for Free Head Double Bulb Under-reamed Pile in Homogeneous Soils - Modified Broms's Theory.

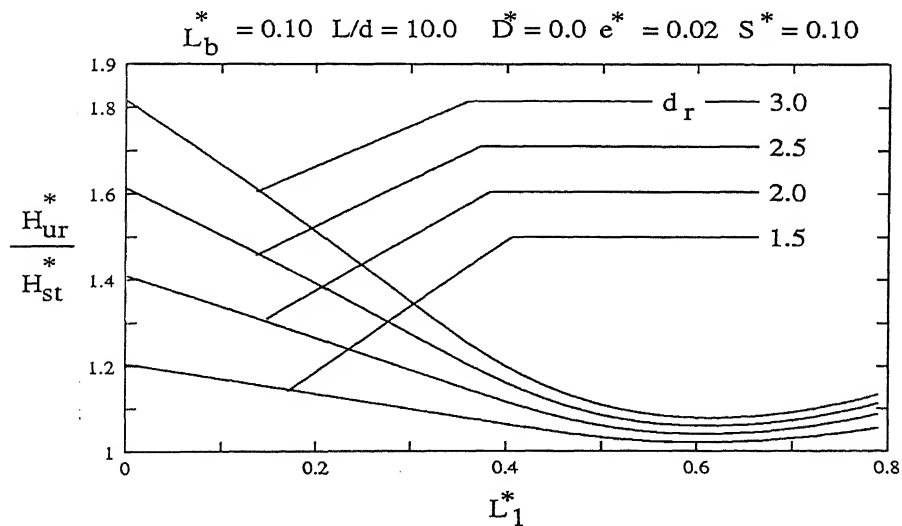


Figure 3.20: Effect of Diameter of Bulb on Ultimate Capacity for Free Head Double Bulb Under-reamed Pile in Homogeneous Soils - Modified Broms's Theory.

from 1.2 to 1.81, a 51% increase in strength with 100% increase in diameter ratio from 1.5 to 3.0. The percentage increase in the ratio,  $H_{ur}^*/H_{st}^*$ , is almost equal for diameter ratio increasing from 1.5 to 2.0, 2.0 to 2.5 and 2.5 to 3.0 (Figure 3.20). The rate of change of the normalised ultimate lateral resistance increases with increase in the diameter ratio (Figure 3.20).

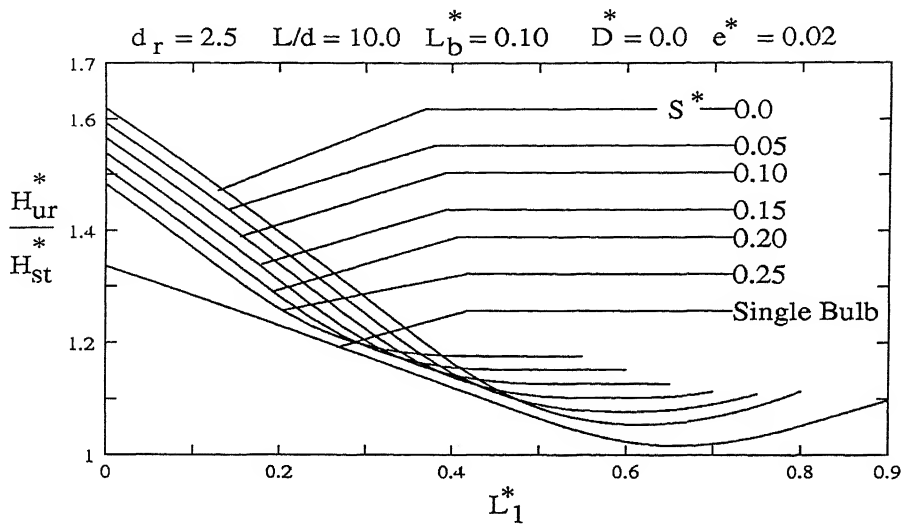


Figure 3.21: Effect of Spacing on Ultimate Capacity for Free Head Double Bulb Under-reamed Pile in Homogeneous Soils - Modified Broms's Theory.

The effect of spacing between the bulbs of the double bulb under-reamed pile according to modified Broms's approach is shown in figure 3.21. For the spacing between the bulbs,  $S^* = 0.0$ , the normalised ultimate lateral resistance is 1.61 whereas it is 1.34, a 20% increase, for single bulb under-reamed pile for  $d_r = 2.5$ ,  $L/d=10$ ,  $L_b^* = 0.1$  and  $e^* = 0.02$  (Figure 3.21). By providing the second bulb to the single bulb under-reamed pile with zero spacing, 20% additional strength is obtained to that of single bulb under-reamed pile (Figure 3.21).

The curves ( $D^* = 0.15$ ) and ( $D^* = 0.0$ ) represent the Broms's and modified Broms's approaches respectively (Figure 3.22). The normalised ultimate lateral resistance is 1.61 and 1.34 for single and double bulb under-reamed pile for  $D^* = 0.0$ ,  $L_b^* = 0.10$ ,  $d_r = 2.5$ ,  $L/d=10$  and  $e^* = 0.02$  (Figures 3.13 and 3.22).

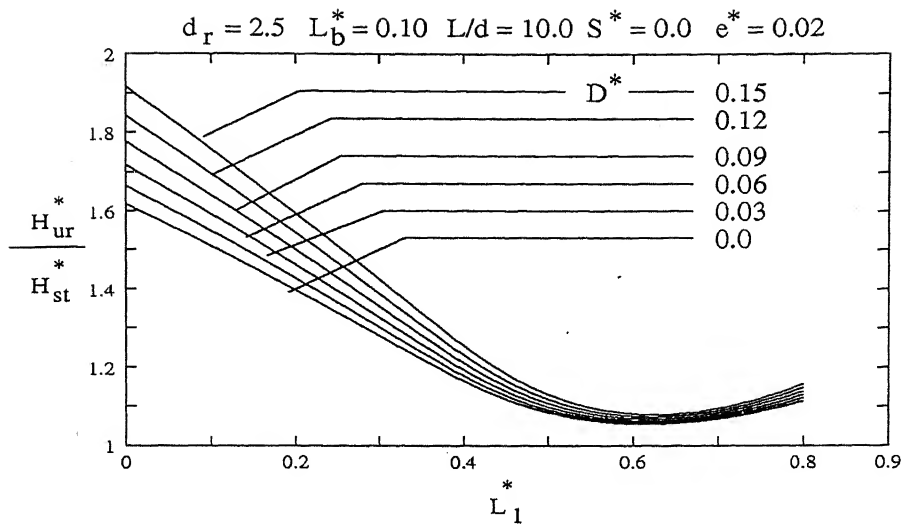


Figure 3.22: Effect of  $D^*$  on Ultimate Capacity for Free Head Double Bulb Under-reamed Pile in Homogeneous Soils - Modified Broms's Theory.

### 3.2.3 Rigid Fixed Head Under-reamed Pile

Fixed head pile is restrained by the pile cap or by a bracing system. Neglecting the cap resistance results in excessively conservative estimates of pile deflections and bending moments.

The ultimate capacity of a fixed head pile is estimated from the following three mechanisms:

- (a) The pile material does not yield while the soil adjacent to it mobilises the ultimate lateral resistance (Short Fixed Head Pile);
- (b) The pile material yields and form a hinge at its top just below the cap (Intermediate Length Pile); and
- (c) The pile material yields in flexure and forms two hinges one at the top (just below the cap) and another at some depth below the ground surface (Long Piles).

The mode of failure of fixed head pile depends on the pile length, shear strength of soils and the stiffness of the pile section.

#### 3.2.3.1 Fixed Head Short Single Bulb Under-reamed Pile

The term "short piles" refer to rigid piles where the lateral load capacity is dependent mainly on the soil resistance. The mode of failure is shown in figure 3.23a with the pile moving laterally as a rigid body. The corresponding distribution of soil reaction is shown in figure 3.23b.

### 3.2.3.1.1 Analysis Based on Broms's Theory

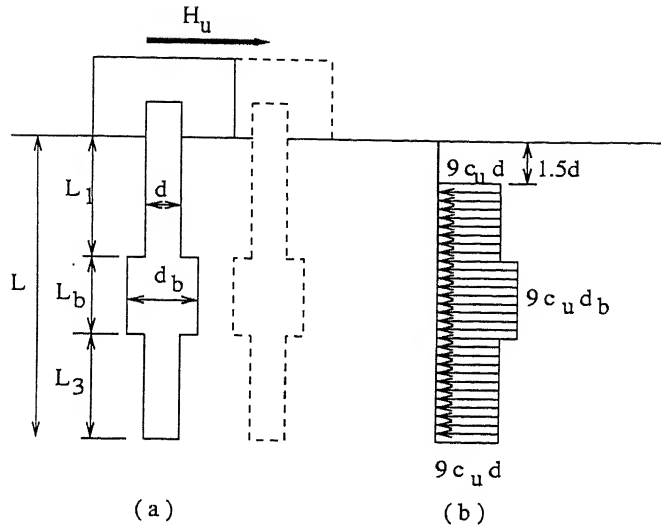


Figure 3.23: Failure Mode of Short Fixed Head Under-reamed Pile: (a) Deflection and (b) Distribution of Forces.

Force equilibrium equation in normalised form is

$$H_u^* = \frac{H_u}{c_u d L} = 9[L_1^* - D^* + d_r L_b^* + L_3^*] \quad (3.19)$$

while the moment equilibrium equation is

$$M_y^* = \frac{M_y}{c_u d L^2} = (9/2)[L_1^{*2} - D^{*2} + d_r \{L_b^{*2} + 2L_1^* L_b^*\} + L_3^{*2} + 2L_1^* L_3^* + 2L_b^* L_3^*] \quad (3.20)$$

### 3.2.3.1.2 Results and Discussion

The ultimate lateral resistance of short fixed head single bulb under-reamed pile is estimated by both Broms's and modified Broms's methods and presented from figures 3.25 through 3.28. The results are plotted between ultimate lateral resistance,  $H_u/c_u d^2$  vs  $L/d$  ratio.

Figure 3.24 depicts the ultimate lateral capacity of short straight shafted pile for different  $L/d$  ratios. It has been noted from figures 3.24 and 3.25 that the ultimate lateral capacity of single bulb under-reamed pile is 1.33 times the straight shafted pile. For the lower  $L/d$  ratio values, there is no significant increase in the ultimate capacity with increase in the length and diameter of the bulb, but at higher  $L/d$  ratio values it increases significantly (Figures 3.25 and 3.26).

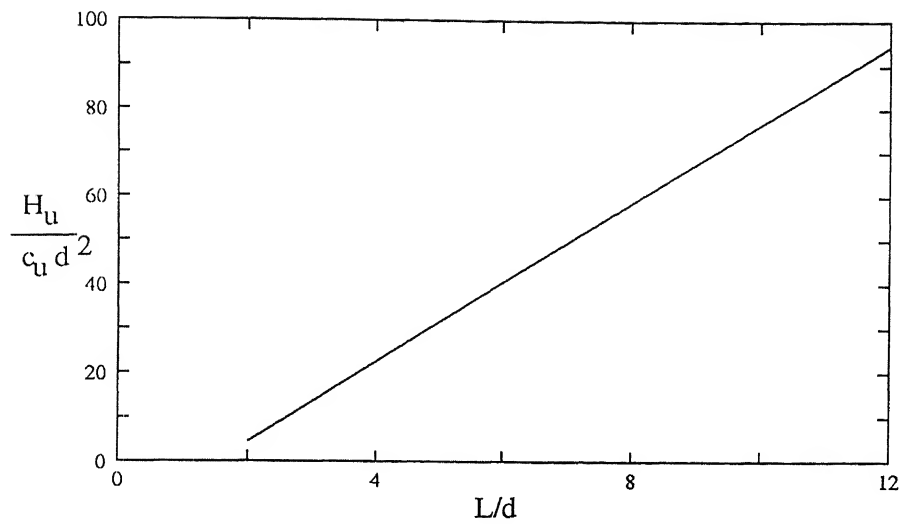


Figure 3.24: Ultimate Capacity of Fixed Head Short Cylindrical Pile.

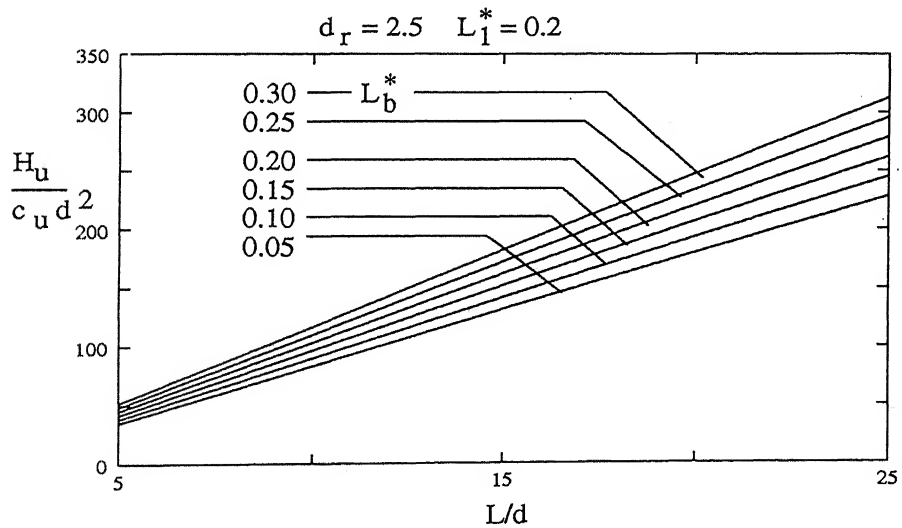


Figure 3.25: Effect of Length of the Bulb on Ultimate Capacity for Fixed Head Short Single Bulb Under-reamed Pile in Homogeneous Soils - Broms's Approach.

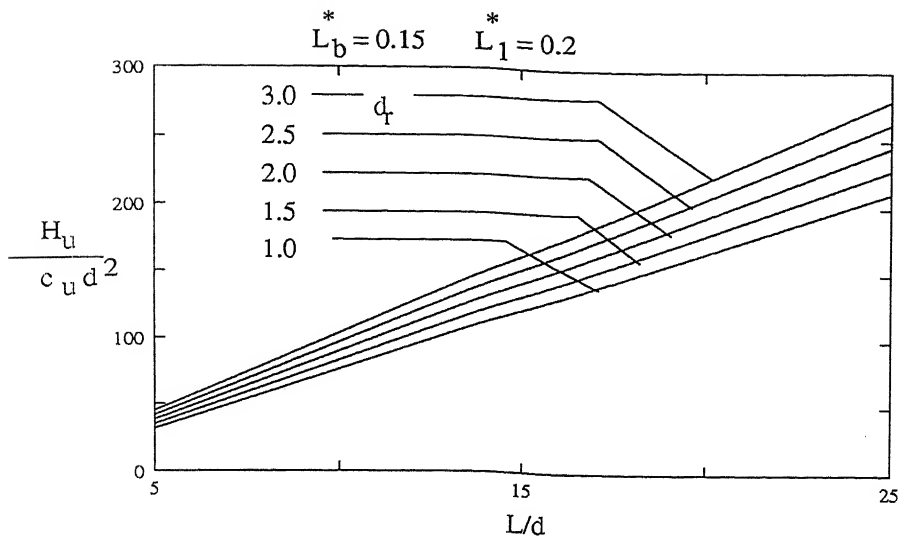


Figure 3.26: Effect of Diameter of the Bulb on Ultimate Capacity for Fixed Head Short Single Bulb Under-reamed Pile in Homogeneous Soils - Broms's Theory.

Figures 3.27 and 3.28 depict the ultimate lateral resistances of fixed head single bulb under-reamed piles by modified Broms's method. From figures 3.26 and 3.28, it is noted that, for  $L_b^* = 0.15$ ,  $L_1^* = 0.2$  and  $d_r = 1.5$ , ultimate lateral resistances are 36% and 50% for Broms's and modified Broms's methods respectively. This indicates that by considering the soil resistance of top  $1\frac{1}{2}$  diameters depth, an additional strength of about 38% can obtain in case of short fixed head pile in homogeneous soils.

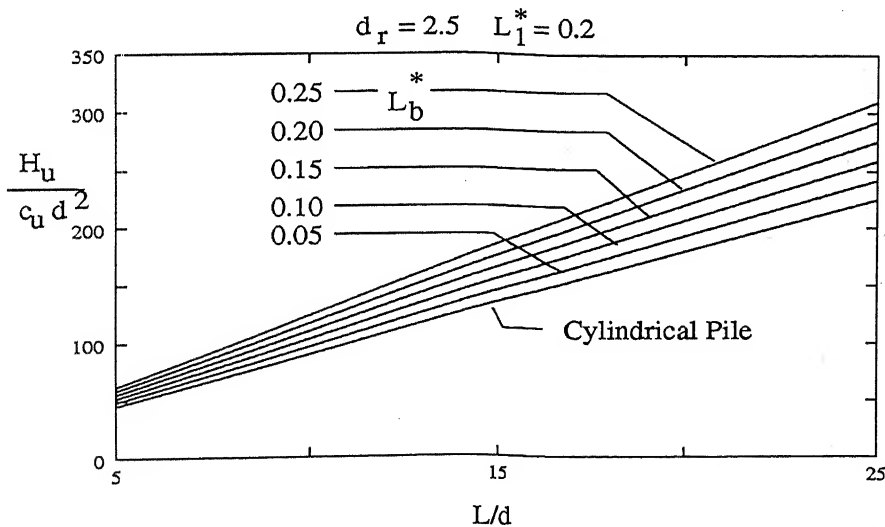


Figure 3.27: Effect of Length of Bulb on Ultimate Capacity for Fixed Head Short Single Bulb Under-reamed Pile in Homogeneous Soils-Modified Broms's Approach.



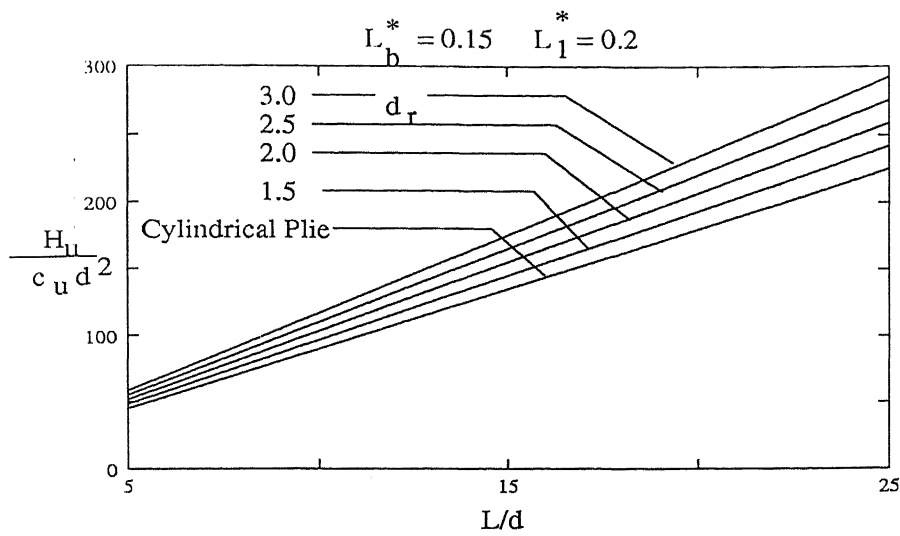


Figure 3.28: Effect of Diameter of Bulb on Ultimate Capacity for Fixed Head Short Single Bulb Under-reamed Pile in Homogeneous Soils-Modified Broms's Approach.

### 3.2.3.2 Rigid Fixed Head Intermediate Length Single Bulb Under-reamed Pile

Long or intermediate length piles are those whose lateral capacity is primarily dependent on the yield moment of the pile itself. The failure mode is illustrated in figure 3.29a. At failure the restraining moment at the head of the pile is equal to the moment capacity of the pile and the pile rotates about a point located some depth below the ground surface. The corresponding distribution of soil reaction is shown in figure 3.29b.

#### 3.2.3.2.1 Analysis Based on Broms's Theory

In the analysis of fixed head intermediate length pile with single bulb, three possible locations of point of rotation are considered: (1) above, (2) within and (3) below the bulb. Kinematics and distribution of forces along the length of pile for the case of point of rotation within the bulb are shown in figure 3.29.

##### a. Point of Rotation Above the Bulb:

$$H_u^* = \frac{H_u}{c_u d L} = 9(2h^* - L_1^* - L_3^* - d_r L_b^* - D^*) \quad (3.21)$$

and

$$2h^{*2} - [d_r \{L_b^{*2} + 2L_1^* L_b^*\} + D^{*2} + L_1^{*2} + L_3^{*2} + 2L_1^* L_3^* + 2L_b^* L_3^*] = M_y^* \quad (3.22)$$

*b. Point of Rotation Within the Bulb:*

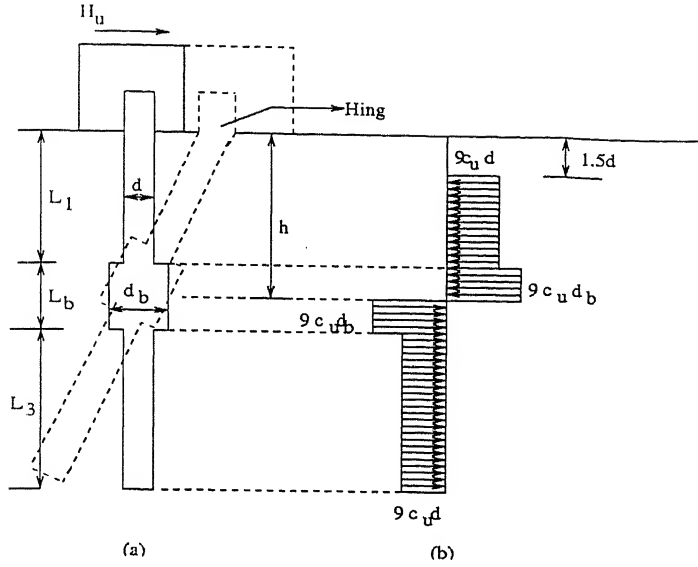


Figure 3.29: Failure Mode of Fixed Head Intermediate Length Under-reamed Pile (a) Kinematics and (b) Distribution of Soil Reaction.

$$H_u^* = \frac{H_u}{c_u d L} = 9[d_r(2h^* - 2L_1^* - L_b^*) + L_1^* - L_3^* - D^*] \quad (3.23)$$

and

$$2d_r h^{*2} - d_r[L_b^* + 2L_1^* L_b^* + 2L_1^*] + L_1^{*2} - L_3^{*2} - 2L_1^* L_3^* - 2L_b^* L_3^* - D^{*2} = M_y^* \quad (3.24)$$

*c. Point of Rotation Below the Bulb:*

$$H_u^* = \frac{H_u}{c_u d L} = 9[2h^* - L_b^* + d_r L_b^* - D^* - 1] \quad (3.25)$$

and

$$2h^{*2} + d_r[L_b^{*2} + 2L_1^* L_b^*] - 2L_1^* L_b^* - L_b^{*2} - D^{*2} - 1 = M_y^* \quad (3.26)$$

### 3.2.3.2.2 Results and Discussion

For fixed head intermediate length single bulb under-reamed pile, the ultimate lateral load capacity is estimated by Broms's and modified Broms's methods and presented in non-dimensional form (Figures 3.30 through 3.33).

The ultimate lateral load capacity increases with increase in length of the bulb. For the length of the bulb,  $L_b^*$ , increasing from 10% to 20% of the length of the pile,

the ultimate lateral capacity increases from 1.25 to 1.48 times the capacity of straight shafted pile, a 19% increase, for  $L/d=10$ ,  $d_r = 2.5$  and  $M_y^* = 200$  (Figure 3.30). No increase in the ratio,  $H_{ur}^*/H_{st}^*$ , with increase in length of the bulb,  $L_b^*$ , for depth of the bulb,  $L_1^*$ , at or below  $0.5L$ . The percentage increase in the normalised ultimate lateral capacity decreases with increase in length of the bulb (Figure 3.30).

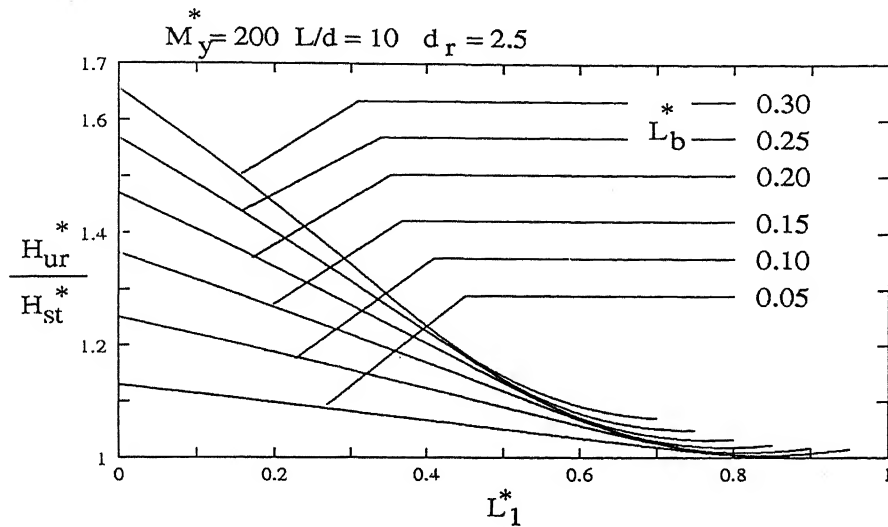


Figure 3.30: Effect of Length of Bulb on Ultimate Capacity for Fixed Head Intermediate Length Under-reamed Pile in Homogeneous Soils-Broms's Approach.

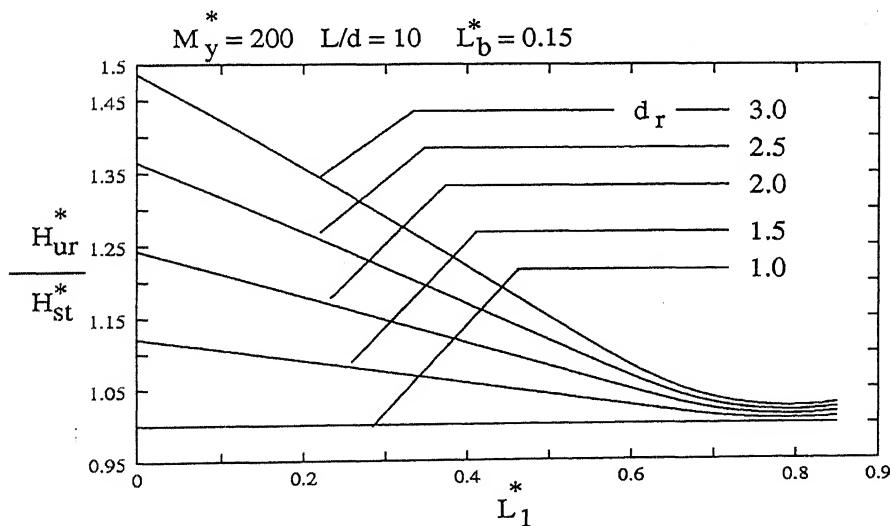


Figure 3.31: Effect of Diameter of Bulb on Ultimate Capacity for Fixed Head Intermediate Length Under-reamed Pile in Homogeneous Soils - Broms's Approach.

By increasing the diameter ratio,  $d_r$ , from 1.0 to 2.0 and 2.0 to 3.0, the capacity increases from 0.975 to 1.24 and 1.24 to 1.48 times the capacity of cylindrical pile, a 27% and 19% increase, for  $L/d=10$ ,  $L_b^* = 0.15$  and  $M_y^* = 200$  (Figure 3.31). No increase

in the normalised ultimate lateral resistance with diameter ratio,  $d_r$ , for the depth of the bulb,  $L_1^* > 0.7$ . The rate of change of ratio,  $H_{ur}^*/H_{st}^*$ , with respect to depth of bulb increases with increase in diameter ratio of the bulb (Figure 3.31).

The length and diameter of the bulb have very similar effect on the ultimate lateral capacity estimated by modified Broms's method. For  $d_r = 2.5$ ,  $L/d=10$  and  $M_y^* = 200$ , the normalised ultimate lateral capacity increases from 1.2 to 1.45 for the length of the bulb increasing from 0.1 to 0.2, a 21% increase (Figure 3.32).

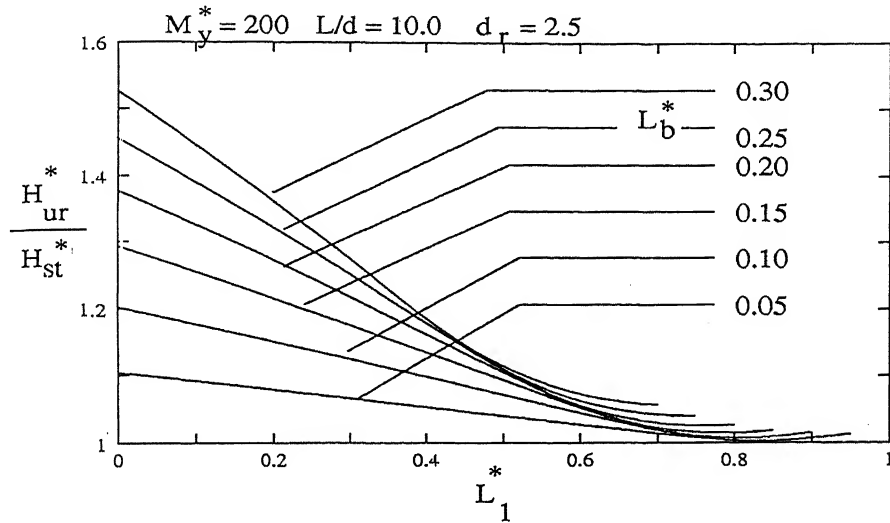


Figure 3.32: Effect of Length of Bulb on Ultimate Capacity for Fixed Head Intermediate Length Under-reamed Pile in Homogeneous Soils - Modified Broms's Approach.

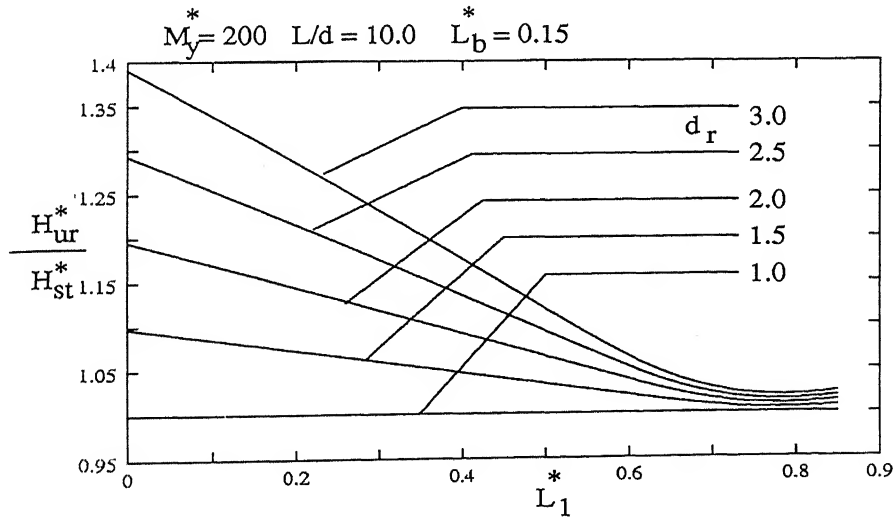


Figure 3.33: Effect of Diameter of Bulb on Ultimate Capacity for Fixed Head Intermediate Length Under-reamed Pile in Homogeneous Soils - Modified Broms's Approach.

For the diameter ratio increasing from 1.5 to 3.0 for  $L_b^* = 0.15$ ,  $L/d=10$  and  $M_y^* = 200$ ,

the ratio,  $H_{ur}^*/H_{st}^*$ , increases from 1.1 to 1.38, a 25% increase (Figure 3.33).

### 3.3 Non-homogeneous Soils

The analyses of under-reamed piles installed in a non-homogeneous soil are presented in the following sections. The undrained strength of the soil is assumed to increase linearly with depth,  $z$ , (Figure 3.34) as  $c_u(z) = c_{u0}(1 + \alpha z/L)$ , where  $c_{u0}$  is the undrained shear strength of the soil at the ground surface and  $\alpha$  is the rate of increase of non-homogeneity of the soil.

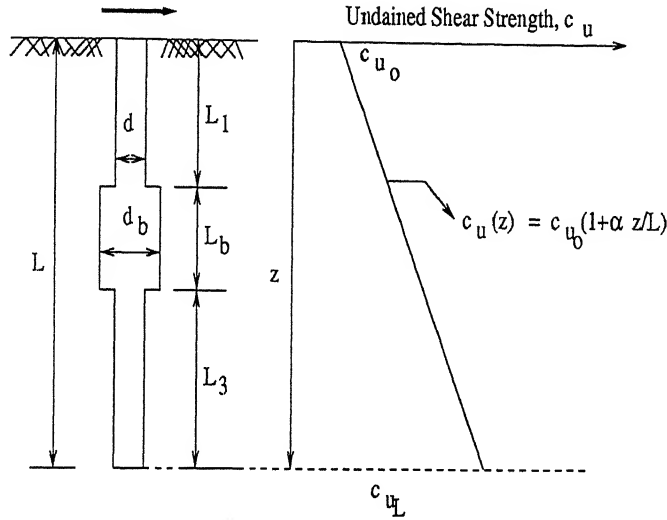


Figure 3.34: Pile Embedded in a Non-homogeneous Soil Stratum.

#### 3.3.1 Rigid Free Head Single Bulb Under-reamed Pile

##### 3.3.1.1 Analysis Based on Broms's Theory

Analysis of free head single bulb under-reamed pile in non-homogeneous soils has been carried out by using the same approach as that for the pile in homogeneous soils, by considering three possible positions of the point of rotation as (1) above, (2) within, and (3) below the bulb. Expressions for estimation of the ultimate lateral load capacity for the three cases of point of rotation are given below. Undrained shear strengths at depths  $L_1$ ,  $L_b$ ,  $h$  and  $L$  are  $c_{uL_1}$ ,  $c_{uL_b}$ ,  $c_{uh}$  and  $c_{uL}$  respectively.

$$c_{uL_1} = c_{u0}(1 + \alpha \frac{L_1}{L}), c_{uL_b} = c_{u0}(1 + \alpha \frac{L_1 + L_b}{L}), c_{uh} = c_{u0}(1 + \alpha \frac{L_1 + L_b + h}{L}) \text{ and } c_{uL} = c_{u0}(1 + \alpha \frac{L}{L}).$$

##### a. Point of Rotation Above the Bulb:

Force equilibrium equation in normalised form,  $H_u^*$  is

$$H_u^* = \frac{H_u}{c_{u0}dL} = (9/2)[h^*\{R_{c1} + 2R_{ch} + 1\} - \{d_r L_b^*(R_{c1} + R_{cb})\} + (R_{ch} + 1)D^* + L_1^*(R_{ch} + R_{c1}) + L_3^*(R_{cb} + R_{cL})] \quad (3.27)$$

and moment equilibrium equation in normalised form is

$$\begin{aligned} h^{*2}[R_{c1} + 4R_{ch} + 1] + h^*[R_{ch}(6e^* - L_1^* - D^*) + R_{c1}(L_1^* + 3e^*) + 3e^* + D^*] - d_r[R_{c1}L_b^*\{L_b^* + 3L_1^* + 3e^*\} + R_{cb}L_b^*\{2L_b^* + 3(L_1^* + e^*)\} - \\ R_{ch}\{D^{*2} + 3e^*D^* + L_1^*(L_1^* + 3e^*)\} - R_{c1}L_1^*(2L_1^* + 3e^*) - R_{cb}L_3^*\{L_3^* + 3(1 - L_3^*)\} - R_{cL}L_3^*\{2L_3^* + 3(1 - L_3^*)\} - 2D^{*2} - 3e^*D^* = 0 \end{aligned} \quad (3.28)$$

where  $R_{c1} = \frac{c_{uL1}}{c_{u0}}$ ,  $R_{cb} = \frac{c_{uLb}}{c_{u0}}$ ,  $R_{ch} = \frac{c_{uh}}{c_{u0}}$ , and  $R_{cL} = \frac{c_{uL}}{c_{u0}}$ .

### b. Point of Rotation Within the Bulb:

Distribution of forces along the length of the pile against the applied lateral load in non-homogeneous cohesive soil for the case of point of rotation lying within the bulb is shown in figure 3.35.

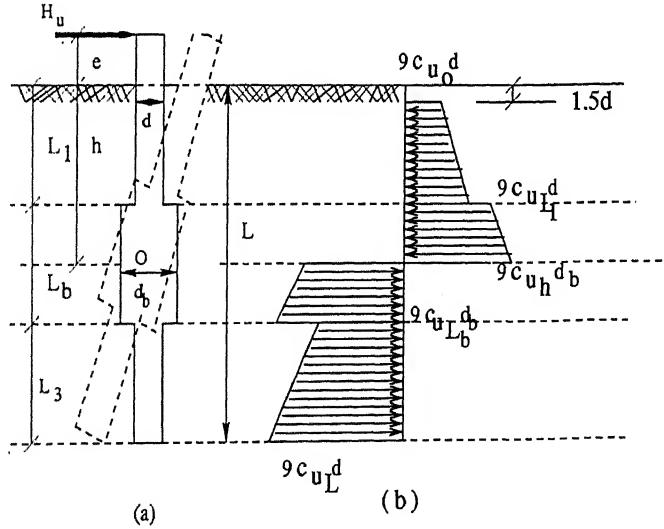


Figure 3.35: Failure Mode of Free Head Single Bulb Under-reamed Pile in Non-Homogeneous Soils (a) Kinematics and (b) Distribution of Forces along the Length of the Pile.

Force and moment equilibrium equations are

$$H_u^* = \frac{H_u}{c_{u0}dL} = (9/2)[h^*\{d_r(R_{c1} + R_{cb} + 2R_{ch})\} + (R_{c1} + 1)(L_1^* - D^*) - R_{c1}L_1^*d_r) - R_{ch}\{d_r(2L_1^* + L_b^*)\} - R_{cb}\{d_r(L_1^* + L_b^*) + L_3^*\} + R_{cL}L_3^*] \quad (3.29)$$

and

$$\begin{aligned} & h^{*2}[d_r\{R_{c1} + 4R_{ch} + R_{cb}\}] + h^*[d_r\{R_{c1}(3e^* + L_1) + R_{cb}(L_1^* + L_b^* + 3e^*) + R_{ch}(6e^* - 2L_1^* - L_b^*)\}] - d_r[R_{c1}(2L_1^{*2} + 3e^*L_1^*) + R_{ch}\{2L_1^*(L_1^* + L_b^*) + L_b^{*2} + 3e^*(2L_1^* + L_b^*)\} + R_{cb}\{2(L_1^* + L_b^*)^2 + 3e^*(L_1^* + L_b^*)\}] \\ & + R_{c1}\{2L_1^{*2} + 3e^*L_1^* - D^*(L_1^* + D^* + 3e^*)\} - R_{cb}L_3^*\{L_3^* + 3(L_1^* + L_b^* + e^*)\} - R_{cL}L_3^*\{2L_3^* + 3(L_1^* + L_b^* + e^*)\} + L_1^{*2} + 3e^*(L_1^* - D^*) - D^*(2D^* + L_1^*) = 0 \end{aligned} \quad (3.30)$$

*c. Point of Rotation Below the Bulb:*

$$H_u^* = \frac{H_u}{c_{u0}dL} = (9/2)[h^*\{R_{cb} + 2R_{ch} + R_{cL}\} + d_r\{L_b^*(R_{c1} + R_{cb})\} + R_{c1}(L_1^* - D^*) - R_{cb}(L_1^* + L_b^*) - R_{ch}(1 + L_1^* + L_b^*) - R_{cL} + L_1^* - D^*] \quad (3.31)$$

and

$$\begin{aligned} & h^{*2}[R_{cb} + 4R_{ch} + R_{cL}] + h^*[R_{cb}\{L_1^* + L_b^* + 3e^*\} - R_{ch}\{L_1^* + L_b^* - 6e^* + 1\} + R_{cL}(1 + 3e^*)] + d_r[R_{c1}L_b^*(L_b^* + 3L_1^* + 3e^*) + R_{cb}L_b^*\{2L_b^* + 3(L_1^* + e^*)\}] + R_{c1}\{2L_1^{*2} + L_1^*D^* - D^{*2} + 3e^*(L_1^* - D^*)\} - R_{cb}\{2(L_1^* + L_b^*)^2 + 3e^*(L_1^* + L_b^*)\} - R_{ch}\{(L_1^* + L_b^*)^2 + 3e^*(L_1^* + L_b^* + 1) + 1\} \\ & - R_{cL}(2 + 3e^*) + L_1^{*2} + 3e^*(L_1^* - D^*) - 2D^{*2} + L_1^*D^* = 0 \end{aligned} \quad (3.32)$$

### 3.3.1.2 Results and Discussion

If the non-homogeneous strength ratios,  $R_{c1}$ ,  $R_{cb}$  and  $R_{cL}$  are equals one i.e. the non-homogeneity factor,  $\alpha = 0$ , the ultimate lateral resistances of the under-reamed piles estimated by the present method are identical to the values predicted by Broms's method. Ultimate lateral resistance of rigid free head single bulb under-reamed pile in non-homogeneous soils estimated by both Broms's and modified Broms's methods are presented in figures 3.36 through 3.43.

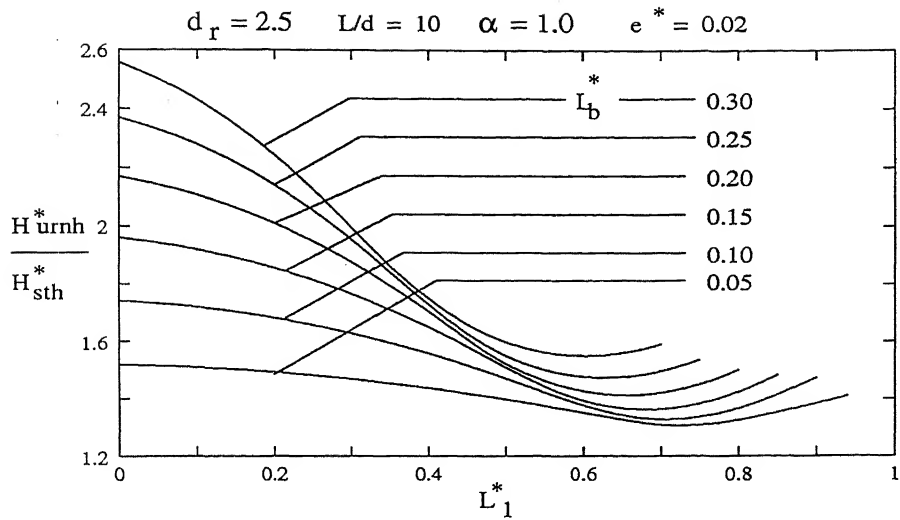


Figure 3.36: Effect of Length of Bulb on Ultimate Capacity for Free Head Single Bulb Under-reamed Pile in Non-homogeneous Soils - Broms's Theory.

For diameter ratio,  $d_r = 2.5$ , length to diameter ratio,  $L/d=10$ ,  $L_b^* = 0.2$ ,  $\alpha = 1.0$  and eccentricity,  $e^* = 0.02$ , the ultimate capacity of under-reamed pile is 2.18 times the cylindrical pile (Figure 3.36), whereas it is 1.92 times (Figure 3.7) in homogeneous soils i.e. a 13.58% increase, due to non-homogeneity. For the length of bulb increasing from 0.1 to 0.2 for  $d_r = 2.5$ ,  $L/d=10$ ,  $\alpha=1.0$  and  $e^* = 0.02$ , the normalised ultimate lateral resistance of the single bulb under-reamed pile increases from 1.76 to 2.18, a 24% increase (Figure 3.36). Percentage increase of the ratio,  $H_{urnh}^*/H_{sth}^*$ , is significant for the length of the bulb,  $L_b^* > 0.25$ , for the bulb at top (Figure 3.36). No significant increase in the normalised ultimate lateral resistance with length of the bulb for the bulb at depth range of  $(0.5 \text{ to } 0.7)L$  (Figure 3.36). From figures 3.7 and 3.36, it is observed that, the percentage increase in the normalised ultimate capacity of under-reamed pile with length of the bulb is more and decreases at a faster rate in homogeneous soils than in non-homogeneous soils.

For the diameter ratio,  $d_r$ , increasing from 1.5 to 3.0 for  $L_b^* = 0.20$ ,  $L/d=10$ ,  $\alpha = 1.0$  and  $e^* = 0.02$ , the normalised ultimate lateral resistance increases from 1.59 to 2.44, a 55% increase (Figure 3.37). No significant increase in the ratio,  $H_{urnh}^*/H_{sth}^*$ , occurs with increase in the diameter ratio for the bulb at or below  $0.6L$  (Figure 3.37). The rate of change of the ratio,  $H_{urnh}^*/H_{sth}^*$ , with respect to the depth of the bulb increases with increase in the diameter ratio of the under-reamed pile. The percentage increase in the ultimate lateral resistance of single bulb under-reamed pile is almost equal with increase in diameter ratio for the bulb at top of the pile (Figure 3.37).

The normalised ultimate lateral resistance is 2.42 and 2.18 for  $L/d$  ratio 5.0 and 10.0 for  $d_r = 2.5$ ,  $L_b^* = 0.20$ ,  $\alpha=1.0$  and  $e^* = 0.02$  (Figure 3.38). The percentage decrease



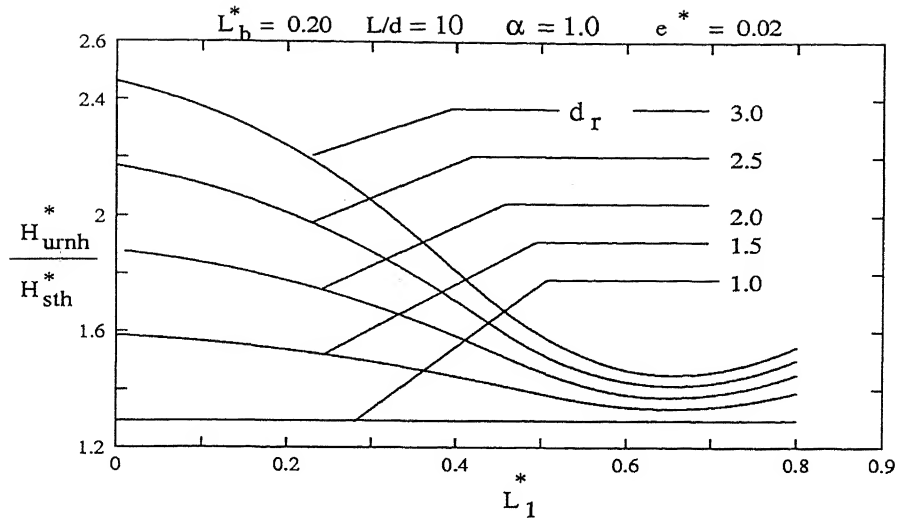


Figure 3.37: Effect of Diameter of Bulb on Ultimate Capacity for Free Head Single Bulb Under-reamed Pile in Non-homogeneous Soils - Broms's Theory.

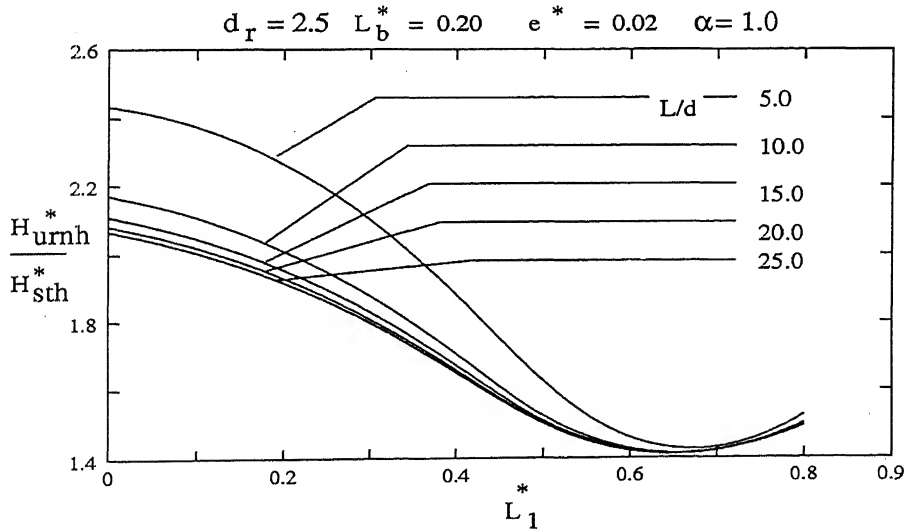


Figure 3.38: Effect of  $L/d$  Ratio on Ultimate Capacity for Free Head Single Bulb Under-reamed Pile in Non-homogeneous Soils - Broms's Theory.

in the normalised ultimate lateral resistance is significant for increase in  $L/d$  ratio from 5.0 to 10.0. No significant decrease in the ratio,  $H_{urnh}^*/H_{sth}^*$ , for greater values of  $L/d$  ( $L/d > 10.0$ ) (Figure 3.38).

Normalised ultimate lateral capacity of under-reamed pile increases with the non-homogeneity factor,  $\alpha$ , (Figure 3.39). At higher values of  $\alpha$ , the ratio,  $H_{urnh}^*/H_{sth}^*$ , increases slightly upto  $L_1^* = 0.2$  and for  $L_1^* > 0.2$  the capacity decreases with depth of the bulb. The percentage increase in the capacity is uniform with the increase of the non-homogeneity factor,  $\alpha$  for  $d_r = 2.5$ ,  $L_b^* = 0.20$ ,  $L/d = 10.0$  and  $e^* = 0.02$  (Figure 3.39).

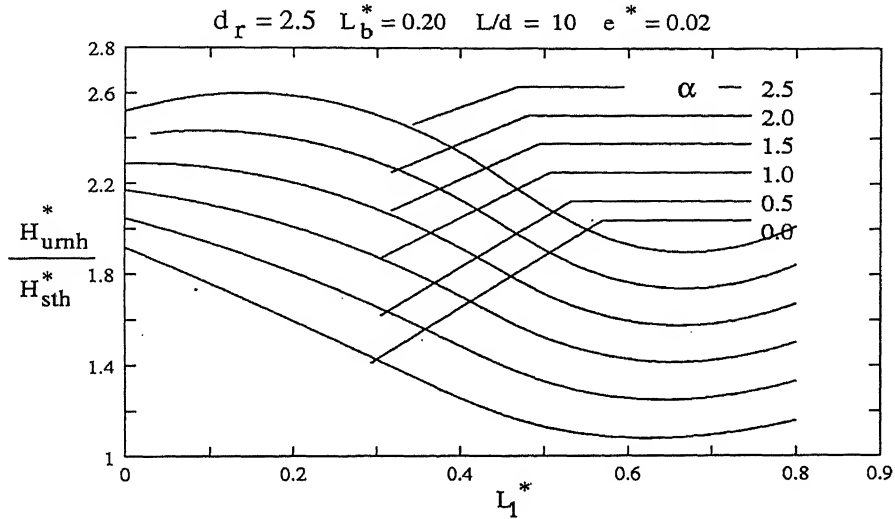


Figure 3.39: Effect of  $\alpha$  on Ultimate Capacity for Free Head Single Bulb Under-reamed Pile in Non-homogeneous Soils - Broms's Theory.

The normalised ultimate lateral resistance of free head single bulb under-reamed pile in non-homogeneous soils estimated based on modified Broms's method is presented in figures 3.40 through 3.43. A 19% and 15% increase in the normalised ultimate lateral resistance occurs with the length of the bulb increasing from 0.1 to 0.2 and 0.2 to 0.3 respectively for  $d_r = 2.5$ ,  $\alpha = 1.0$ ,  $L/d = 10$ ,  $D^* = 0.0$  and  $e^* = 0.02$  (Figure 3.40). The rate of change of normalised ultimate lateral resistance with respect to the depth of the bulb increases with increase in length of the bulb.

For the diameter ratio,  $d_r$ , increasing from 1.0 to 2.0 and 2.0 to 3.0, a 35% and 26% increase, in the normalised ultimate lateral resistance occurs for  $L/d = 10$ ,  $L_b^* = 0.2$ ,  $D^* = 0.0$ ,  $\alpha = 1.0$  and  $e^* = 0.02$  (Figure 3.41). No significant increase in the ratio,  $H_{urnh}^*/H_{sth}^*$ , with increase in diameter ratio of the bulb for the depth of the bulb at or below  $0.6L$  from the ground surface (Figure 3.41). The rate of change of the normalised ultimate lateral resistance with respect to depth of bulb increases with increase in diameter ratio.

For the non-homogeneity factor,  $\alpha$ , increasing from 0.0 to 1.0 and 1.0 to 2.0 for  $d_r = 2.5$ ,  $L/d = 10.0$ ,  $L_b^* = 0.20$ ,  $D^* = 0.0$  and  $e^* = 0.02$ , the normalised ultimate lateral

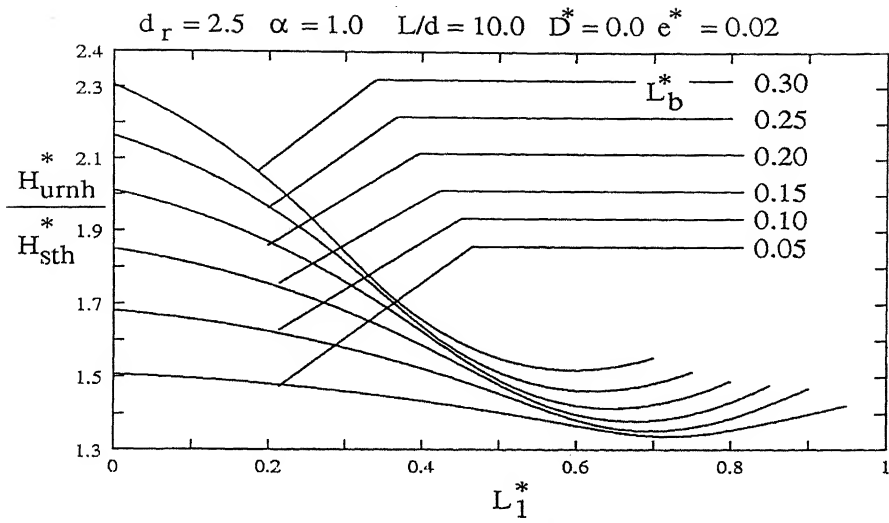


Figure 3.40: Effect of Length of Bulb on Ultimate Capacity for Free Head Single Bulb Under-reamed Pile in Non-homogeneous Soils - Modified Broms's Theory.

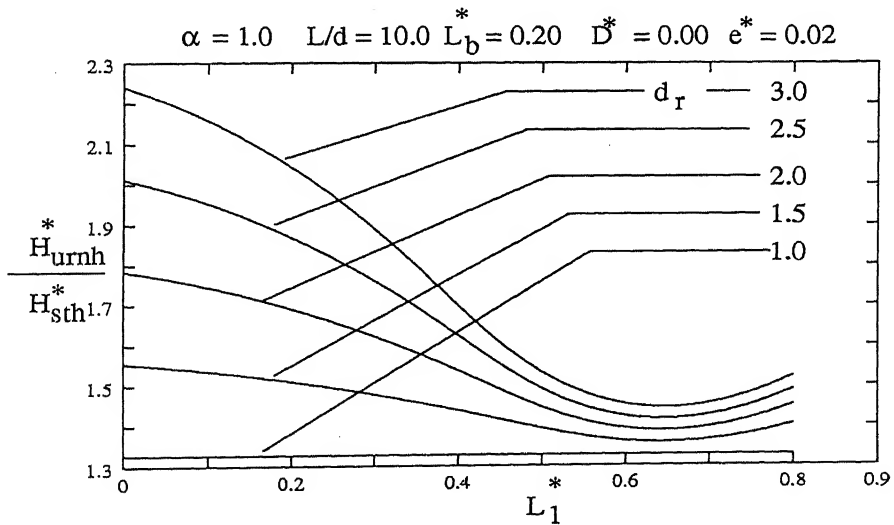


Figure 3.41: Effect of Diameter of Bulb on Ultimate Capacity for Free Head Single Bulb Under-reamed Pile in Non-homogeneous Soils - Modified Broms's Theory.

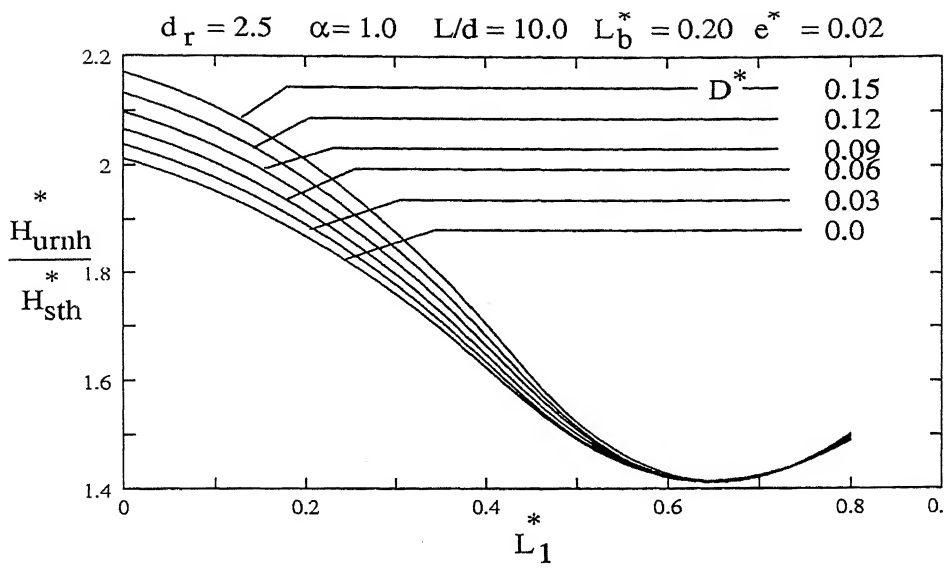


Figure 3.42: Effect of  $D^*$  on Ultimate Capacity for Free Head Single Bulb Under-reamed Pile in Non-homogeneous Soils - Modified Broms's Theory.

resistance increases from 1.6 to 2.0 and 2.0 to 2.4, a 25% and 20% increase (Figure 3.43). The percentage increase in the ratio,  $H_{urnh}^*/H_{sth}^*$ , is almost uniform with increase in the non-homogeneity factor,  $\alpha$  (Figure 3.43). For larger values of non-homogeneity factor,  $\alpha > 0.2$ , the normalised ultimate lateral resistance decreases at a faster rate for the depth of bulb below  $0.2L$ , for  $d_r = 2.5$ ,  $L/d = 10.0$ ,  $L_b^* = 0.20$ ,  $D^* = 0.0$  and  $e^* = 0.02$  (Figure 3.43).

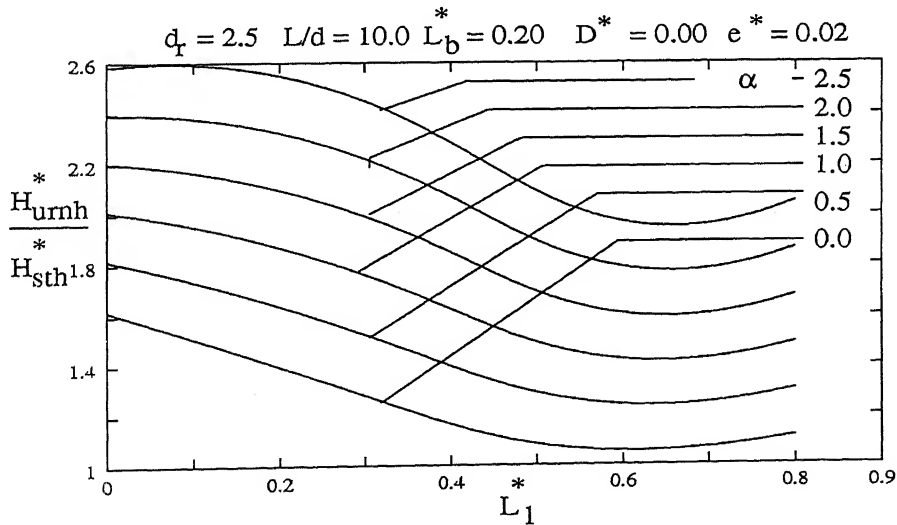


Figure 3.43: Effect of  $\alpha$  on Ultimate Capacity for Free Head Single Bulb Under-reamed Pile in Non-homogeneous Soils - Modified Broms's Theory.

### 3.3.2 Rigid Free Head Double Bulb Under-reamed Pile

The failure mechanism and the resulting distribution of mobilised and simplified soil reaction for double bulb under-reamed pile in non-homogeneous soils as shown in figure 3.44.

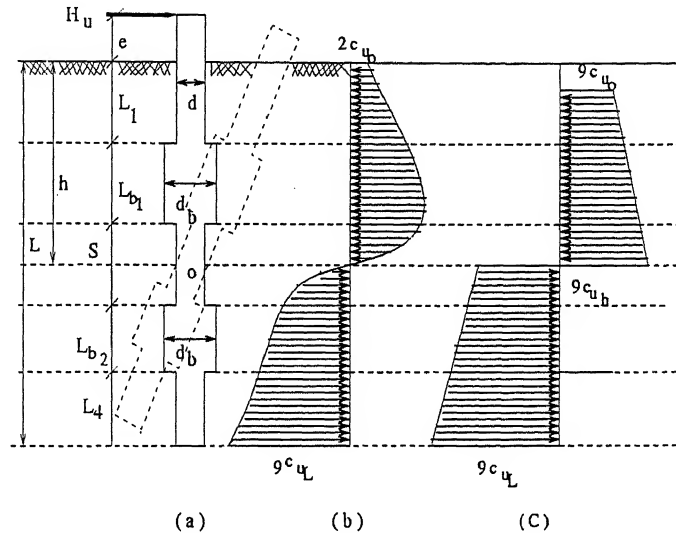


Figure 3.44: Distribution of Soil Reaction in Non-homogeneous Soils - Broms's Theory  
(a) Kinematics, (b) Probable Distribution and (c) Simplified Soil Reaction.

Consider the double bulb under-reamed pile of diameter,  $d$ , and length,  $L$ . The bulb lengths and diameters are  $L_{b1}$ ,  $L_{b2}$ ,  $d_{b1}$  and  $d_{b2}$  respectively. Depth of the bulb from the ground surface and length of pile below the bottom bulb are  $L_1$  and  $L_4$ . Spacing between the two bulbs is  $S$ . Pile rotates about a point,  $O$ , at a depth  $h$ , from the ground surface due to an applied lateral load,  $H_u$ , with an eccentricity,  $e$ , above the ground surface (Figure 3.44).

#### 3.3.2.1 Analysis Based on Broms's Theory

Five possible locations of depth of point of rotation are considered in analysing the double bulb under-reamed pile in non-homogeneous soils. The possible locations are (1) above the two bulbs (2) within the top bulb (3) in between the two bulbs (4) within the bottom bulb and (5) below the bottom bulb as in the case of analysis of piles in homogeneous soils.

##### *a. Point of Rotation Above the Two Bulbs:*

Force and moment equilibrium equations, once again are

$$H_u^* = \frac{H_u}{c_{u0}dL} = (9/2)[h^*\{1 + R_{c1} + 2R_{ch}\} - d_r\{L_{b1}^*(R_{c1} + R_{cb1}) + L_{b2}^*(R_{cs} + R_{cb2})\} - D^* - R_{ch}(L_1^* + D^*) - R_{c1}L_1^* - S^*(R_{cb1} + R_{cs}) - L_4^*(R_{cb2} + R_{cL})] \quad (3.33)$$

and

$$\begin{aligned} & h^{*2}[R_{c1} + 4R_{ch} + 1] + h^*[3e^* + D^* + R_{ch}(6e^* - L_1^* - D^*) + R_{c1}(L_1^* + 3e^*)] - 2D^{*2} - 3e^*D^* - R_{ch}\{D^{*2} + L_1^{*2} + 3e^*(L_1^* + D^*)\} - R_{c1}(2L_1^{*2} \\ & + 3e^*L_1^*) - R_{cb1}S^*\{S^* + 3(L_1^* + L_{b1}^* + e^*)\} - R_{cs}S^*\{2S^* + 3(L_1^* + e^* + L_{b1}^*)\} - R_{cb2}L_4^*\{L_4^* + 3(1 - L_4^*)\} - R_{cL}L_4^*\{2L_4^* + 3(1 - L_4^*)\} - \\ & d_r[R_{c1}L_{b1}^*\{L_{b1}^* + 3(L_1^* + e^*)\} + R_{cb1}L_{b1}^*\{2L_{b1}^* + 3(L_1^* + e^*)\} + R_{cb2}L_{b2}^*\{L_{b2}^* + 3(S^* + L_{b1}^* + L_1^* + e^*)\} + R_{cb2}L_{b2}^*\{2L_{b2}^* + 3(S^* + L_1^* + L_{b1}^* + e^*)\}] \\ & = 0 \end{aligned} \quad (3.34)$$

$$\text{where } R_{c1} = \frac{c_{uL1}}{c_{u0}}, R_{cb1} = \frac{c_{uLb1}}{c_{u0}}, R_{cb2} = \frac{c_{uLb2}}{c_{u0}}, R_{cs} = \frac{c_{uS}}{c_{u0}}, R_{cL} = \frac{c_{uL}}{c_{u0}}$$

**b. Point of Rotation Within the Top Bulb:**

$$\begin{aligned} H_u^* = \frac{H_u}{c_{u0}dL} = (9/2)[h^*\{d_r(R_{c1} + 2R_{ch} + R_{cb1})\} - d_r\{R_{c1}L_1^* + R_{ch}(2L_1^* + L_{b1}^*) \\ + R_{cb1}(L_1^* + L_{b1}^*) + R_{cs}L_{b2}^* + R_{cb2}L_{b2}^*\} + L_1^* - D^* + R_{c1}(L_1^* - D^*) - S^*(R_{cb1} \\ + R_{cs}) - L_4^*(R_{cb2} + R_{cL})] \end{aligned} \quad (3.35)$$

and

$$\begin{aligned} & h^{*2}[d_r\{R_{c1} + 4R_{ch} + R_{cb1}\}] + h^*[d_r\{R_{c1}(L_1^* + 3e^*) + R_{ch}(6e^* - 2L_1^* - L_{b1}^*) \\ & + R_{cb1}(L_1^* + L_{b1}^* + 3e^*)\}] - d_r[R_{c1}L_1^*(2L_1^* + 3e^*) + R_{ch}\{L_1^{*2} + (L_1^* + L_{b1}^*)^2 \\ & + 3e^*(2L_1^* + L_{b1}^*)\} + R_{cb1}\{2(L_1^* + L_{b1}^*)^2 + 3e^*(L_1^* + L_{b1}^*)\} + R_{cs}L_{b2}^*\{L_{b2}^* \\ & + 3(S^* + L_1^* + L_{b1}^* + e^*)\} + R_{cb2}L_{b2}^*\{2L_{b2}^* + 3(S^* + L_{b1}^* + L_1^* + e^*)\}] + \\ & L_1^*(L_1^* + 3e^*) - 2D^{*2} - 3e^*D^* + L_1^*D^* + R_{c1}\{2L_1^{*2} - D^*(L_1^* + D^*) \\ & + 3e^*(L_1^* - D^*)\} - R_{cb1}S^*\{S^* + 3(L_1^* + L_{b1}^* + e^*)\} - R_{cs}S^*\{2S^* + 3(L_1^* \\ & + L_{b1}^* + e^*)\} - R_{cb2}L_4^*\{L_4^* + 3(1 - L_4^*)\} - R_{cL}L_4^*\{2L_4^* + 3(1 - L_4^*)\} = 0 \end{aligned} \quad (3.36)$$

पुस्तकालय काशीनाथ केशवदास  
भारतीय प्रौद्योगिकी संस्थान दिल्ली  
अवधि १९९४-१९९७  
134987

### c. Point of Rotation Between the Two Bulbs:

The kinematics and distribution of forces along the pile for the case of point of rotation lying between the two bulbs shown in figure 3.45.

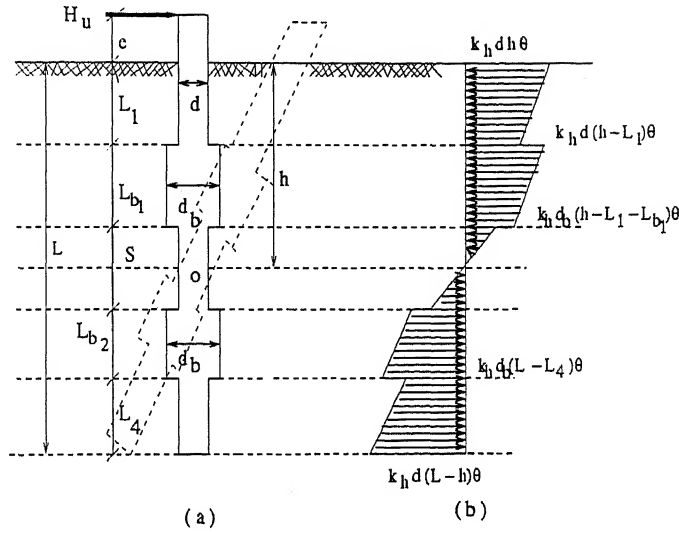


Figure 3.45: Failure Mode of Double Bulb Under-reamed Pile in Non-homogeneous Soils  
(a) Kinematics and (b) Distribution of Forces along the Pile Length.

$$H_u^* = \frac{H_u}{c_{u0} d L} = (9/2)[h^*(R_{cb1} + 2R_{ch} + R_{cs}) + d_r\{L_{b1}^*(R_{c1} + R_{cb1}) - L_{b2}^*(R_{cs} + R_{cb2})\} + (L_1^* - D^*)(1 + R_{c1}) - R_{cb1}(L_1^* + L_{b1}^*) - R_{ch}(2L_1^* + L_{b1}^* + S^*) - R_{cs}(L_1^* + L_{b1}^* + S^*) - L_4^*(R_{cb2} + R_{cL})] \quad (3.37)$$

and

$$\begin{aligned} & h^{*2}[R_{cb1} + 4R_{ch} + R_{cs}] + h^*[R_{cb1}(3e^* + L_1^* + L_{b1}^*) + R_{ch}(6e^* - 2L_1^* - 2L_{b1}^* - S^*) + R_{cs}(L_1^* + L_{b1}^* + S^* + 3e^*)] + d_r[R_{c1}L_{b1}^*\{L_{b1}^* + 3(L_1^* + e^*)\} + R_{cb1}L_{b1}^*\{2L_{b1}^* + 3(L_1^* + e^*)\} - R_{cs}L_{b2}^*\{2L_{b2}^* + 3(1 - L_{b2}^* - L_4^*)\}] \\ & + L_1^*(L_1^* + 3e^*) - 2D^{*2} + D^*(L_1^* - 3e^*) + R_{c1}\{2L_1^{*2} - L_1^*D^* - D^{*2} + 3e^*(L_1^* - D^*) - R_{cb1}\{2(L_1^* + L_{b1}^*)^2 + 3e^*(L_1^* + L_{b1}^*)\} - \\ & R_{ch}\{2(L_1^* + L_{b1}^*)^2 + 6e^*(L_1^* + L_{b1}^*) + S^*(S^* + 2L_1^* + 2L_{b1}^* + 3e^*)\} - \\ & R_{cs}\{2(L_1^* + L_{b1}^*)^2 + 4S^*(L_1^* + L_{b1}^*)2S^{*2} + 3e^*(L_1^* + L_{b1}^* + S^*)\} - \\ & R_{cb2}L_4^*\{L_4^* + 3(1 - L_4^*)\} - R_{cL}L_4^*\{2L_4^* + 3(1 - L_4^*)\} = 0 \end{aligned} \quad (3.38)$$

*d. Point of Rotation Within the Bottom Bulb:*

$$H_u^* = \frac{H_u}{c_{u0} dL} = (9/2)[h^*\{d_r(R_{c_s} + 2R_{c_h} + R_{c_{b_2}})\} + d_r\{L_{b_1}^*(R_{c_1} + R_{c_{b_1}}) - (R_{c_s} - 2R_{c_h})(L_1^* + L_{b_1}^* + S^*) - R_{c_h}L_{b_2}^* - R_{c_{b_2}}(1 - L_4^*)\} + (L_1^* - D^*)(1 + R_{c_1}) + S^*(R_{c_{b_2}} + R_{c_s}) - L_4^*(R_{c_{b_2}} + R_{c_L})] \quad (3.39)$$

and

$$\begin{aligned} & h^{*2}d_r[R_{c_s} + 4R_{c_h} + R_{c_{b_2}}] + h^*d_r[3e^*(R_{c_s} + 2R_{c_h} + R_{c_{b_2}}) + (L_1^* + L_{b_1}^*)(R_{c_s} \\ & - 2R_{c_h} + R_{c_{b_2}}) + 2S^*(S^* - R_{c_h}) + L_{b_2}^*(R_{c_{b_2}} - R_{c_h})] + d_r[R_{c_1}L_{b_1}^*\{L_{b_1}^* + 3(L_1^* \\ & + e^*)\} + R_{c_{b_1}}L_{b_1}^*\{2L_{b_1}^* + 3(L_1^* + e^*)\} - R_{c_s}\{2(L_1^{*2} + L_{b_1}^{*2} + S^{*2}) + 4L_{b_1}^* \\ & (L_1^* + S^*) + 4L_1^*S^* + 3e^*(L_1^* + L_{b_1}^* + S^*)\} - R_{c_h}\{2(L_1^{*2} + L_{b_1}^{*2} + S^{*2}) \\ & + 4(L_1^*L_{b_1}^* + L_1^*S^* + L_{b_1}^*S^*) + 6e^*(L_1^* + L_{b_1}^* + S^*) + L_{b_2}^*(L_{b_2}^* + 2L_1^* \\ & + 2L_{b_1}^* + 2S^*) + 3e^*L_{b_2}^*\} - 2R_{c_{b_2}}L_1^*\{L_{b_1}^* + 2(L_{b_1}^* + S^* + L_{b_2}^*) + 2L_{b_1}^*(L_{b_1}^* \\ & 2S^* + 2L_{b_2}^*) + 2S^{*2} + 2L_{b_2}^*(2S^* + L_{b_2}^*) + 3e^*(1 - L_4^*)\} + L_1^{*2} - 2D^{*2} + \\ & 3e^*L_1^* + D^*(L_1^* + e^*) + R_{c_1}\{2L_1^{*2} - D^*(L_1^* + D^*) + 3e^*(L_1^* - D^*) \\ & + S^{*2}(R_{c_{b_1}} + R_{c_s}) + 3(R_{c_{b_1}} + R_{c_s})(L_1^* + L_{b_1}^* + e^*)\} - L_4^{*2}(R_{c_{b_2}} + 2R_{c_L}) - \\ & 3(R_{c_{b_2}} + R_{c_L})(1 - L_4^* + e^*) = 0 \end{aligned} \quad (3.40)$$

*e. Point of Rotation Below the Two Bulbs:*

$$H_u^* = \frac{H_u}{c_{u0} dL} = (9/2)[h^*(R_{c_{b_2}} + 2R_{c_h} + R_{c_L}) + d_r\{L_{b_1}^*(R_{c_1} + R_{c_{b_1}}) + L_{b_2}^*(R_{c_{b_2}} + R_{c_s})\} + (L_1^* - D^*)(1 + R_{c_1}) + S^*(R_{c_{b_1}} + R_{c_s}) - R_{c_{b_2}}(1 - L_4^*) - R_{c_h}(L_1^* + L_{b_1}^* + L_{b_2}^* + S^* + 1) - R_{c_L}] \quad (3.41)$$

and

$$\begin{aligned} & h^{*2}[R_{c_{b_2}} + 4R_{c_h} + R_{c_L}] + h^*[R_{c_{b_2}}(3e^* + 1 - L_4^*) - R_{c_h}(2 - L_4^* - 6e^*) + \\ & R_{c_L}(1 + 3e^*)] + d_r[L_{b_1}^{*2}(R_{c_1} + 2R_{c_{b_1}}) + 3(R_{c_1} + R_{c_{b_1}})(L_1^* + e^*) + L_{b_2}^{*2}(R_{c_s} \\ & + 2R_{c_{b_2}}) + 3(R_{c_s} + R_{c_{b_2}})(L_1^* + L_{b_1}^* + e^*)] + R_{c_1}\{2L_1^{*2} - L_1^*D^* - D^{*2} + \\ & 3e^*(L_1^* - D^*)\} + S^{*2}(R_{c_{b_1}} + 2R_{c_s}) + 3(R_{c_{b_1}} + R_{c_s})(L_1^* + L_{b_1}^* + e^*) - \\ & (2R_{c_{b_2}} + R_{c_h})(1 - L_4^*)^2 - 3e^*(R_{c_{b_2}} + R_{c_h})(1 - L_4^*) - R_{c_h}(3e^* + 1) - R_{c_L}(2 \\ & + 3e^*) + L_1^{*2} - 2D^{*2} + L_1^*D^* + 3e^*(L_1^* - D^*) = 0 \end{aligned} \quad (3.42)$$



### 3.3.2.2 Results and Discussion

Results for the double bulb under-reamed pile in non-homogeneous soils are presented for  $L_{b1} = L_{b2} = L_b$ . In non-homogeneous soils, by providing an additional bulb to the single bulb under-reamed pile for  $L_b^* = 0.2$ ,  $d_r = 2.5$ ,  $L/d=10$ ,  $e^* = 0.02$  with spacing,  $S^* = 0.05$ , and non-homogeneity factor,  $\alpha = 1.0$ , the ultimate lateral capacity is 2.78 times the capacity of straight shafted pile, whereas it is 2.18 times for single bulb under-reamed pile, a 28% increase (Figures 3.36 and 3.46).

The normalised ultimate lateral resistance increases from 2.18 to 2.78 and 2.78 to 2.92 with the length of the bulb increasing from 0.1 to 0.2 and 0.2 to 0.3 respectively, for  $d_r = 2.5$ ,  $L/d=10$ ,  $S^* = 0.1$ ,  $e^* = 0.02$  and  $\alpha=1.0$ , a 27.5% and 5% increase (Figure 3.46). The percentage increase in the normalised ultimate lateral resistance decreases with increase in length of the bulb. No significant increase in the ratio,  $H_{urnh}^*/H_{sth}^*$ , for increase in length of the bulb,  $L_b^* > 0.2$  (Figure 3.46).

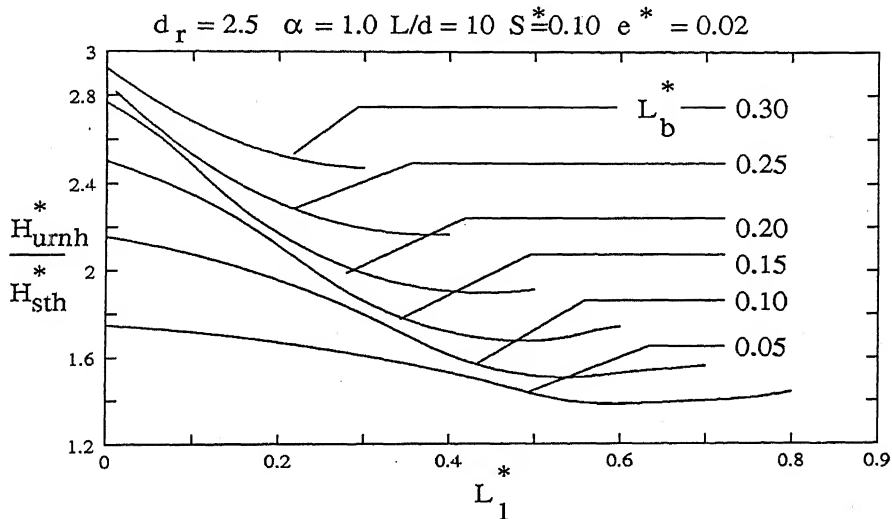


Figure 3.46: Effect of Length of Bulb on Ultimate Capacity for Free Head Double Bulb Under-reamed Pile in Non-homogeneous Soils - Broms's Theory.

For the diameter ratio,  $d_r$ , increasing from 1.5 to 3.0, the normalised ultimate lateral resistance increases from 1.6 to 2.24, a 40% increase, for  $L_b^* = 0.2$ ,  $L/d=10$ ,  $S^* = 0.05$ ,  $\alpha=1.0$  and  $e^* = 0.02$  (Figure 3.47). No significant increase in the ratio,  $H_{urnh}^*/H_{sth}^*$ , with increase in the diameter ratio for the depth of bulb at or below  $0.5L$  (Figure 3.47). Rate of change of the normalised ultimate lateral resistance increases with increase in the diameter ratio.

The ultimate lateral resistance of under-reamed pile is 3.44 and 2.82 times that of the straight shafted pile for  $L/d$  ratios 5.0 and 10.0 respectively, for  $d_r = 2.5$ ,  $L_b^* = 0.2$ ,  $S^* = 0.05$ ,  $\alpha=1.0$  and  $e^* = 0.02$  (Figure 3.48). The normalised ultimate lateral resistance decreases with increase in  $L/d$  ratio. No significant decrease in the ratio,  $H_{urnh}^*/H_{sth}^*$ ,

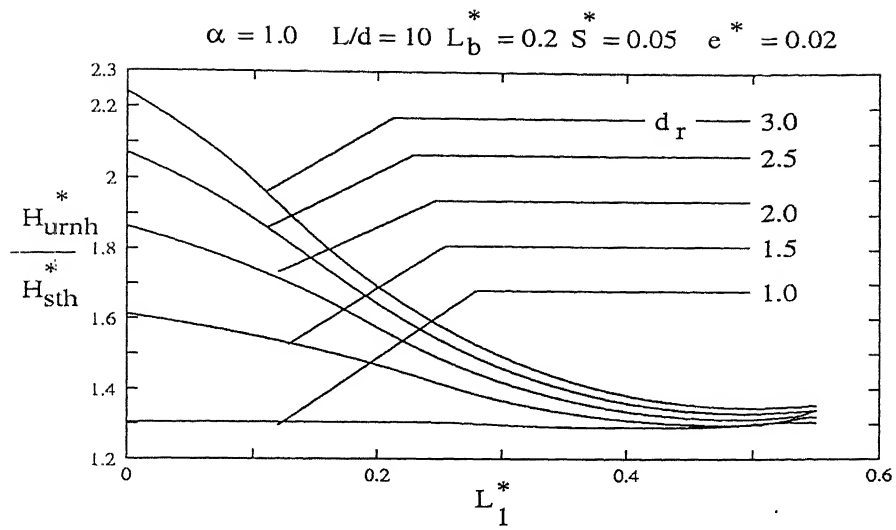


Figure 3.47: Effect of Diameter of Bulb on Ultimate Capacity for Free Head Double Bulb Under-reamed Pile in Non-homogeneous Soils - Broms's Theory.

for the  $L/d$  ratio greater than 10 (Figure 3.48). The rate of change of the normalised ultimate lateral resistance with respect to depth of the bulb is same for  $L/d$  ratio 5.0 through 25.0.

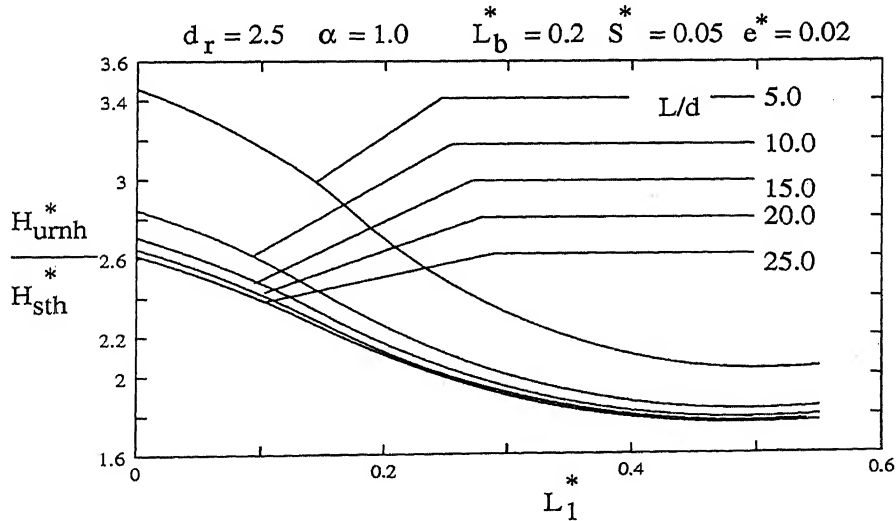


Figure 3.48: Effect of  $L/d$  Ratio on Ultimate Capacity for Free Head Double Bulb Under-reamed Pile in Non-homogeneous Soils - Broms's Theory.

The effect of spacing between the bulbs in case of double bulb under-reamed pile in non-homogeneous soils is shown figure 3.49. The normalised ultimate lateral resistance is 2.9 for the spacing between the bulbs,  $S^* = 0.0$ , whereas it is 2.18 for single bulb under-reamed pile for  $d_r = 2.5$ ,  $L/d=10$ ,  $L_b^* = 0.2$ ,  $\alpha=1.0$  and  $e^* = 0.02$  (Figure 3.49). Provision of second bulb gives 33% additional strength to single bulb under-reamed pile

in case of non-homogeneous soils (Figure 3.49) whereas it is 30% in case of homogeneous soils (Figure 3.18).

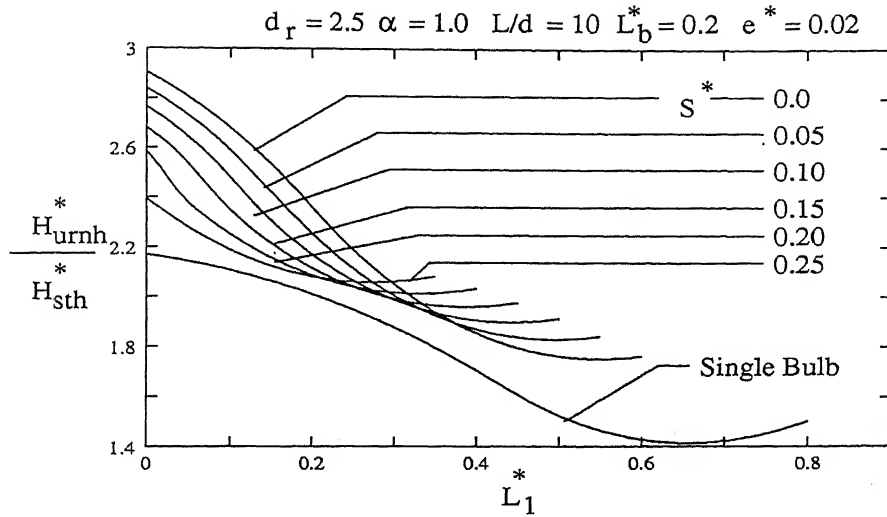


Figure 3.49: Effect of Spacing on Ultimate Capacity for Free Head Double Bulb Under-reamed Pile in Non-homogeneous Soils - Broms's Theory.

Normalised ultimate lateral resistance increases with increase in non-homogeneity factor,  $\alpha$ , (Figure 3.50). The normalised ultimate lateral resistance increases from 2.45 to 2.85 and 2.85 to 3.2, a 16% and 12% increase, with the non-homogeneity factor increasing from 0.0 to 1.0 and 1.0 to 2.0, for  $d_r = 2.5$ ,  $L/d=10$ ,  $L_b^* = 0.2$ ,  $S^* = 0.05$  and  $e^* = 0.02$  (Figure 3.50).

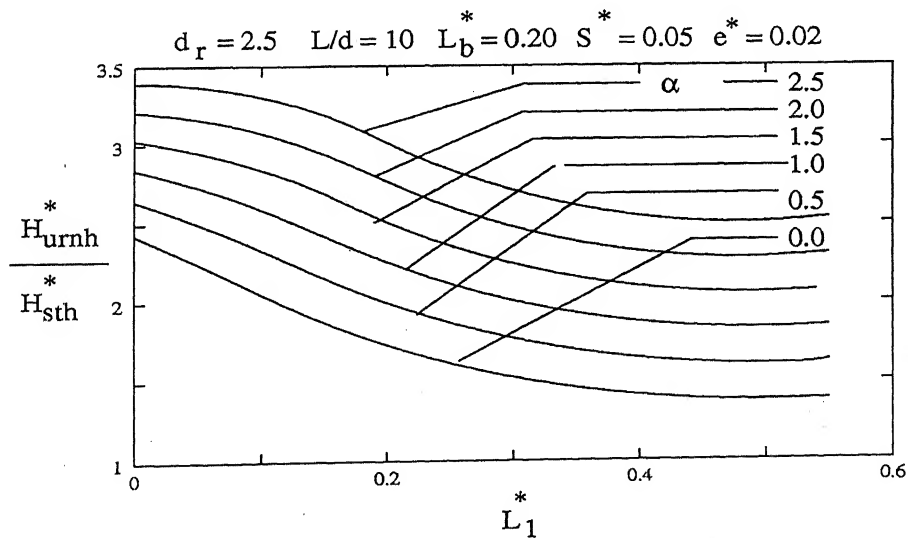


Figure 3.50: Effect of  $\alpha$  on Ultimate Capacity for Free Head Double Bulb Under-reamed Pile in Non-homogeneous Soils - Broms's Theory.

The normalised ultimate lateral resistance increases from 2.0 to 2.5 and 2.5 to 2.62

with the length of the bulb,  $L_b^*$ , increasing from 0.1 to 0.2 and 0.2 to 0.3, a 25% and 5% increase, for  $d_r = 2.5$ ,  $L/d=10$ ,  $D^* = 0.0$ ,  $S^* = 0.05$ ,  $\alpha=1.0$  and  $e^* = 0.02$  (Figure 3.51). Percentage increase in the ratio,  $H_{urnh}^*/H_{sth}^*$ , decreases with increase in length of the bulb,  $L_b^*$ . No significant increase in the normalised ultimate lateral resistance for length of the bulb,  $L_b^* > 0.25$ , for the bulb at top of the pile (Figure 3.51).

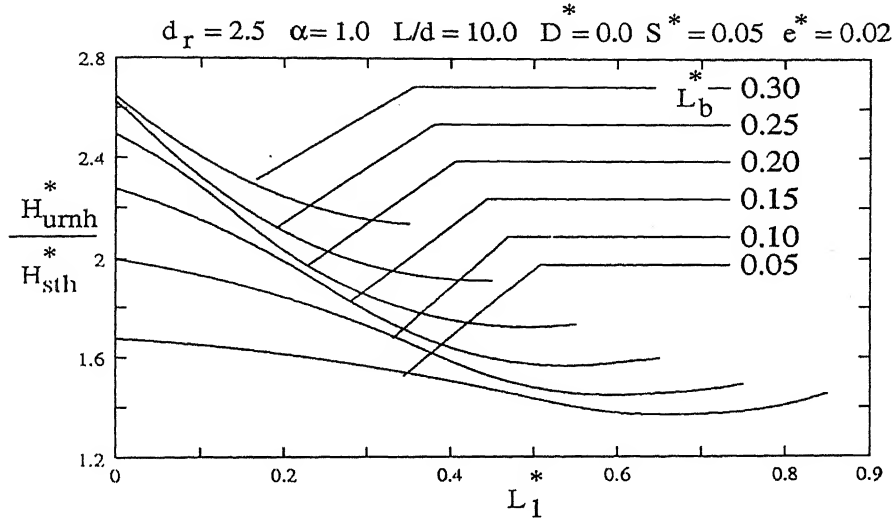


Figure 3.51: Effect of Length of Bulb on Ultimate Capacity for Free Head Double Bulb Under-reamed Pile in Non-homogeneous Soils - Modified Broms's Theory.

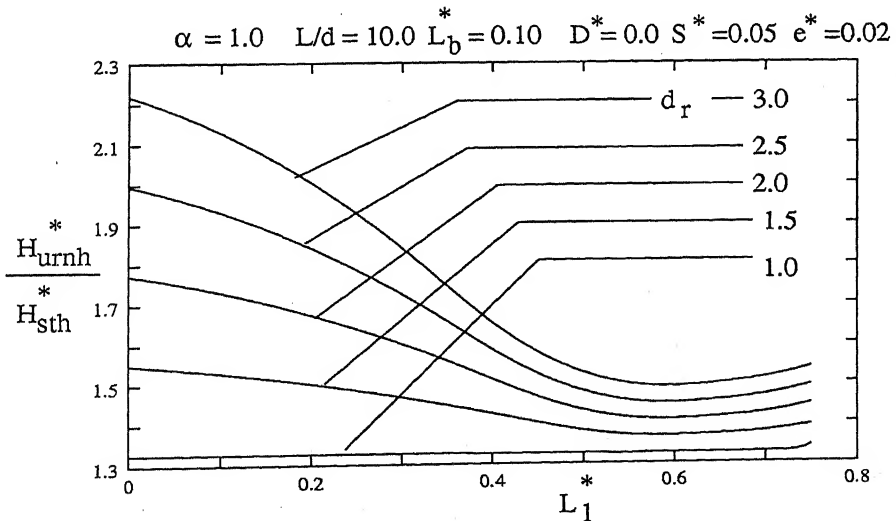


Figure 3.52: Effect of Diameter of Bulb on Ultimate Capacity for Free Head Double Bulb Under-reamed Pile in Non-homogeneous Soils - Modified Broms's Theory.

The ratio,  $H_{urnh}^*/H_{sth}^*$ , increases from 1.32 to 1.78 and 1.78 to 2.22, a 35% and 25% increase, with diameter ratio,  $d_r$ , increasing from 1.0 to 2.0 and 2.0 to 3.0 for  $L/d=10$ ,

$L_b^* = 0.1$ ,  $D^* = 0.0$ ,  $S^* = 0.05$ ,  $\alpha = 1.0$  and  $e^* = 0.02$  (Figure 3.52). Rate of change of the normalised ultimate lateral resistance increases with increase in diameter ratio. No significant increase in the ratio,  $H_{urnh}^*/H_{sth}^*$ , for diameter ratio,  $d_r > 0.5$  (Figure 3.52).

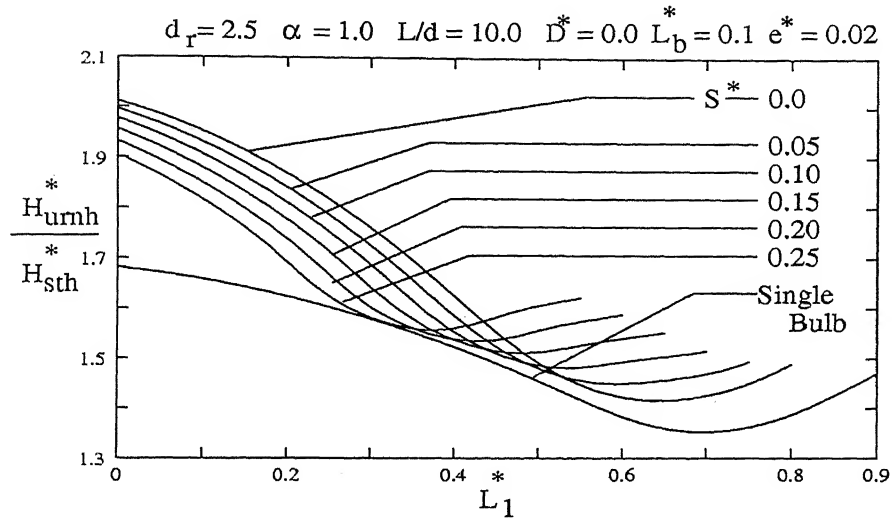


Figure 3.53: Effect of Spacing on Ultimate Capacity for Free Head Double Bulb Under-reamed Pile in Non-homogeneous Soils - Modified Broms's Theory.

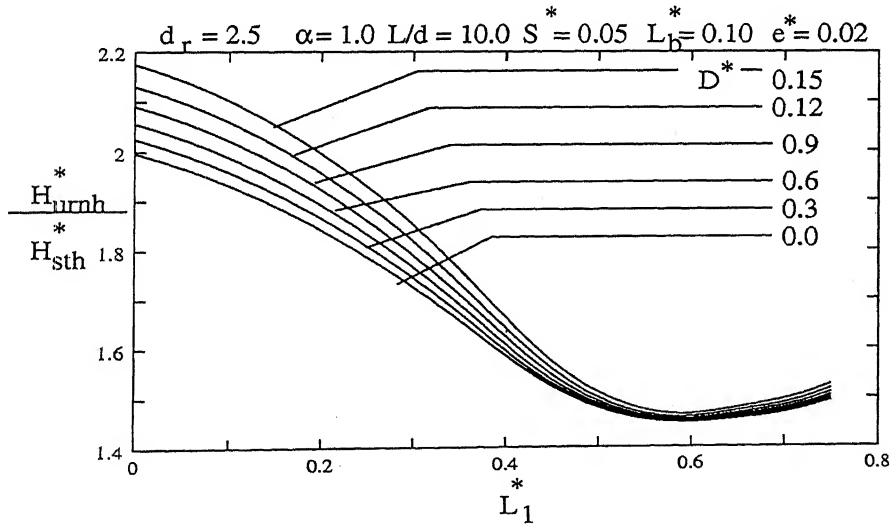


Figure 3.54: Effect of  $D^*$  on Ultimate Capacity for Free Head Double Bulb Under-reamed Pile in Non-homogeneous Soils - Modified Broms's Theory.

The normalised ultimate lateral resistance for single and double bulb, with zero spacing, under-reamed piles are 1.68 and 2.02, a 20% increase, for  $d_r = 2.5$ ,  $\alpha = 1.0$ ,  $L/d=10$ ,  $D^* = 0.0$ ,  $L_b^* = 0.1$  and  $e^* = 0.02$  (Figure 3.53). The ratio,  $H_{urnh}^*/H_{sth}^*$ , decreases with increase in spacing between the bulbs. No increase in the ratio,  $H_{urnh}^*/H_{sth}^*$ , occurs for the provision of second bulb with depth range of  $0.4L$  or below, for  $d_r = 2.5$ ,  $\alpha = 1.0$ ,

$L/d=10$ ,  $D^* = 0.0$ ,  $L_b^* = 0.1$  and  $e^* = 0.02$  (Figure 3.53).

### 3.3.3 Rigid Fixed Head Short Single Bulb Under-reamed Pile

The mode of failure and corresponding distribution of soil reaction of rigid fixed head under-reamed pile in non-homogeneous soils moving laterally as a rigid body is shown in figure 3.55.

#### 3.3.3.1 Analysis Based on Broms's Theory

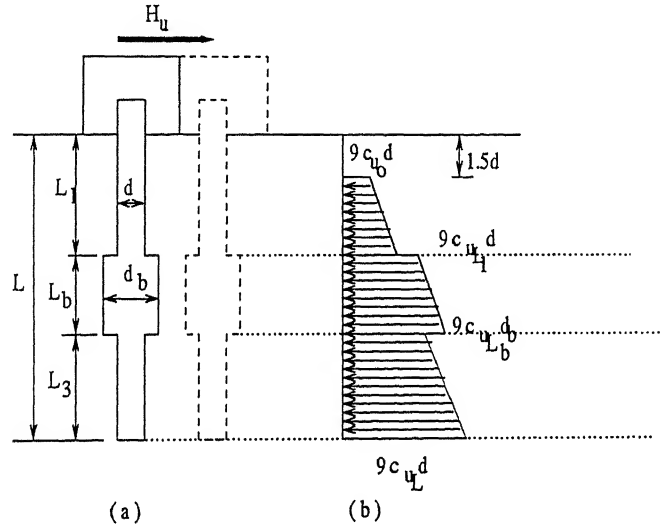


Figure 3.55: Failure Mode of Short Fixed Head Under-reamed Pile in Non-homogeneous Soils (a) Deflection and (b) Forces along the Pile Length.

From force and moment equilibrium equations are

$$H_u^* = \frac{H_u}{c_{u0} d L} = (9/2)[(R_{c1} + 1)(L_1^* - D^*) + d_r \{L_b^*(R_{c1} + R_{cb})\} + L_3^*(R_{cb} + R_{cL})] \quad (3.43)$$

and

$$M_y^* = \frac{M_y}{c_{u0} d L^2} = (9/6)[2L_1^{*2} - D^{*2} - L_1^* D^* + R_{c1}(L_1^{*2} + D^* L_1^* - 2D^{*2}) + d_r \{R_{c1}(2L_b^{*2} + 3L_1^* L_b^*) + R_{cb}(L_b^{*2} + 3L_1^* L_b^*)\} + R_{cb}\{2L_3^{*2} + 3L_3^*(L_1^* + L_b^*)\} + R_{cL}(L_3^{*2} + 3L_1^* L_3^* + 3L_b^* L_3^*)] \quad (3.44)$$

### 3.3.3.2 Results and Discussion

Estimated ultimate lateral resistances of the short rigid fixed head single bulb under-reamed piles in non-homogeneous soils are presented figure 3.56 through 3.58. The ultimate lateral resistance increases with increase in both the length and the diameter of the bulb and the non-homogeneity factor of the soil. From figures 3.25 and 3.56, it is observed that the ultimate lateral capacity,  $H_u/c_u d^2$ , is 100 and 140 in homogeneous and non-homogeneous soils respectively for diameter ratio,  $d_r = 2.5$ , and non-homogeneity factor,  $\alpha = 1.0$ , a 40% increase, in case of short fixed head pile.

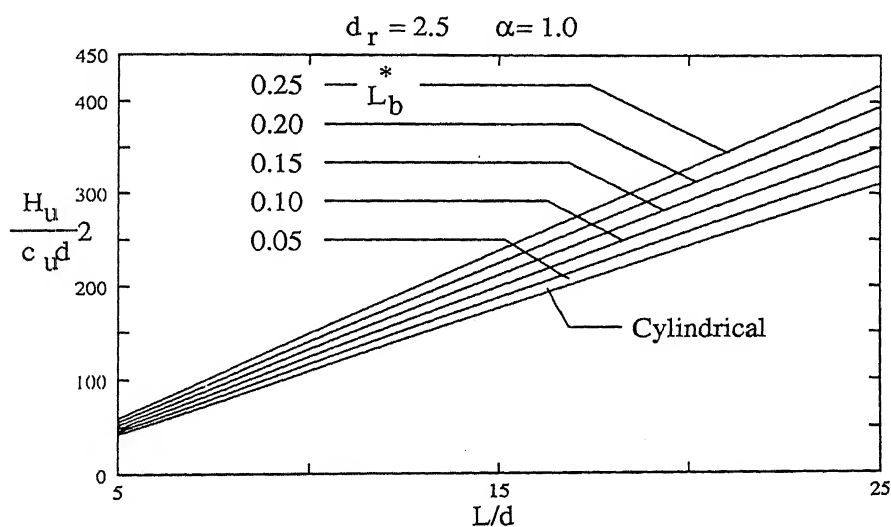


Figure 3.56: Effect of Length of Bulb on Ultimate Capacity for Fixed Head Short Single Bulb Under-reamed Pile in Non-homogeneous Soils-Broms's Approach.

With increase in the length of bulb, significant increase in the ultimate lateral capacity is obtained for larger  $L/d$  ratio. Similarly for the length of the bulb,  $L_b^* = 0.15$ , and at diameter ratio,  $d_r = 2.0$ , the ultimate lateral resistance in homogeneous and non-homogeneous soils are 36 and 50 respectively (Figures 3.26 and 3.57).

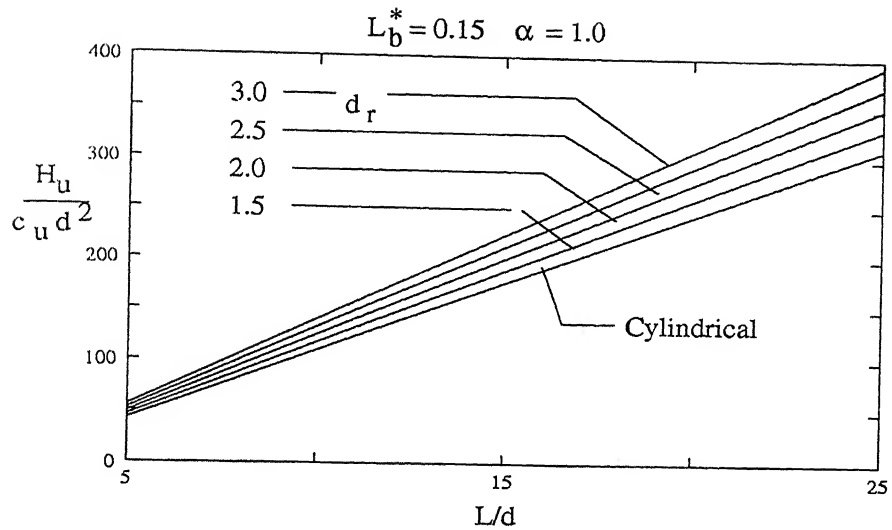


Figure 3.57: Effect of Diameter of Bulb on Ultimate Capacity for Fixed Head Short Single Bulb Under-reamed Pile in Non-homogeneous Soils-Broms's Approach.

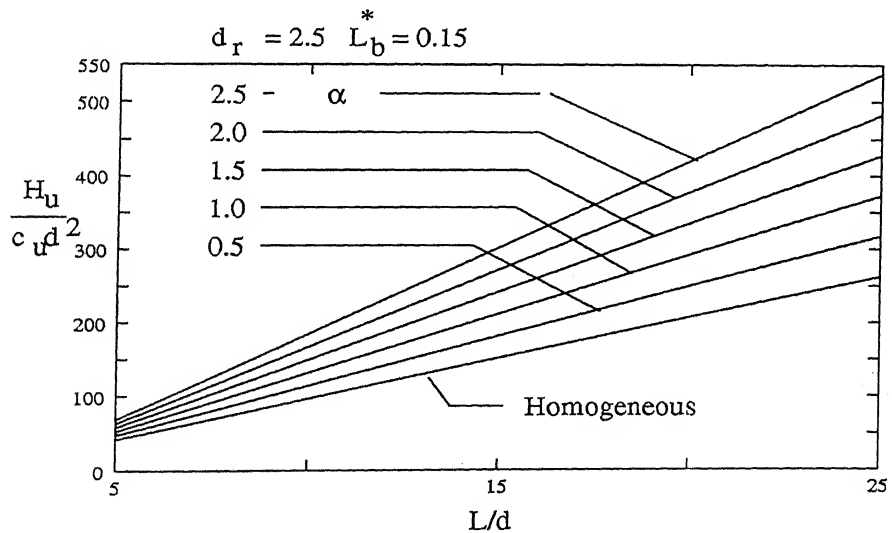


Figure 3.58: Effect of  $\alpha$  on Ultimate Capacity for Fixed Head Short Single Bulb Under-reamed Pile in Non-homogeneous Soils - Broms's Approach.



### 3.3.4 Rigid Fixed Head Intermediate Length Single Bulb Under-reamed Pile

#### 3.3.4.1 Analysis Based on Broms's Theory

In the analysis of fixed head intermediate length pile with single bulb, three possible locations of point of rotation are considered: (1) above, (2) within and (3) below the bulb. Kinematics and distribution of forces for the case of depth of point of rotation lying within the bulb is shown in figure 3.59.

##### a. Point of Rotation Above the Bulb:

$$H_u^* = \frac{H_u}{c_{u0} d L} = (9/2)[h^* \{2R_{ch} + 1 + R_{c1}\} + (R_{ch} + 1)D^* - \{d_r L_b^* (R_{cb} + R_{c1})\} + L_3^* (R_{cb} + R_{cL}) + L_1^* (R_{ch} + R_{c1})] \quad (3.45)$$

and

$$h^{*2} [4R_{ch} + R_{c1} + 1] + h^* [R_{c1} L_1^* - R_{ch} (L_1^* + D^*) + D^*] - d_r [R_{cb} (2L_b^{*2} + 3L_1^* L_b^*) + R_{c1} (3L_1^* L_b^* + L_b^{*2})] - R_{c1} (2L_b^{*2}) - R_{cb} \{3L_3^* (L_1^* + L_b^*) + L_3^{*2}\} - R_{ch} (L_1^{*2} + D^{*2}) - R_{cL} \{3L_3^* (L_b^* + L_1^*) + 2L_3^{*2}\} - 2D^{*2} = M_y^* \quad (3.46)$$

##### b. Point of Rotation Within the Bulb:

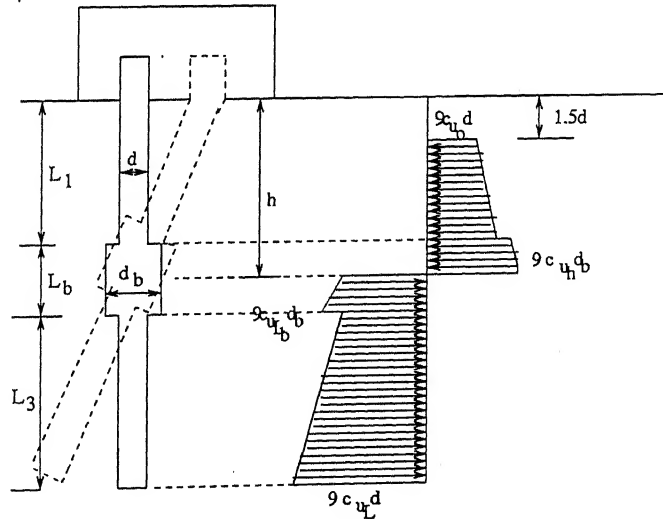


Figure 3.59: Failure Mode of Fixed Head Intermediate Length Under-reamed Pile in Non-homogeneous Soils.

$$H_u^* = \frac{H_u}{c_{u0} dL} = (9/2)[h^*\{d_r(2R_{ch} + R_{c1} + R_{cb}) + R_{c1}(L_1^* - D^* - L_1^* d_r) + L_1^* - D^* - R_{cb}\{d_r(L_1^* + L_b^*) + L_3^*\} - R_{ch}\{d_r(L_b^* + 2L_1^*)\} + R_{cL}L_3^*] \quad (3.47)$$

and

$$h^{*2}[d_r\{4R_{ch} + R_{cb} + R_{c1}\}] + h^*[d_r\{R_{cb}(L_1^* + L_b^*) + (R_{c1}L_1^*) - R_{ch}(L_b^* + 2L_1^*)\}] - d_r[2R_{c1}L_1^{*2} + R_{ch}(L_b^{*2} + 2L_1^*L_b^* + 2L_1^{*2}) + R_{cb}\{2(L_1^* + L_b^*)^2\}] + R_{c1}(2L_1^{*2} - L_1^*D^* - D^{*2}) - R_{cL}\{3L_3^*(L_1^* + L_b^*) + 2L_3^{*2}\} - R_{cb}\{L_3^{*2} + 3L_3^*(L_1^* + L_b^*)\} + L_1^{*2} + L_1^*D^* - 2D^{*2} = M_y^* \quad (3.48)$$

### c. Point of Rotation Below the Bulb:

$$H_u^* = \frac{H_u}{c_{u0} dL} = (9/2)[h^*\{2R_{ch} + R_{cb} + R_{cL}\} + d_r\{R_{c1}(L_1^* - D^*) + L_b^*(R_{c1} + R_{cb}) - R_{ch}(L_1^* + L_b^* + 1) - R_{cb}(L_1^* + L_b^*) - R_{cL} + L_1^* - D^*\}] \quad (3.49)$$

and

$$h^{*2}[4R_{ch} + R_{cb} + R_{cL}] + h^*[(R_{cb} - R_{ch})(L_1^* + L_b^*) + R_{cL} - R_{ch}] + d_r[R_{c1}(3L_1^*L_b^* + L_b^{*2}) + R_{cb}(2L_b^{*2} + 3L_1^*L_b^*)] + R_{c1}(2L_1^{*2} - D^{*2} + L_1^*D^*) - (L_1^* + L_b^*)^2 (2R_{cb} + R_{ch}) + R_{ch} - 2R_{cL} + L_1^{*2} + L_1^*D^* - 2D^{*2} = M_y^* \quad (3.50)$$

### 3.3.4.2 Results and Discussion

Normalised ultimate lateral resistance for fixed head intermediate length under-reamed pile in non-homogeneous soils is estimated by Broms's and modified Broms's approaches and presented from figures 3.60 through 3.65.

The normalised ultimate lateral resistance increases with increase in length of the bulb. For the length of the bulb increasing from 0.1 to 0.2 and 0.2 to 0.3, the normalised ultimate lateral resistance increases from 1.36 to 1.58 and 1.58 to 1.78, a 16% and 13% increase, for  $d_r = 2.5$ ,  $L/d=10$ ,  $M_y^* = 200$  and  $\alpha = 1.0$  (Figure 3.60), whereas it is from 1.25 to 1.48 and 1.48 to 1.66 for homogeneous soil (Figure 3.30). No increase in the ratio,  $H_{urnh}^*/H_{sth}^*$ , with increase in length of the bulb,  $L_b^*$ , for depth of the bulb at or below  $0.5L$ . The rate of change of the ratio,  $H_{urnh}^*/H_{sth}^*$ , with respect to depth of the bulb increases with increase in length of the bulb,  $L_b^*$  (Figure 3.60).

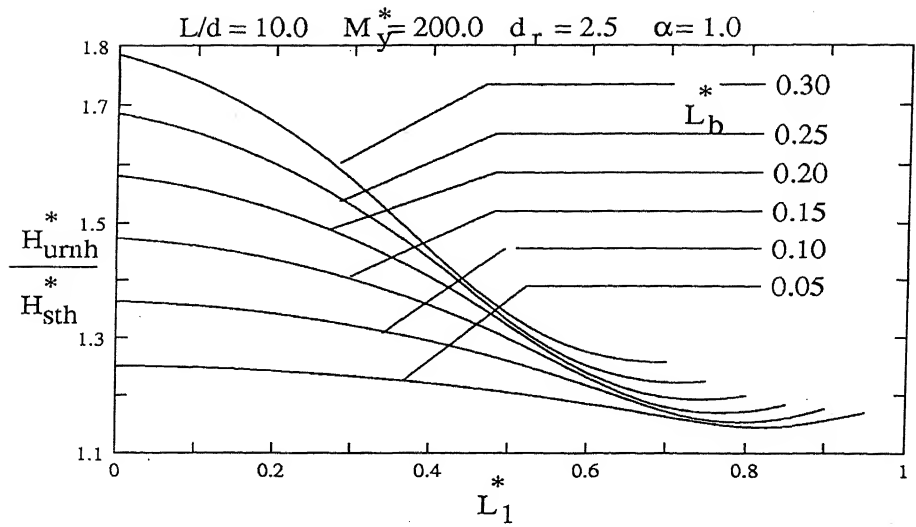


Figure 3.60: Effect of Length of Bulb on Ultimate Capacity for Fixed Head Intermediate Length Under-reamed Pile in Non-homogeneous Soils - Broms's Approach.

For diameter ratio,  $d_r$ , increasing from 1.0 to 2.0 and 2.0 to 3.0, normalised ultimate lateral resistance increases from 1.14 to 1.44 and 1.44 to 1.72, a 26% and 19% increase, for  $L_b^* = 0.2$ ,  $L/d=10$ ,  $M_y^* = 200$  and  $\alpha = 1.0$  (Figure 3.61). Percentage increase in the ratio,  $H_{urnh}^*/H_{sth}^*$ , decreases with increase in diameter ratio,  $d_r$ . No significant increase in the ratio,  $H_{urnh}^*/H_{sth}^*$ , with increase in the diameter ratio,  $d_r$ , for the depth of bulb,  $L_1^* > 0.6$ .

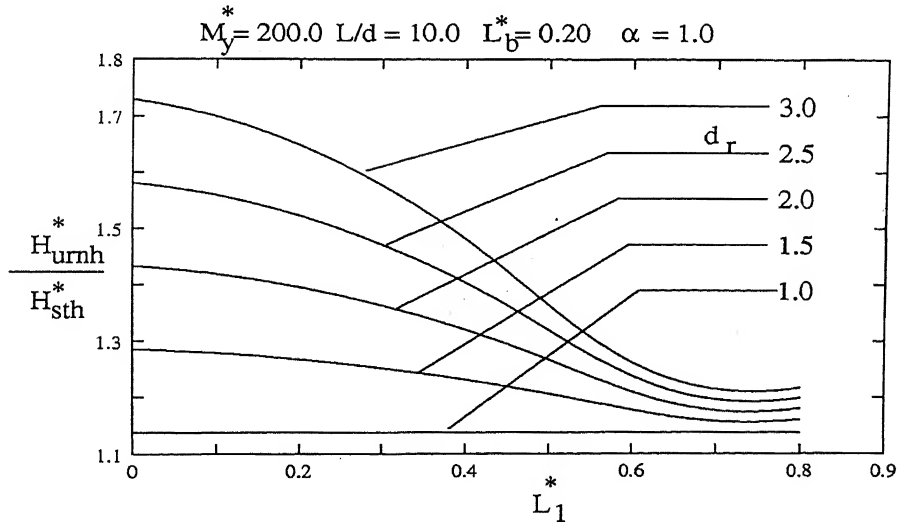


Figure 3.61: Effect of Diameter of Bulb on Ultimate Capacity for Fixed Head Intermediate Length Under-reamed Pile in Non-homogeneous Soils - Broms's Approach.

For the non-homogeneity factor,  $\alpha$ , increasing from 0.0 to 1.0 and 1.0 to 2.0, for  $L/d=10$ ,  $L_b^* = 0.2$ ,  $M_y^* = 200$  and  $d_r = 2.5$ , the normalised ultimate lateral resistance

increases from 1.48 to 1.58 and 1.58 to 1.7, a 7% and 8% increase (Figure 3.62). For larger values of non-homogeneity factor,  $\alpha > 0.2$ , the normalised ultimate lateral resistance increases slightly upto the depth of the bulb,  $L_1^* = 0.2$  and decreases at a faster rate below this depth (Figure 3.62). The percentage increase in the ratio,  $H_{urnh}^*/H_{sth}^*$ , is almost uniform with increase in the non-homogeneity factor.

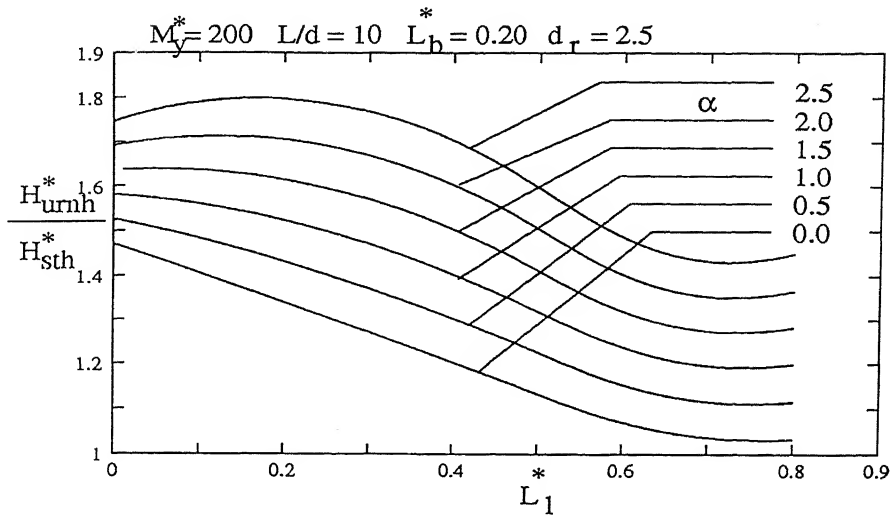


Figure 3.62: Effect of  $\alpha$  on Ultimate Capacity for Fixed Head Intermediate Length Under-reamed Pile in Non-homogeneous Soils - Broms's Approach.

The length and diameter of the bulb and the non-homogeneity factor of the soil have very similar effect on the ultimate lateral capacity obtained by modified Broms's approach.

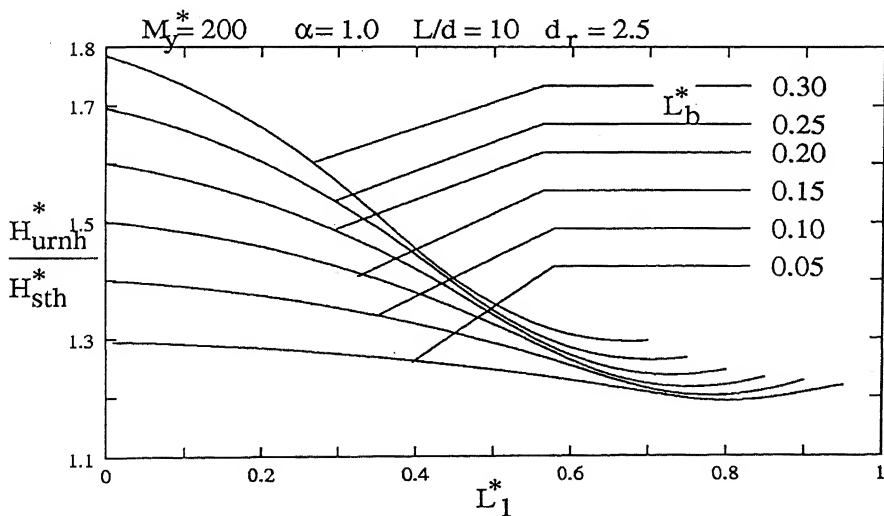


Figure 3.63: Effect of Length of Bulb on Ultimate Capacity for Fixed Head Intermediate Length Under-reamed Pile in Non-homogeneous Soils - Modified Broms's Theory.

For the length of the bulb,  $L_b^*$ , increasing from 0.1 to 0.2 and 0.2 to 0.3, normalised ultimate lateral resistance increases from 1.4 to 1.6 and 1.6 to 1.79, 14% and 12% increase, for  $d_r = 2.5$ ,  $L/d=10$ ,  $M_y^* = 200$  and  $\alpha = 1.0$  (Figure 3.63). The ratio,  $H_{urnh}^*/H_{sth}^*$ , increases from 1.18 to 1.46 and 1.46 to 1.74, a 24% and 19% increase, with diameter ratio,  $d_r$ , increasing from 1.0 to 2.0 and 2.0 to 3.0, for  $L/d=10$ ,  $L_b^* = 0.2$ ,  $M_y^* = 200$  and  $\alpha = 1.0$  (Figure 3.64). For the non-homogeneity factor,  $\alpha$ , increasing from 0.0 to 1.0 and 1.0 to 2.0, a 16% and 14% increase in normalised ultimate lateral resistance, for  $L/d=10$ ,  $L_b^* = 0.2$ ,  $d_r = 2.5$  and  $M_y^* = 200$  (Figure 3.65).

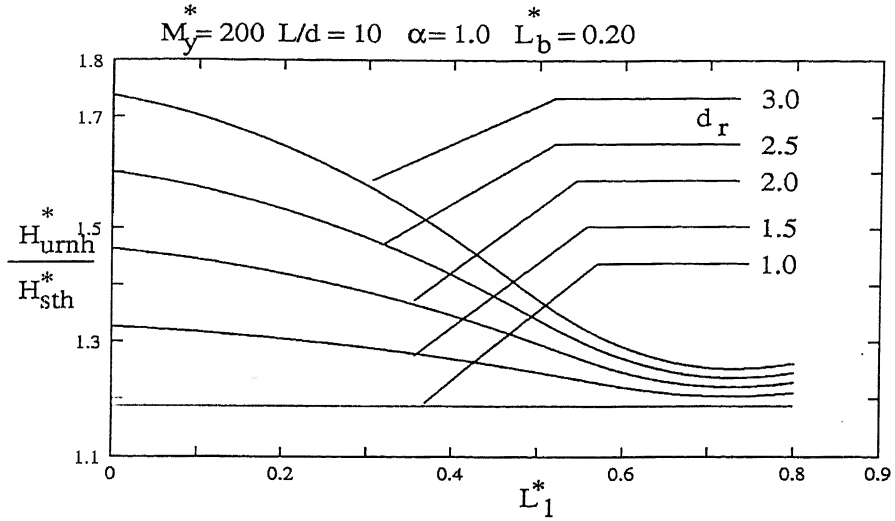


Figure 3.64: Effect of Diameter of Bulb on Ultimate Capacity for Fixed Head Intermediate Length Under-reamed Pile in Non-homogeneous Soils - Modified Broms's Theory.

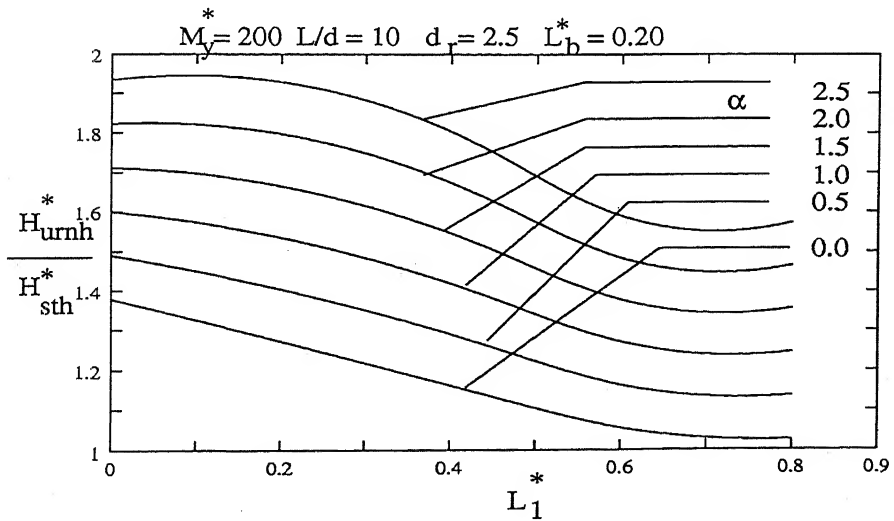


Figure 3.65: Effect of  $\alpha$  on Ultimate Capacity for Fixed Head Intermediate Length Under-reamed Pile in Non-homogeneous Soils - Modified Broms's Theory.

# Normalised Ultimate Capacities of Cylindrical Pile

Normalised ultimate capacity,  $H_u^* = H_u/c_u dL$ , of the cylindrical pile is presented with respect to the  $L/d$  ratio, for homogeneous and non-homogeneous soils (Figures 3.66 and 3.67 ) based on Broms's theory.

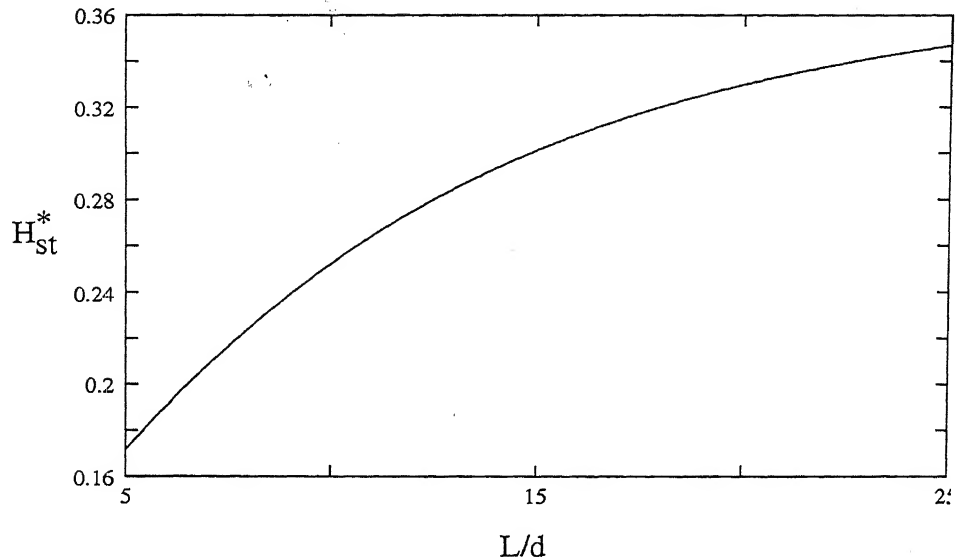


Figure 3.66: Normalised Ultimate Lateral Capacity of Cylindrical Pile for Homogeneous Soils-Broms's Theory.

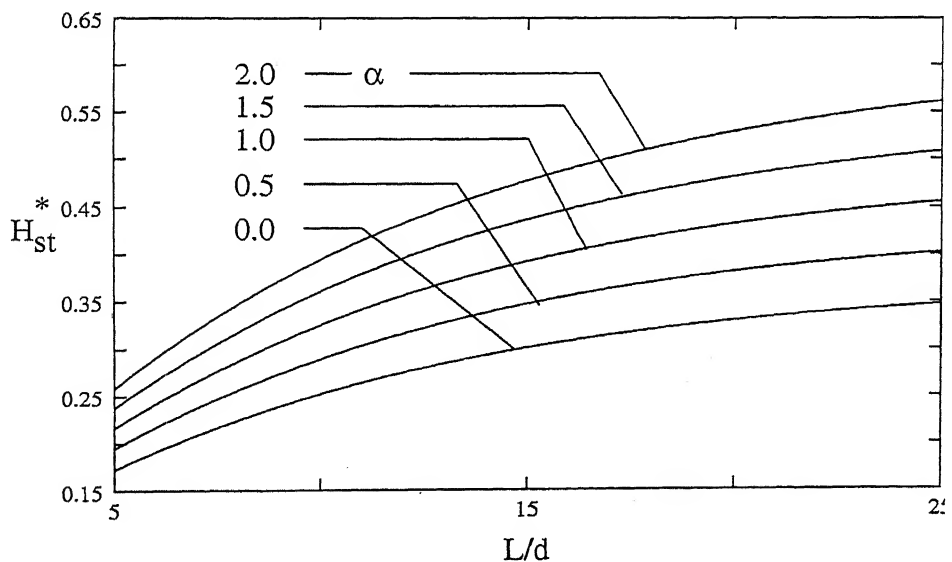


Figure 3.67: Normalised Ultimate Lateral Capacity of Cylindrical Pile in Non-homogeneous Soils-Broms's Theory.

# Chapter 4

## Deformation at Working Loads

### 4.1 General

In designing pile foundations to resist lateral loads, the criterion for design in majority of the cases is not the ultimate lateral capacity of the piles, but the permissible/allowable deflection of the piles. The allowable deflection may be relatively large for structures like retaining walls, but only small movements can be tolerated in structures such as bridge abutments and foundations of tall structures. Design practice in the past has frequently made use of empirical information for pile design; for example, that provided by McNulty (1956) from full-scale lateral load tests. In recent years, theoretical approaches for predicting lateral movements have been developed. One may broadly classify these approaches into three categories: (a) Subgrade reaction approach which ignores the continuous nature of soil and simulates its lateral resistance against the pile through a set of independent, linear or non-linear distributed springs (Matlock & Reese, 1960; Matlock, 1970; etc), (b) Elastic continuum approach which involve integration of Mindlin (1936) equations for displacements due to a subsurface point load acting within a half space (Poulos, 1971 a, 1971 b; Banerjee & Davies, 1978), and (c) Finite-element formulations which invariably discretise both the pile and the surrounding soil into axisymmetric elements and rigorously enforce the boundary conditions at the pile-soil interface (Randolph, 1981). In spite of the disadvantages of the subgrade reaction approach, this model provides a relatively simple means of analysis.

At working loads, the deflections of a single pile or of a pile group can be considered to increase approximately linearly with the applied load. Part of lateral deflection is caused by the deformation of the soil at the time of loading and part by consolidation and creep subsequent to loading. The deformation caused by consolidation and creep increase with time.

Some simplifications are now considered in the description of the deformation of the soil medium, in order to avoid large number of numerical equations that would result from

a complete three dimensional modeling of the problem. The main simplification is that the horizontal loading of the soil at the soil-pile interface will produce mainly horizontal displacements. The subgrade modulus of the soil is considered to be constant with depth in case of homogeneous and to increase linearly with depth in non-homogeneous soils.

The conventional approach to analyse the response of a vertical pile to applied lateral loads and moments, has been to consider the soil to be a Winkler type of foundation. Winkler (1867) assumed the reaction of the subsoil to depend solely on the settlement/displacement of this point and to be independent of the settlements of neighboring points. Additionally Winkler assumed the reaction of the subsoil to be proportional to settlement. The two assumptions together represent an arrangement of independent elastic springs. The governing differential equation (Hetenyi 1946), for the pile shown in figure 4.1 can be written as

$$EI \frac{d^4 y}{dx^4} = p - q = p - ky \quad (4.1)$$

where  $E$  is the elastic modulus of the pile,  $I$  its moment of inertia,  $y$  the deflection of the pile along its length,  $x$ ,  $p$  the distributed load applied along the length of the pile,  $q$  the soil response, and  $k=k_h \cdot d$ ,  $k_h$ -denotes the modulus of subgrade reaction of the soil and  $d$ -the diameter of the pile. Usually piles are loaded only at the top and  $p=0$ .

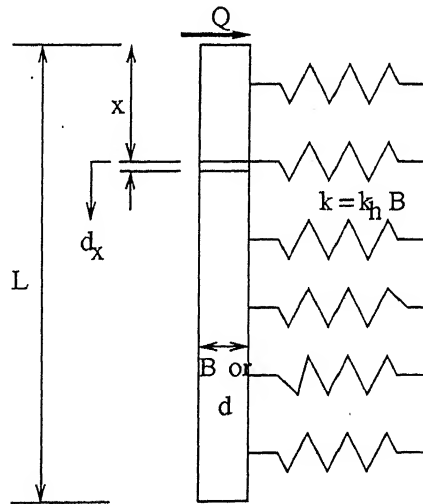


Figure 4.1: Pile in Winkler Foundation.

The analysis of pile behavior using the subgrade reaction approach requires a knowledge of the variation of  $k_h$  along the length of the pile. A comprehensive discussion on  $k_h$ , the modulus of subgrade reaction, is given by Terzaghi (1955). The most common assumptions are that the coefficient of subgrade reaction increases linearly with depth for a normally consolidated clay or remains constant with depth for an overconsolidated clay.



Solutions of Eq. 4.1 for simple boundary conditions have been given by Chang (1937) and Hetenyi (1946), the former treating the pile as an infinite beam. Solutions in the form of infinite series have been obtained for Eq. 4.1 with  $k_h$  varying linearly or parabolically with depth (Reddy & Valsangkar 1966; Snitko 1968). Finite difference methods appear to be more commonly used than analytical methods. Results of these investigations obtain deflections, moments and shear force along the length of the pile, as long as the soil behaves as a linear elastic material. The relation between the load and the deflection of the pile at top would be linear, and is similar to the stress-strain relation of a soil in C-U test (Broms 1964). Under normal working loads, the deflection near the top of the pile would be sufficiently large to cause the pressures exerted by the soil to be outside the linear range. In such cases, use of secant modulus for  $k_h$ , and repeated application of the trial and error methods for solution of Eq. 4.1 have been recommended (Davisson & Gill 1963).

Kubo (1965) suggested an approach, based on an experimental study. The pressure,  $q$ , due to soil, on unit width of the pile, is given as

$$q = n_h x^m y^n \quad (4.2)$$

where  $n_h$ ,  $m$ , and  $n$  are constants. The recommended values of  $m$  and  $n$  respectively are 1 and 0.5. Solution of Eq. 4.1 with  $q$  given by Eq. 4.2 is difficult, due to the nonlinear nature of the relation.

The form of the relation suggested by Kondner (1963) for cohesive soils (curve (a) of Fig. 4.2) is somewhat similar to the relation (Eq. 4.2). The curve is described by

$$q = \frac{y}{a + by} \quad (4.3)$$

where  $q$  is the stress at any displacement  $y$ , and  $a$  and  $b$  are constants, with  $a=1/k_h$  and  $b=1/q_{max}$ .

A simple approximation to curve (a) of fig. 4.2 is a bi-linear relation (curve b) which is described by

$$q = k_h y \quad \text{if} \quad y \leq y_o \quad \text{or} \quad q < q_{max} \quad (4.4)$$

and

$$q = q_{max} \quad \text{if} \quad y > y_o \quad (4.5)$$

where  $q_{max}$  is the yield stress and  $y_o = q_{max}/k_h$ . Eqs. 4.4 and 4.5 describe an elasto-plastic material, i.e., a material that is elastic upto a stress level,  $q_{max}$ , and flows plastically once the stress level reaches  $q_{max}$ .

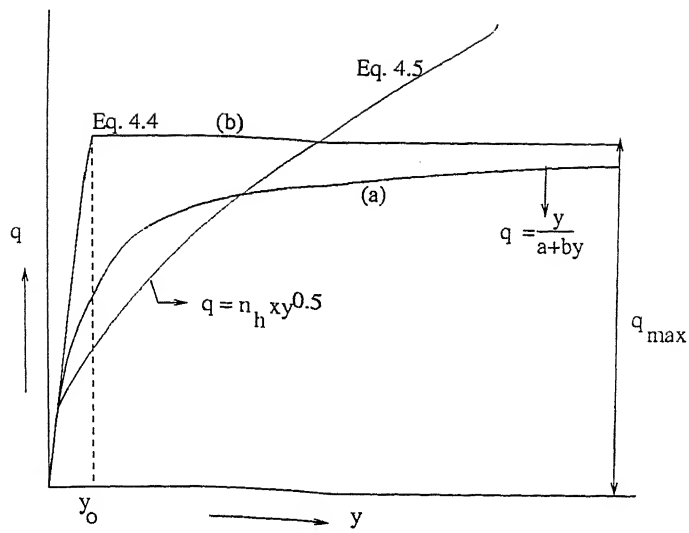


Figure 4.2: Stress - Displacement Relation

Vesic (1961) has found that the coefficient of subgrade reaction,  $k_h$ , can be related to the modulus of elasticity,  $E_s$ , and Poisson's ratio,  $\nu_s$ , of the soil and the stiffness of the pile,  $E_p I_p$ , as

$$k_h = \frac{0.65}{d} \cdot \left( \frac{E_s d^4}{E_p I_p} \right)^{\frac{1}{12}} \cdot \frac{E_s}{(1 - \nu_s^2)}$$

## 4.2 Homogeneous Soils

In the following analysis, it is assumed that the coefficient of subgrade reaction is constant with the depth.

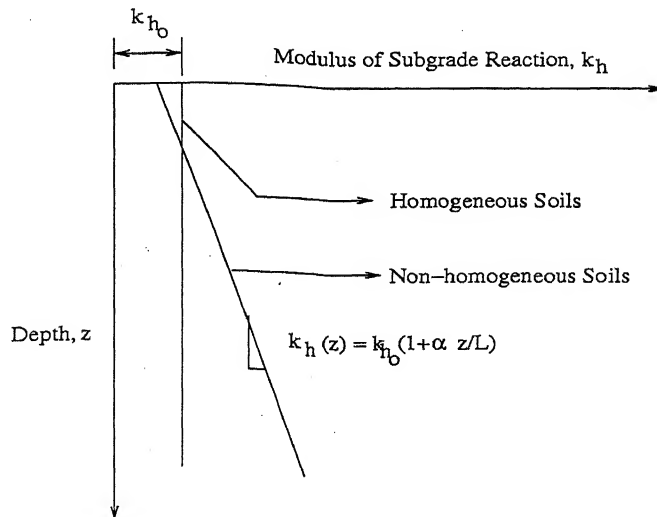


Figure 4.3: Modulus of Subgrade Reaction in Homogeneous and Non-homogeneous Soils.

## 4.2.1 Rigid Free Head Single Bulb Under-reamed Pile

### 4.2.1.1 Analysis

Using Winkler's subgrade reaction approach, deformation of single bulb under-reamed pile is analysed by considering the three possible cases for the point of rotation of the pile: (a) above; (b) within and (c) below the bulb as in case of ultimate capacity. Soil reaction along the length of the pile for the case of point of rotation within the bulb is shown in figure 4.4. In this analysis, expressions for force and moment equilibrium are identical for the three cases of point of rotation, because of rigid body rotation of the pile.

The diameter and length of the pile are  $d$  and  $L$  respectively. The bulb diameter is  $d_b$ . Depth of the top of bulb from the ground surface, length of the bulb and length of pile from the bottom of bulb to tip of the pile are  $L_1$ ,  $L_b$  and  $L_3$  respectively. The pile rotates as a rigid body about a point,  $O$ , at a depth,  $h$ , from the ground surface due to an applied load,  $H_u$ , with an eccentricity,  $e$ , above the ground surface (Figure 4.4 a).

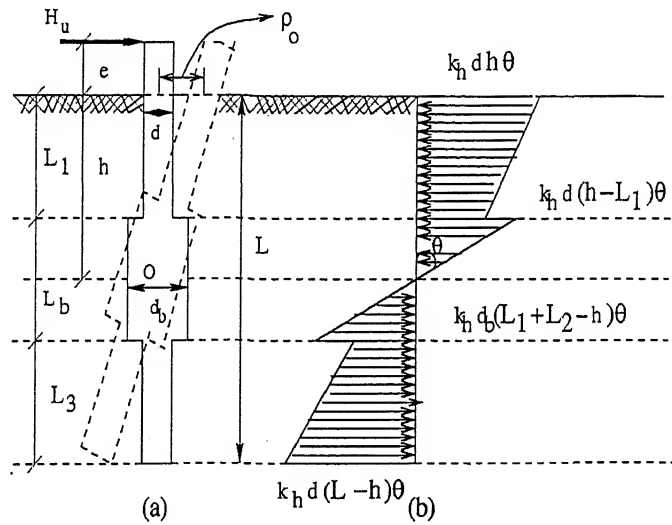


Figure 4.4: Definition Sketch (a) Kinematics of Under-reamed Pile and (b) Distribution of Forces along the Pile.

Normalised form of force equilibrium expression, in terms of the rotation coefficient,  $I_\theta$ , is

$$I_\theta = \frac{2H}{k_h d L^2 \theta} = h^* (2d_r L_b^* - 2L_b^* + 2) + L_b^{*2} + 2L_1^* L_b^* - 2d_r L_1^* L_b^* - d_r L_b^{*2} - 1 \quad (4.6)$$

$$\theta = \left( \frac{H}{k_h d L^2} \right) (I_\theta^*)$$

where  $I_{\theta}^* = \frac{2}{I_{\theta}}$

and the normalised depth of the point of rotation,  $h^*$ , from the moment equilibrium, is

$$h^* = \frac{C.d_r - D}{A.d_r - B} \quad (4.7)$$

where  $A = 3L_b^{*2} + 6L_1^*L_b^* + 6e^*L_b^*$ ;

$B = 3L_b^{*2} + 6L_1^*L_b^* + 6e^*L_b^* - 6e^* - 3$ ;

$C = 6L_1^*L_b^{*2} + 2L_b^{*3} + 3e^*L_b^{*2} + 6L_1^{*2}L_b^* + 6e^*L_1^*L_b^*$ ; and

$D = 6L_1^{*2}L_b^* + 2L_b^{*3} + 6L_1^*L_b^{*2} + 6e^*L_1^*L_b^* + 3e^*L_b^{*2} - 3e^* - 2$ .

$$\rho_{\theta}^* = I_{\theta}^*.h^* \quad \text{and} \quad \rho = \left(\frac{H}{k_h d L^2}\right)(\rho_{\theta}^*)$$

Rotation,  $\theta$ , of the pile is calculated by solving the above the two equations and the deformation of the top of the pile,  $\rho$ , is  $h.\theta$ .

#### 4.2.1.2 Results and Discussion

Deformations of rigid free head single bulb under-reamed pile in homogeneous soil are estimated by using Winkler's subgrade reaction approach. Deformation of an under-reamed pile,  $\rho_{ur}^*$ , is normalised with respect to that of the straight shafted pile,  $\rho_{st}^*$ . The normalised deformation coefficient,  $\rho_{ur}^*/\rho_{st}^*$ , of an under-reamed pile increases with increase in depth of bulb from the ground surface upto a depth of  $(0.5 \text{ to } 0.7)L$  and decreases with further increase in the depth of bulb (Figure 4.5).

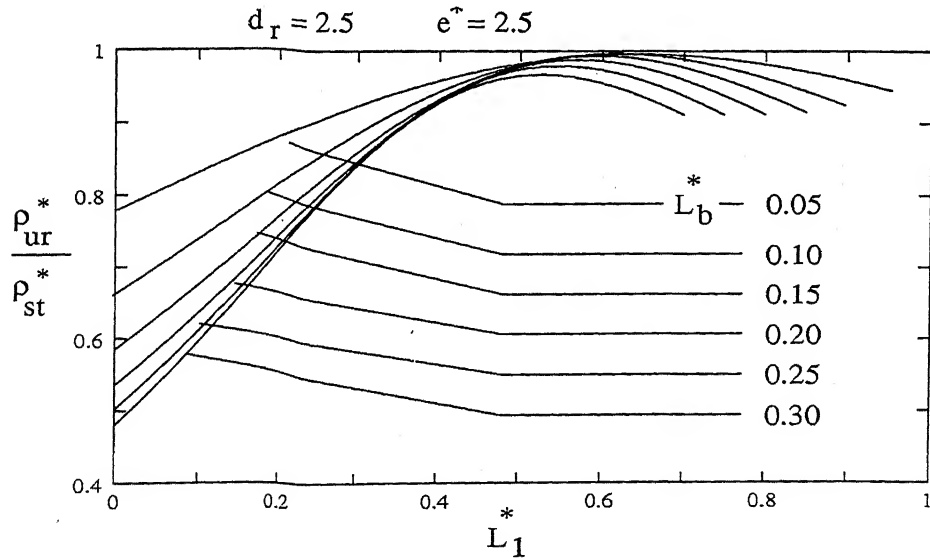


Figure 4.5: Effect of Length of Bulb on Normalised Deformation Coefficient for Rigid Free Head Single Bulb Under-reamed Pile in Homogeneous Soils.

The deformation of under-reamed pile is the same as that of the cylindrical pile for the depth of bulb,  $L_1^* = \frac{L_1}{L}$ , lying in the range of (0.5 to 0.7)L. The normalised deformation coefficient,  $\rho_{ur}^*/\rho_{st}^*$ , is 0.67 for  $L_b^* = 0.10$  and 0.54 for  $L_b^* = 0.20$  and for the bulb at ground surface, the diameter ratio,  $d_r = 2.5$  and  $e^* = 0.02$ . Deformation decreases by 19% for 100% increase in length of the bulb from 0.1 to 0.2 (Figure 4.5). Rate of change of the ratio,  $\rho_{ur}^*/\rho_{st}^*$ , with depth of the bulb, increases with increase in length of the bulb. No significant decrease in the deformation occurs with increase in length of bulb greater than 0.15 (Figure 4.5).

The ratio,  $\rho_{ur}^*/\rho_{st}^*$ , is 0.81 for  $d_r = 1.5$  and 0.52 for  $d_r = 3.0$  for the bulb at top and length of bulb,  $L_b^* = 0.15$  (Figure 4.6). A 36% decrease in deformation is obtained for doubling the diameter of the bulb from 0.15 to 0.30 (Figure 4.6). The percentage decrease in normalised deformation coefficient decreases with increase in the diameter ratio (Figure 4.6). Rate of change of the normalised deformation coefficient with depth of the bulb increases with increase in diameter ratio (Figure 4.6).

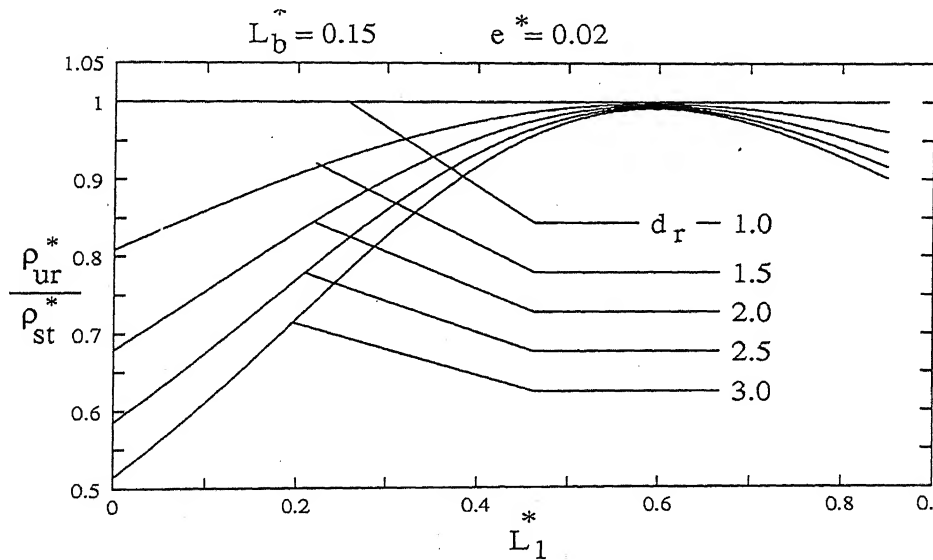


Figure 4.6: Effect of Diameter of Bulb on Normalised Deformation Coefficient for Rigid Free Head Single Bulb Under-reamed Pile in Homogeneous Soils.

The normalised deformation coefficient appears to be independent of eccentricity,  $e^*$ , varying from 0.01 to 0.05 for  $L_b^* = 0.15$  and  $d_r = 2.5$  (Figure 4.7).

## 4.2.2 Rigid Free Head Double Bulb Under-reamed Pile

### 4.2.2.1 Analysis

Deformation of double bulb under-reamed pile is analysed by considering five possible cases for the location of the point of rotation along the length of the pile. Soil reaction along the length of the pile for the case of point of rotation within the bulb is shown in

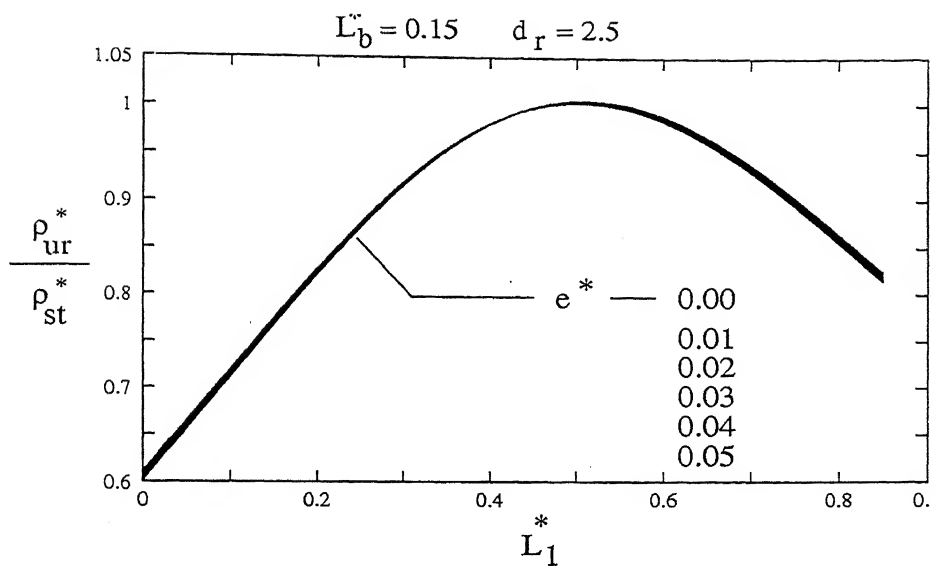


Figure 4.7: Effect of Eccentricity on Normalised Deformation Coefficient for Rigid Free Head Single Bulb Under-reamed Pile in Homogeneous Soils.

figure 4.8.

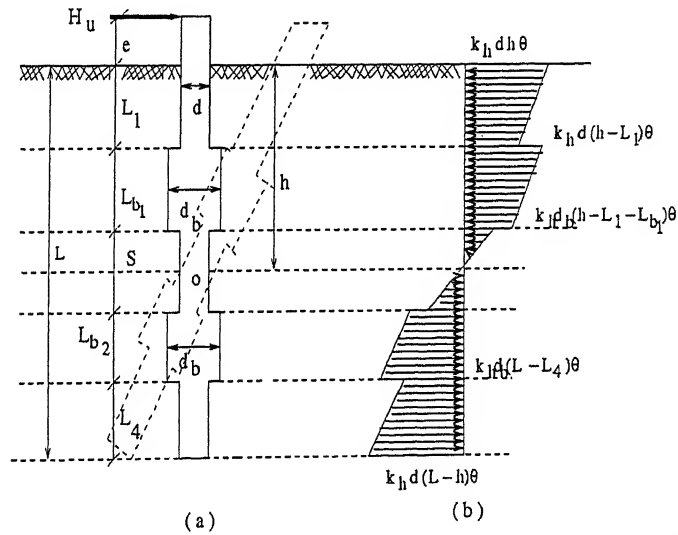


Figure 4.8: Definition Sketch for Double Bulb Under-reamed Pile in Homogeneous Soils  
(a) Kinematics and (b) Distribution of Forces.

Normalised force equilibrium expression, in terms of the rotation coefficient,  $I_\theta$ , is

$$I_\theta = \frac{2H}{K_h d L^2 \theta} = h^* [2L_1^* + 2S^* + 2L_4^* + d_r \{2L_{b1}^* + 2L_{b2}^*\}] - L_1^{*2} - S^{*2} - 2L_1^* S^* - 2L_{b1}^* S^* - 2L_1^* L_4^* - 2L_{b1}^* L_4^* - 2S^* L_4^* - 2L_{b2}^* L_4^* - L_4^{*2} - d_r \{2L_1^* L_{b1}^* + L_{b1}^{*2} + 2L_1^* L_{b2}^* + 2L_{b1}^* L_{b2}^* + 2S^* L_{b1}^* + L_{b2}^{*2}\} \quad (4.8)$$

$$\theta = \left( \frac{H}{k_h d L^2} \right) (I_\theta^*)$$

where  $I_\theta^* = \frac{2}{I_\theta}$

and the normalised depth of point of rotation,  $h^*$ , from the moment equilibrium, is

$$h^* = \frac{C.d_r + D}{A.d_r + B} \quad (4.9)$$

where

$$A = 3L_{b_1}^{*2} + 6L_1^* L_{b_1}^* + 6e^* L_{b_1}^* + 3L_{b_2}^{*2} + 6L_1^* L_{b_2}^* + 6S^* L_{b_2}^*$$

$$B = 3L_1^{*2} + 6e^* L_1^* + 6S^* L_1^* + 6S^* L_2^* + 3S^{*2} + 6e^* S^* + 3L_4^{*2} + 6L_{b_2}^* L_4^* + 6S^* L_4^* + 6L_{b_1}^* L_4^* + 6L_1^* L_4^* + 6e^* L_4^*$$

$$C = 2L_{b_1}^{*3} + 6L_1^* L_{b_1}^{*2} + 6L_1^{*2} L_{b_1}^* + 6e^* L_1^* L_{b_1}^* + 3e^* L_{b_1}^{*2} + 6L_1^* L_{b_2}^{*2} + 6L_{b_1}^* L_{b_2}^{*2} + 6S^* L_{b_2}^{*2} + 6L_1^{*2} L_{b_2}^* + 12L_1^* L_{b_1}^* L_{b_2}^* + 12L_1^* S^* L_{b_2}^* + 6L_{b_1}^{*2} L_{b_2}^* + 12L_{b_1}^* S^* L_{b_2}^* + 6S^{*2} L_{b_2}^* + 6e^* L_1^* L_{b_2}^* + 6e^* L_{b_1}^* L_{b_2}^* + 6e^* S^* L_{b_2}^* + 2L_{b_2}^{*3} + 3e^* L_{b_2}^{*2}$$

$$D = 2L_1^{*3} + 3e^* L_1^{*2} + 6L_1^* S^{*2} + 6L_1^{*2} S^* + 12L_1^* L_{b_1}^* S^* + 6L_{b_1}^* S^{*2} + 6L_{b_1}^{*2} S^* + 2S^{*3} + 3e^* S^{*2} + 6e^* L_1^* S^* + 6e^* L_{b_1}^* S^* + 6L_4^{*2} (L_1^* + L_{b_1}^* + S^* + L_{b_2}^*) + 12L_{b_1}^* L_{b_2}^* (L_1^* + L_4^*) + 12S^* L_{b_2}^* L_4^* + 6L_{b_2}^{*2} L_4^* + 12S^* L_1^* L_4^* + 12S^* L_{b_1}^* L_4^* + 6S^{*2} L_4^* + 12L_1^* L_{b_1}^* L_4^* + 6L_{b_1}^{*2} L_4^* + 6L_1^{*2} L_4^* + 6e^* L_1^* L_4^* + 6e^* L_{b_1}^* L_4^* + 6e^* S^* L_4^* + 6e^* L_{b_2}^* L_4^* + 2L_4^{*3} + 3e^* L_4^{*2}$$

$$\rho_\theta^* = I_\theta^* . h^* \quad \text{and} \quad \rho = \left( \frac{H}{k_h d L^2} \right) (\rho_\theta^*)$$

#### 4.2.2.2 Results and Discussion

For the double bulb under-reamed piles in homogeneous soils, the deformation is quantified and described in the form of normalised deformation coefficient,  $\rho_{ur}^* / \rho_{st}^*$ , as a function

of depth of the bulb,  $L_1^*$ , from the ground surface. Lengths and diameters of the two bulbs are considered to be the same. The ratio,  $\rho_{ur}^*/\rho_{st}^*$ , increases with increase in depth of the bulb upto a depth of  $(0.5 \text{ to } 0.7)L$  and decreases with further increase in depth of the bulb.

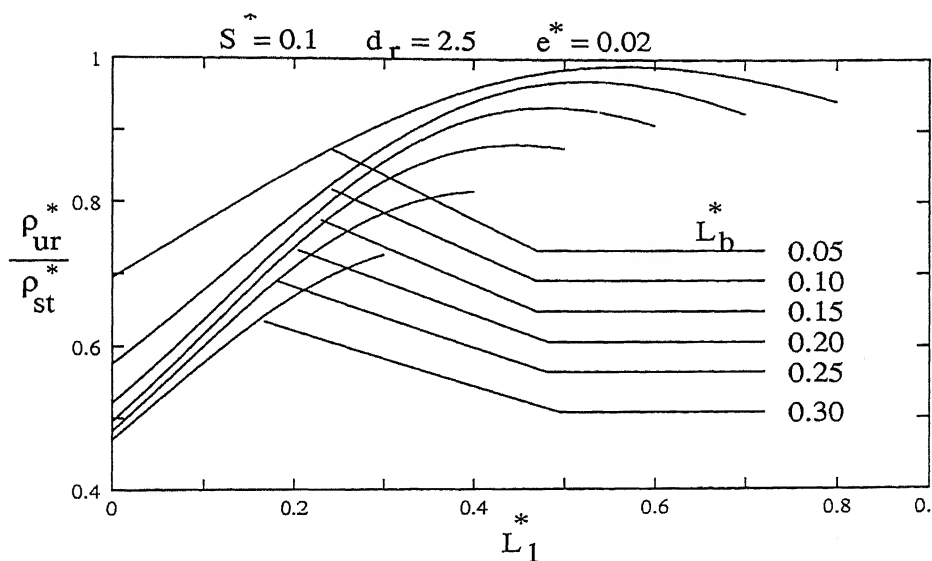


Figure 4.9: Effect of Length of Bulb on Normalised Deformation Coefficient for Rigid Free Head Double Bulb Under-reamed Pile in Homogeneous Soils.

Significant decrease in the normalised deformation coefficient occurs for the length of the bulb,  $L_b^*$ , increasing from 0.05 upto 0.15 for  $d_r = 2.5$ ,  $S^* = 0.1$  and  $e^* = 0.02$ . However no significant decrease in deformation occurs for further increase in length of the bulb (Figure 4.9). The normalised deformation coefficient is 0.58 and 0.50 for  $L_b^* = 0.10$  and 0.2 respectively for  $d_r = 2.5$ ,  $S^* = 0.1$  and  $e^* = 0.02$ . A 14% decrease in deformation occurs for doubling the length of the bulb from 0.1 to 0.2 (Figure 4.9). The percentage decrease in the ratio,  $\rho_{ur}^*/\rho_{st}^*$ , is less with increase in length of the bulb for bulb at the top, but is significant for bulb at bottom of the pile (Figure 4.9).

For the lengths of the bulbs,  $L_{b1}^* = L_{b2}^* = L_b^* = 0.1$ , with spacing,  $S^* = 0.1$  and  $e^* = 0.02$ , the normalised deformation coefficient is 0.80 and 0.51, for  $d_r = 1.5$  and 3.0 respectively, a 36% decrease in the deformation (Figure 4.10). The percentage decrease in the normalised deformation coefficient is significant for the bulb at top and bottom of the pile. No significant percentage decrease in deformation occurs for the bulb at  $(0.5 \text{ to } 0.7)L$  (Figure 4.10). The rate of change in the ratio,  $\rho_{ur}^*/\rho_{st}^*$ , with depth of the bulb,  $L_1^*$ , for  $L_b^* = 0.1$ ,  $S^* = 0.1$  and  $e^* = 0.02$  increases with increase in the diameter ratio (Figure 4.10).

The effect of spacing on the deformation of double bulb under-reamed pile in homogeneous soils is described in the figure 4.11. By providing one more bulb with zero spacing to the single bulb under-reamed pile, the normalised deformation coefficient for



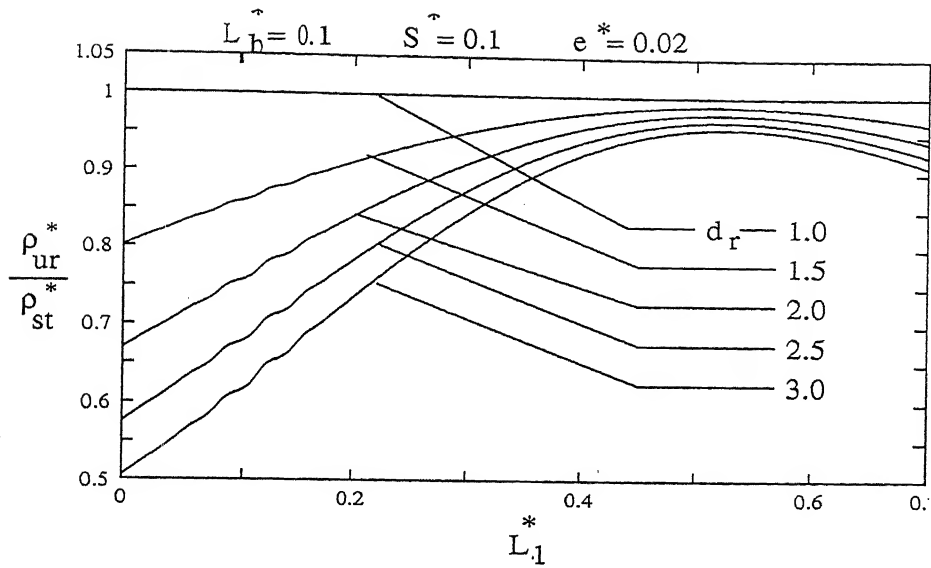


Figure 4.10: Effect of Diameter of Bulb on Normalised Deformation Coefficient for Rigid Free Head Double Bulb Under-reamed Pile in Homogeneous Soils.

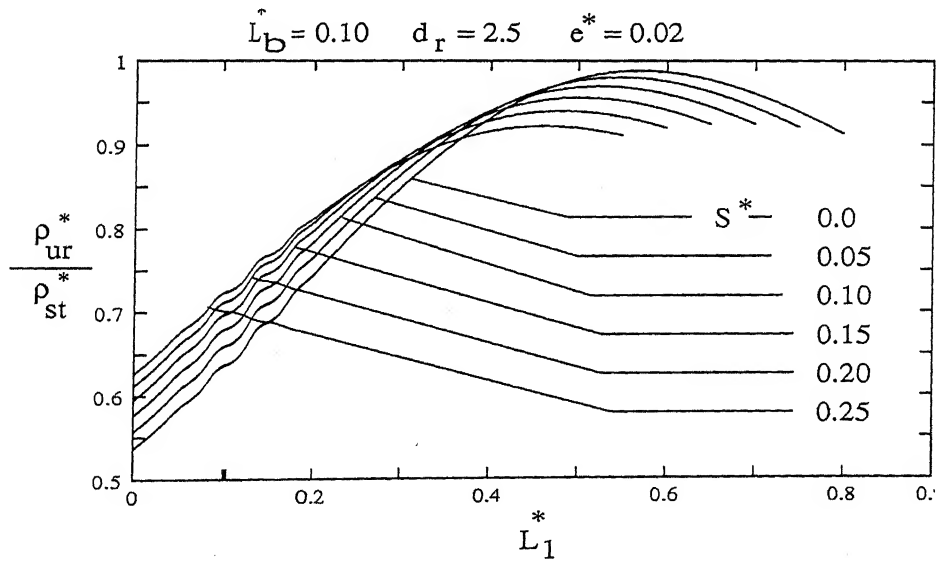


Figure 4.11: Effect of Spacing on Normalised Deformation Coefficient for Rigid Free Head Double Bulb Under-reamed Pile in Homogeneous Soils.

$d_r = 2.5$ ,  $L_b^* = 0.10$  and  $e^* = 0.02$  decreases from 0.67 to 0.48, a 28% decrease in the deformation (Figure 4.11). The rate of change in the ratio,  $\rho_{ur}^*/\rho_{st}^*$ , with depth of the bulb is nearly the same for different spacings in between the bulbs. The normalised deformation coefficient decreases with increase in the spacing for  $d_r = 2.5$ ,  $L_b^* = 0.10$  and  $e^* = 0.02$  (Figure 4.11).

### 4.3 Non-homogeneous Soils

In the analysis of non-homogeneous soils, coefficient of subgrade reaction is considered to increase linearly with depth. The coefficient of subgrade reaction at any depth ( $z$ ) of the soil,  $k_h(z) = k_{h0}(1 + \alpha z/L)$ , where  $\alpha$  is the rate of increase of the coefficient of subgrade reaction with depth and  $k_{h0}$  is the coefficient of subgrade reaction at the ground surface. The coefficient of subgrade reaction at depths  $L_1$ ,  $h$  and  $L$  are denoted as  $k_{hL_1}$ ,  $k_{hh}$  and  $k_{hL}$  respectively.

$$k_{hL_1} = k_{h0}(1 + \alpha \frac{L_1}{L}), k_{hh} = k_{h0}(1 + \alpha \frac{h}{L}), k_{hL_b} = k_{h0}(1 + \alpha \frac{L_1 + L_b}{L}) \text{ and } k_{hL} = k_{h0}(1 + \alpha \frac{L}{L})$$

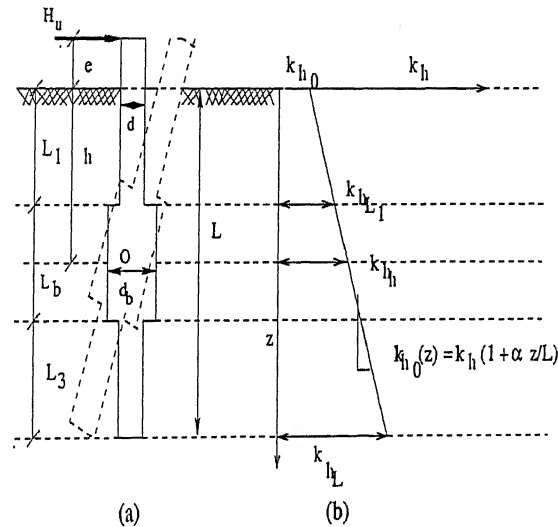


Figure 4.12: Variation of Coefficient of Subgrade Reaction in Non-homogeneous Soils.

#### 4.3.1 Rigid Free Head Single Bulb Under-reamed Pile

##### 4.3.1.1 Analysis

Deformation of single bulb under-reamed pile in non-homogeneous soil is analysed by considering the three possible locations of point of rotation along the length of the pile. Coefficient of subgrade reaction,  $k_h$ , is consider to increase linearly with depth,  $z$ , below the ground surface. Soil reaction along the length of the pile for the case of point of rotation within the bulb is shown in figure 4.13.

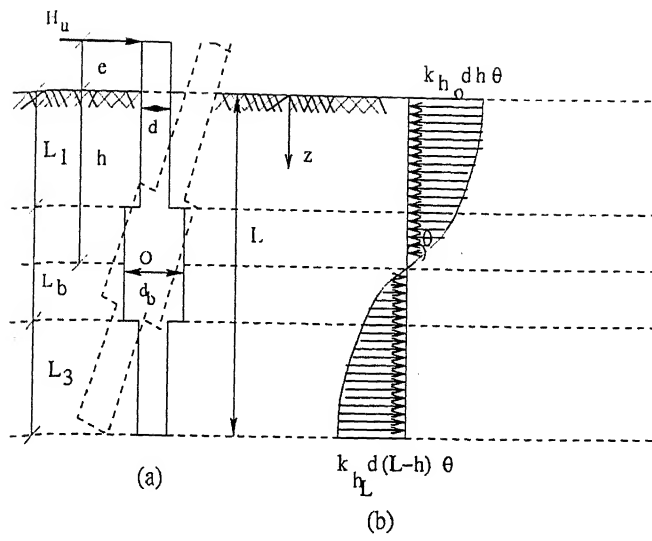


Figure 4.13: Definition Sketch of Rigid Free Head Single Bulb Under-reamed Pile in Non-homogeneous Soil (a) Kinematics and (b) Distribution of Forces.

Normalised force equilibrium expression, in terms of the rotation coefficient,  $I_\theta$ , is

$$I_\theta = \frac{H}{k_{h0} d L \theta} = \int_0^{L_1} (1 + \alpha z^*) (h^* - z^*) dz + \int_{L_1}^{L_1+L_b} d_r (1 + \alpha z^*) (h^* - z^*) dz + \int_{L_1+L_b}^L (1 + \alpha z^*) (h^* - z^*) dz \quad (4.10)$$

$$\theta = \left( \frac{H}{k_h d L^2} \right) (I_\theta^*)$$

where  $I_\theta^* = \frac{2}{I_\theta}$

and the normalised point of rotation,  $h^*$ , from the moment equilibrium, is

$$h^* = \frac{A}{B} \quad (4.11)$$

where

$$A = \int_0^{L_1} \{z^{*2} + e^* z^* + \alpha(z^{*3} + e^* z^{*2})\} dz + \int_{L_1}^{L_1+L_b} \{z^{*2} + e^* z^* + \alpha(z^{*3} + e^* z^{*2})\} d_r dz + \int_{L_1+L_b}^L \{z^{*2} + e^* z^* + \alpha(z^{*3} + e^* z^{*2})\} dz$$

$$B = \int_0^{L_1} \{z^* + e^* + \alpha(z^{*2} + e^* z^*)\} dz + \int_{L_1}^{L_1+L_b} \{z^* + e^* + \alpha(z^{*2} + e^* z^*)\} d_r dz + \int_{L_1+L_b}^L \{z^* + e^* + \alpha(z^{*2} + e^* z^*)\} dz$$

$$\alpha(z^{*2} + e^*z^*)\}d\tau.dz + \int_{L_1+L_b}^{L_1} \{z^* + e^* + \alpha(z^{*2} + e^*z^*)dz$$

$$\rho_\theta^* = I_\theta^*.h^* \quad \text{and} \quad \rho = \left(\frac{H}{k_h d L^2}\right)(\rho_\theta^*)$$

#### 4.3.1.2 Results and Discussion

Deformations of rigid free head single bulb under-reamed pile in non-homogeneous soils are quantified and described in the normalised deformation coefficient,  $\rho_{urnh}^*/\rho_{sth}^*$ , as a function of depth of bulb from the ground surface,  $L_1^*$ . The coefficient of subgrade reaction in non-homogeneous soils varies as  $k_h(z) = k_{h0}(1 + \alpha z/L)$  as shown in figure 4.12. If the non-homogeneity factor,  $\alpha$ , equals zero, the estimated deformations of the under-reamed pile become identical to the values estimated for piles in homogeneous soils. The normalised deformation coefficient of under-reamed pile increases with increase in depth of bulb from the ground surface upto a depth of  $(0.5 \text{ to } 0.7)L$  and decreases with further increase in depth of the bulb.

The normalised deformation coefficient,  $\rho_{urnh}^*/\rho_{sth}^*$ , is 0.57 and 0.46 at  $L_b^*=0.1$  and 0.2 respectively for the bulb at the top of the pile,  $d_r = 2.5$ ,  $\alpha = 1.0$  and  $e^* = 0.02$ , a 19% decrease in the deformation for the length of bulb increases by 100% from 0.1 to 0.2 (Figure 4.14). Percentage decrease in the normalised deformation coefficient decreases with increase in the length of the bulb for bulb at ground surface. Rate of change of the ratio,  $\rho_{urnh}^*/\rho_{sth}^*$ , with respect to the depth of bulb increases with increase in the length of the bulb (Figure 4.14).

The ratios,  $\rho_{urnh}^*/\rho_{sth}^*$ , are 0.68 and 0.45 respectively for diameter ratio,  $d_r=1.5$  and 3.0 for the bulb at ground surface,  $L_b^* = 0.15$ ,  $\alpha = 1.0$  and  $e^* = 0.02$ , a 34% decrease, in the normalised deformation coefficient (Figure 4.15). For the bulb at  $0.55L$ , the ratio,  $\rho_{urnh}^*/\rho_{sth}^*$ , is the same for cylindrical and for different diameter ratios of under-reamed pile (Figure 4.15). The rate of change of normalised deformation coefficient with respect to the depth of the bulb increases with increase in the diameter ratio of under-reamed pile (Figure 4.15).

The effect of non-homogeneity factor,  $\alpha$ , on the deformation of under-reamed pile in non-homogeneous soils is described in figure 4.16. The normalised deformation coefficient decreases with increase in the non-homogeneity of the soil. The rate of change of the ratio,  $\rho_{urnh}^*/\rho_{sth}^*$ , with respect to the depth of the bulb decreases with increase in the non-homogeneity factor,  $\alpha$ , for  $d_r = 2.5$ ,  $L_b^* = 0.15$  and  $e^* = 0.02$  (Figure 4.16).

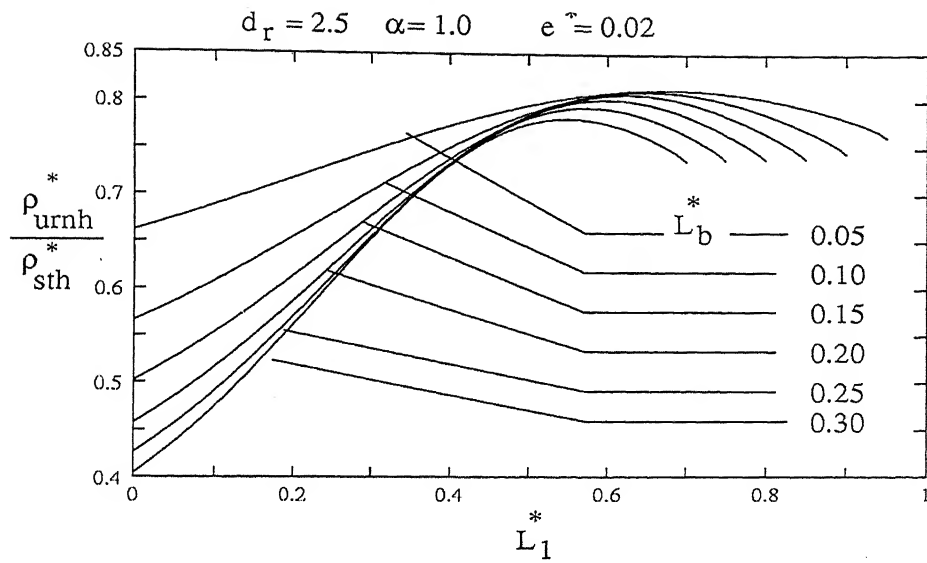


Figure 4.14: Effect of Length of Bulb on Normalised Deformation Coefficient for Rigid Free Head Single Bulb Under-reamed Pile in Non-homogeneous Soils.

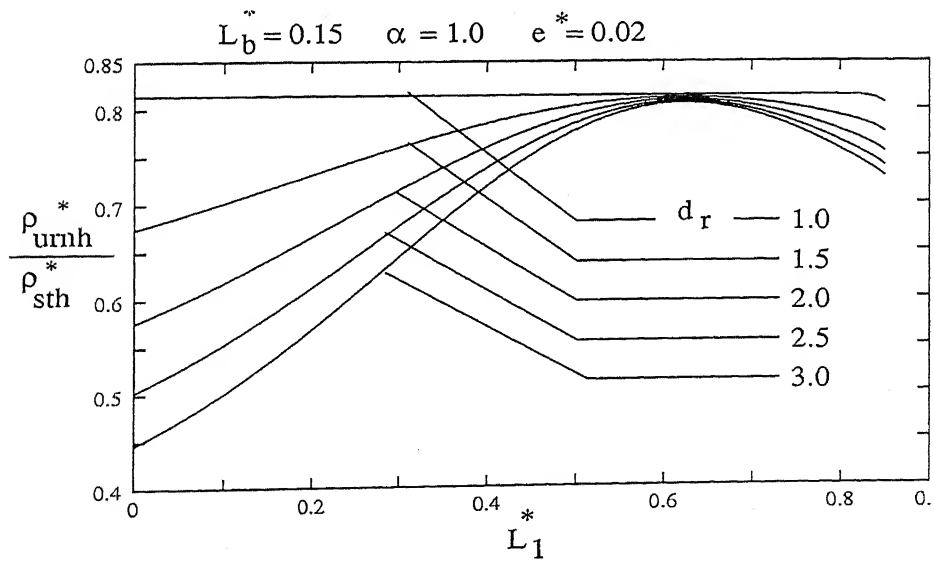


Figure 4.15: Effect of Diameter of Bulb on Normalised Deformation Coefficient for Rigid Free Head Single Bulb Under-reamed Pile in Non-homogeneous Soils.

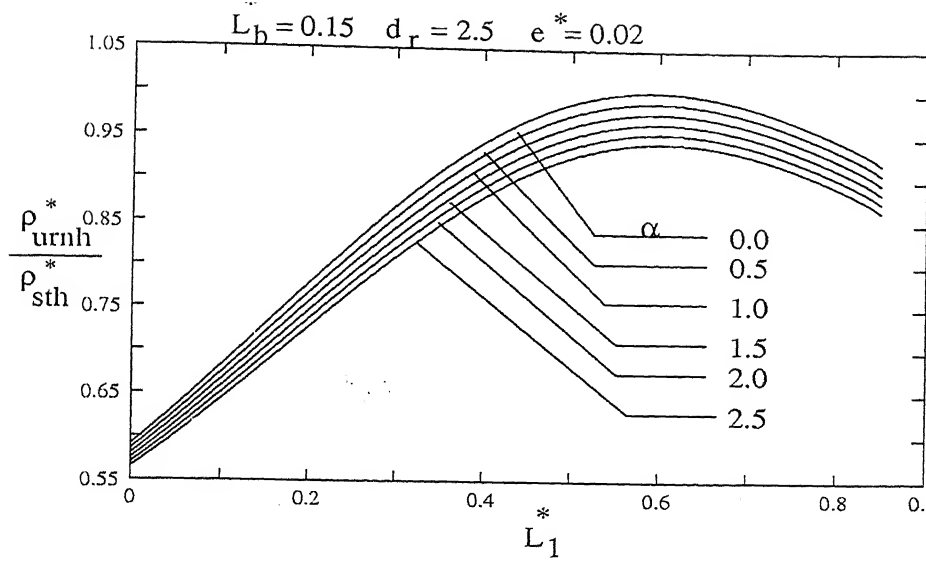


Figure 4.16: Effect of  $\alpha$  on Normalised Deformation Coefficient for Rigid Free Head Single Bulb Under-reamed Pile in Non-homogeneous Soils.

### 4.3.2 Rigid Free Head Double Bulb Under-reamed Pile

The failure mechanism and the resulting qualitative distribution of mobilized soil reaction at failure for double bulb under-reamed pile in non-homogeneous soil is as shown in figure 4.17.

#### 4.3.2.1 Analysis

Consider the double bulb under-reamed pile of diameter  $d$ , length  $L$  and bulb diameter as  $d_b$ . Depth of the bulb from the ground surface, length of bulbs and the length of the pile below the bottom bulb are  $L_1$ ,  $L_{b1}$ ,  $L_{b2}$  and  $L_4$  respectively. Spacing between the bulbs is  $S$ . The load,  $H_u$ , is applied with an eccentricity,  $e$ . The depth of point of rotation is  $h$  from the ground surface. The possible locations of the point of rotation along the length of the pile are (1) above the top bulb (2) within the top bulb (3) in between the two bulbs (4) within the bottom bulb and (5) below the bottom bulb. Equilibrium expressions for all case of point of rotations are identical because of rigid rotation of the pile. Soil reaction and kinematics of double bulb under-reamed pile in non-homogeneous soils for the case of depth of point of rotation lying between the two bulbs are shown in figure 4.17.

Normalised form of force equilibrium expression, in terms of the rotation coefficient,  $I_\theta$ , is

$$I_\theta = \frac{H}{k_{h0} d L \theta} = \int_0^{L_1} a \cdot dz + \int_{L_1}^{L_1+L_{b1}} a \cdot dr \cdot dz + \int_{L_1+L_{b1}}^{L_1+L_{b1}+S} a \cdot dz + \int_{L_1+L_{b1}+S}^{L-L_4} a \cdot dr \cdot dz$$

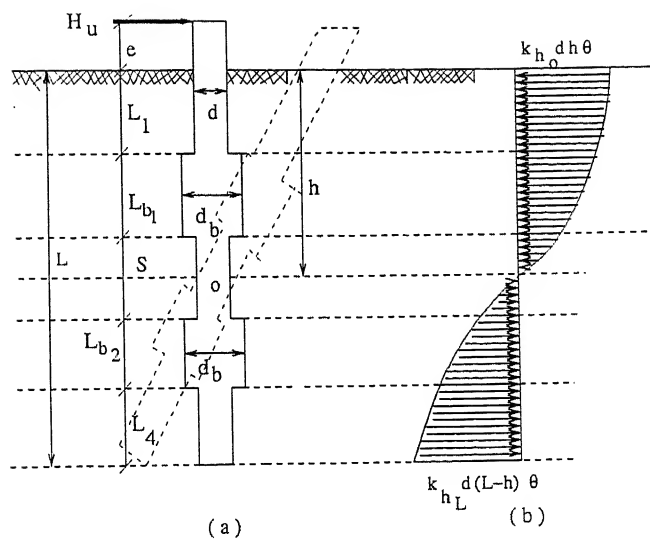


Figure 4.17: Definition Sketch of Rigid Free Head Double Bulb Under-reamed Pile - Non-homogeneous Soils (a) Kinematics and (b) Distribution of Forces.

$$+ \int_{L-L_4}^L a.dz \quad (4.12)$$

where  $a = (1 + \alpha z^*)(h^* - z^*)$ ,  $\theta = (\frac{H}{k_h d L^2})(I_\theta^*)$  and  $I_\theta^* = \frac{1}{I_\theta}$  and the normalised depth of point of rotation,  $h^*$ , from the moment equilibrium, is

$$h^* = \frac{A}{B} \quad (4.13)$$

where

$$\begin{aligned} A &= \int_0^{L_1} b.dz + \int_{L_1}^{L_1+L_{b1}} b.d_r.dz + \int_{L_1+L_{b1}}^{L_1+L_{b1}+S} b.dz + \int_{L_1+L_{b1}+S}^{L-L_4} b.d_r.dz + \int_{L-L_4}^L b.dz \\ B &= \int_0^{L_1} c.dz + \int_{L_1}^{L_1+L_{b1}} c.d_r.dz + \int_{L_1+L_{b1}}^{L_1+L_{b1}+S} c.dz + \int_{L_1+L_{b1}+S}^{L-L_4} c.d_r.dz + \int_{L-L_4}^L c.dz \\ b &= z^{*2} + e^*z^* + \alpha(z^{*3} + e^*z^{*2}) \\ c &= z^* + e^* + \alpha(z^{*2} + e^*z^*) \end{aligned}$$

$$\rho_\theta^* = I_\theta^*.h^* \quad \text{and} \quad \rho = (\frac{H}{k_h d L^2})(\rho_\theta^*)$$

#### 4.3.2.2 Results and Discussion

Deformations of rigid free head double bulb under-reamed pile in non-homogeneous soils are estimated and presented in the form of normalised deformation coefficient,  $\rho_{urnh}^*/\rho_{sth}^*$ , as a function of the depth of bulb from the ground surface,  $L_1^*$  in figures 4.18 through 4.21. The normalised deformation coefficient is maximum for the depth of bulb at  $(0.5$  to  $0.7)L$ .

For the diameter ratio,  $d_r=2.5$ ,  $S^* = 0.1$ ,  $\alpha = 1.0$  and  $e^* = 0.02$ , the normalised deformation coefficient,  $\rho_{urnh}^*/\rho_{sth}^*$ , is 0.48 and 0.41 for the length of the bulb,  $L_b^* = 0.1$

and 0.2 respectively, a 15% decrease (Figure 4.18). The ratio,  $\rho_{urnh}^*/\rho_{sth}^*$ , is 0.54 and 0.46 for single bulb under-reamed pile for the same set of parameters (Figure 4.14). By providing one additional bulb to the single bulb under-reamed pile in non-homogeneous soils, 15% and 7% decreases in the deformations occur for  $L_b^* = 0.1$  and 0.2 respectively (Figures 4.14 and 4.18). The rate of increase of the normalised deformation coefficient with respect to the depth of the bulb increases with increase in the depth of the bulb (Figure 4.18).

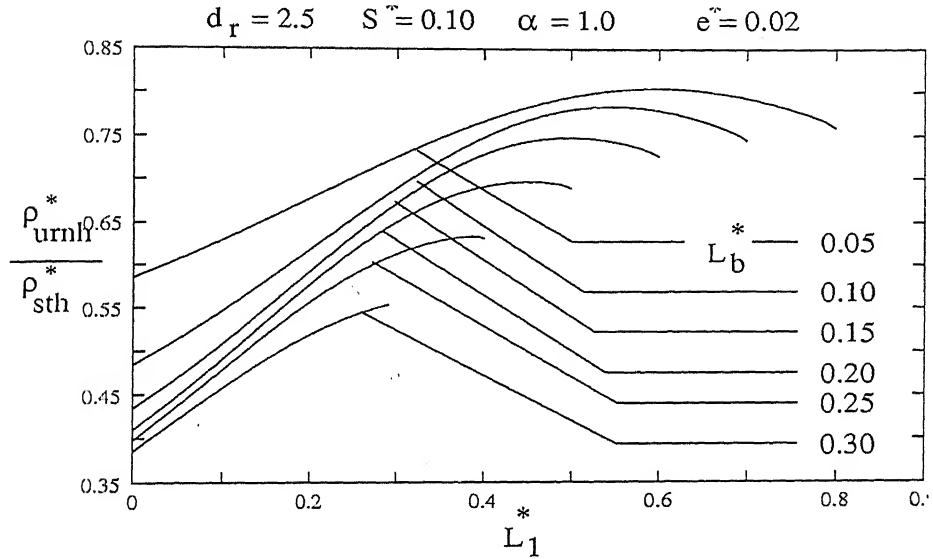


Figure 4.18: Effect of Length of Bulb on Normalised Deformation Coefficient for Rigid Free Head Double Bulb Under-reamed Pile in Non-homogeneous Soils.

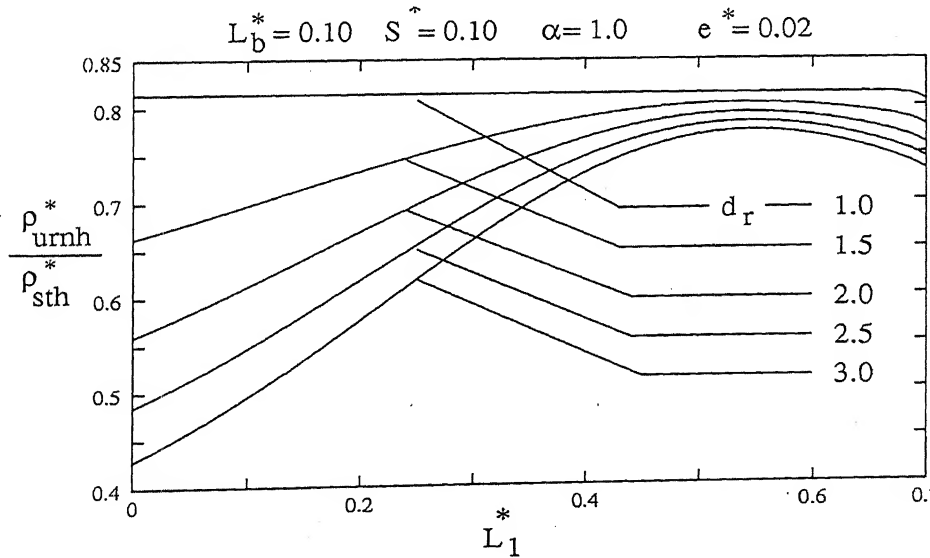


Figure 4.19: Effect of Diameter of Bulb on Normalised Deformation Coefficient for Rigid Free Head Double Bulb Under-reamed Pile in Non-homogeneous Soils.

The ratio,  $\rho_{urnh}^*/\rho_{sth}^*$ , is 0.66 and 0.43 for diameter ratios,  $d_r = 1.5$  and 3.0 for the bulb



at the top of the pile with  $L_b^* = 0.1$ ,  $S^* = 0.1$ ,  $\alpha = 1.0$  and  $e^* = 0.02$ , a 35% decrease (Figure 4.19). No significant decrease in the ratio,  $\rho_{urnh}^*/\rho_{sth}^*$ , is observed with increase in the diameter ratio for the bulb at mid length of the pile (Figure 4.19). Rate of increase in the normalised deformation coefficient increases with increase in the diameter ratio.

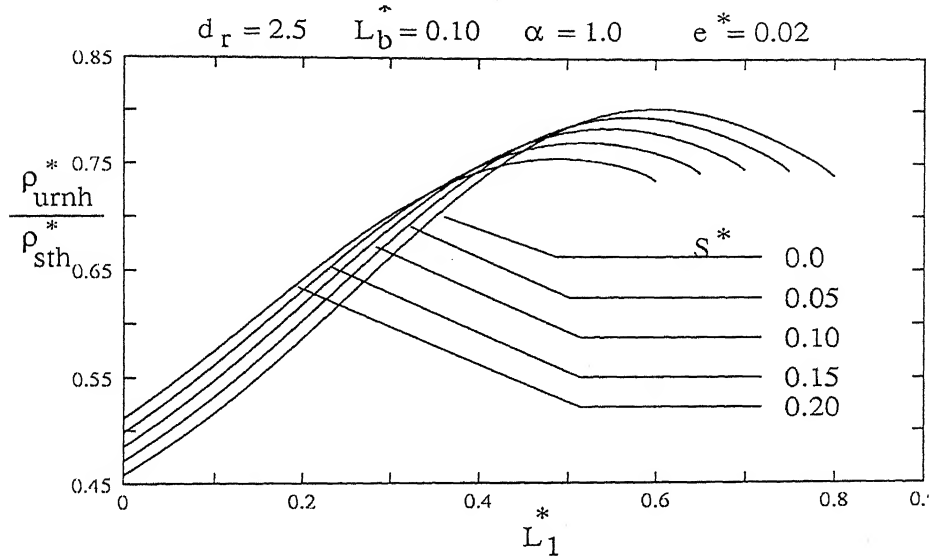


Figure 4.20: Effect of Spacing on Normalised Deformation Coefficient for Rigid Free Head Double Bulb Under-reamed Pile in Non-homogeneous Soils.

The normalised deformation coefficient increases with increase in spacing between the bulbs (Figure 4.20). For double bulb under-reamed pile in non-homogeneous soils with zero spacing, the normalised deformation coefficient is 0.46 for  $d_r = 2.5$ ,  $L_b^* = 0.10$ ,  $\alpha = 1.0$  and  $e^* = 0.02$ , whereas it is 0.55 for single bulb under-reamed pile (16% decrease) for the same set of parameters (Figure 4.20). The rate of change in the ratio,  $\rho_{urnh}^*/\rho_{sth}^*$ , with respect to depth of the bulb is the same for different values of spacing between the bulbs of double bulb under-reamed pile (Figure 4.20).

The effect of non-homogeneity factor,  $\alpha$ , on the deformation of double bulb under-reamed pile in non-homogeneous soils is presented in figure 4.21. The normalised deformation coefficient decreases with increase in the non-homogeneity of the soil. A 16% and 18% decrease in the deformation is observed with increase in the non-homogeneity factor from 0 to 1.0 and 1.0 to 2.0 respectively for  $d_r = 2.5$ ,  $L_b^* = 0.1$ ,  $S^* = 0.1$  and  $e^* = 0.02$  (Figure 4.21).

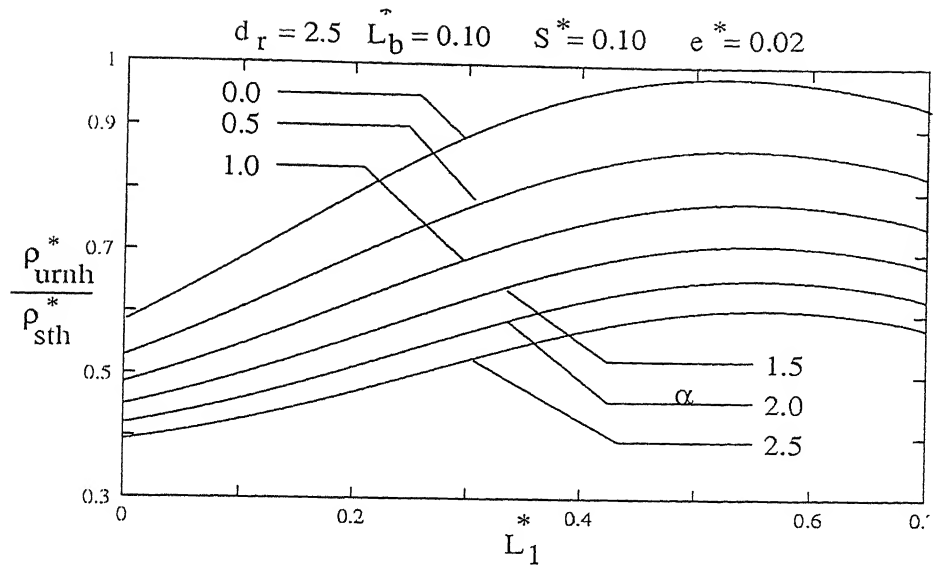


Figure 4.21: Effect of  $\alpha$  on Normalised Deformation Coefficient for Rigid Free Head Double Bulb Under-reamed Pile in Non-homogeneous Soils.

### 4.3.3 Validation

Closed form solutions given by Hetenyi (1946) for the lateral deflections at the ground surface of free headed rigid pile and constant  $k_h$  with depth are

$$\rho = \frac{4H(1+1.5e/L)}{k_h dL}$$

$$\theta = \frac{6H(1+2e/L)}{k_h dL^2}.$$

If the diameter ratio,  $d_r$ , equals 1, expressions to estimate the deformation for single and double bulb under-reamed piles in homogeneous soils are identical to the solutions given by Hetenyi (1946). In case of non-homogeneous soils, if the non-homogeneity factor,  $\alpha$ , equals zero, expression become identical to homogeneous ones.

### 4.3.4 Verification from the Test Results

Results of single and double bulb under-reamed piles from the proposed analysis are compared with the test results conducted by CBRI, Roorkee. Model tests have been conducted on single and double bulb under-reamed piles in silty sand for different  $L/d$  ratios. Bulb diameter was 2.5 times the shaft diameter of the pile (5 cm). The spacing between the two bulbs was 1.5 times the bulb diameter in case of double bulb under-reamed piles. The load was applied very close to the ground level and hence the displacements at load level were taken as displacements at ground level. Tests results are shown in figures 4.22 and 4.23.

Ultimate lateral load capacity of the cylindrical pile for different  $L/d$  ratios (10, 15

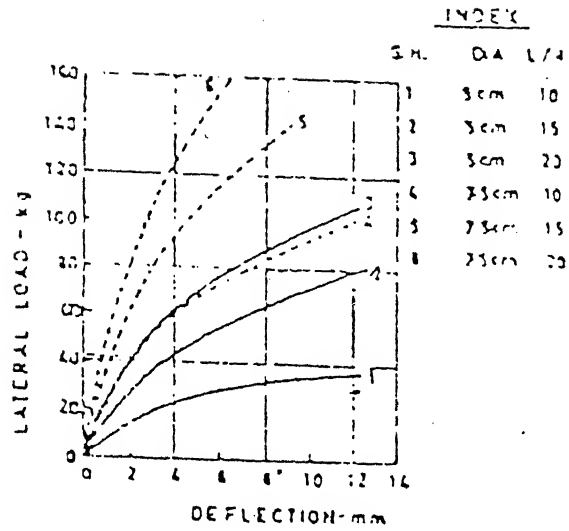


Figure 4.22: Effect of Depth in Straight Shaft Piles Under Lateral Loads.

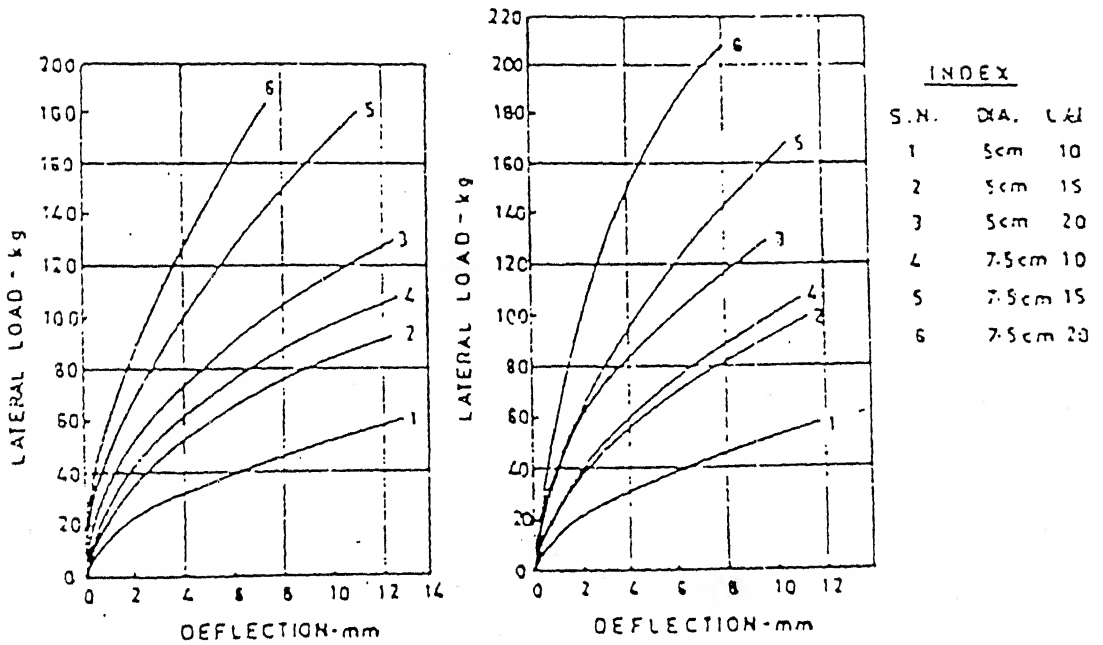


Figure 4.23: Effect of Depth in (a) Single and (b) Double Bulb Under-reamed Pile.

and 20) are used to back calculate undrained shear strengths of the soil at the surface,  $c_{u0}$ , of the cylindrical pile for different non-homogeneity factors,  $\alpha$ , by modified Broms's theory (Table 4.1).

L/d	$H_{u_{meas}}$ (kg)	$c_{u0}$ (kg/cm <sup>2</sup> )				
		$\alpha = 0.0$	0.50	1.00	1.50	2.00
10	46.67	0.0741	0.0645	0.0574	0.0517	0.0471
15	106.00	0.0978	0.0848	0.0751	0.0674	0.0613
20	158	0.1023	0.0885	0.0782	0.0702	0.0637

Table 4.1: Variation of Initial Undrained Shear Strength of the Soil for Different L/d Ratios of the Cylindrical Pile.

Predicted and measured ultimate capacities for the single and double bulb under-reamed piles in non-homogeneous soils are presented in tables 4.2 and 4.3 respectively. From table 4.2, the predicted ultimate lateral load capacity is 17% lower than the measured capacity for L/d=10 for  $\alpha = 0$ . For L/d=15 and 20, predicted ultimate lateral load capacities are 16.5% and 16.2% higher than the measured values (Table 4.2).

L/d	$H_{u_{meas}}$ (kg)	$H_{u_{pred}}$ (kg)				
		$\alpha = 0.0$	0.50	1.00	1.50	2.00
10	83.33	69.309	68.08	67.15	66.267	65.564
15	122.45	142.625	139.499	137.033	134.971	133.517
20	171.80	199.654	195.482	192.185	189.876	187.734

Table 4.2: Comparison of Test Results for Ultimate Capacity of Single Bulb Under-reamed Pile in Non-homogeneous Soils.

For double bulb under-reamed pile, predicted lateral load capacity is 18% lower and 21% and 27% higher than the measured values for L/d =10, 15 and 20 respectively for  $\alpha = 0.0$  (Table 4.3).

L/d	$H_{u_{meas}}$ (kg)	$H_{u_{pred}}$ (kg)				
		$\alpha = 0.0$	0.50	1.00	1.50	2.00
10	89.55	73.073	72.549	72.308	71.199	70.156
15	131.82	159.98	158.553	157.200	155.784	154.941
20	175.65	223.963	220.65	217.882	215.816	214.057

Table 4.3: Comparison of Test Results for Ultimate Capacity of Double Bulb Under-reamed Pile in Non-homogeneous Soils.

Subgrade moduli of the soil at surface,  $k_{h0}$ , for different L/d ratios (10,15 and 20) and loadings for cylindrical pile are calculated and presented in the respective tables from 4.4 through 4.6 for non-homogeneity factor,  $\alpha = 0.0$  to 2.0.

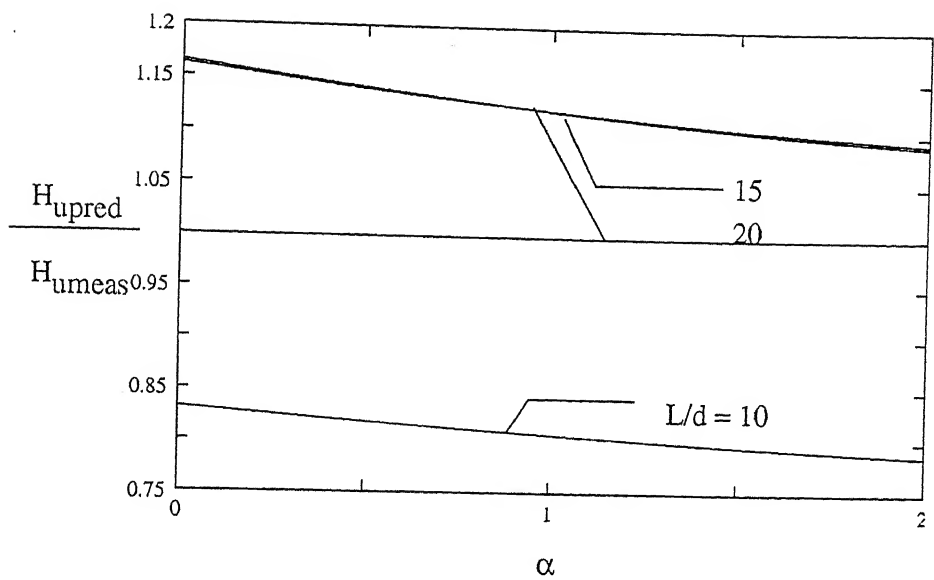


Figure 4.24: Comparison of Test Results for Ultimate Capacity of Single Bulb Under-reamed Pile in Non-homogeneous Soils.

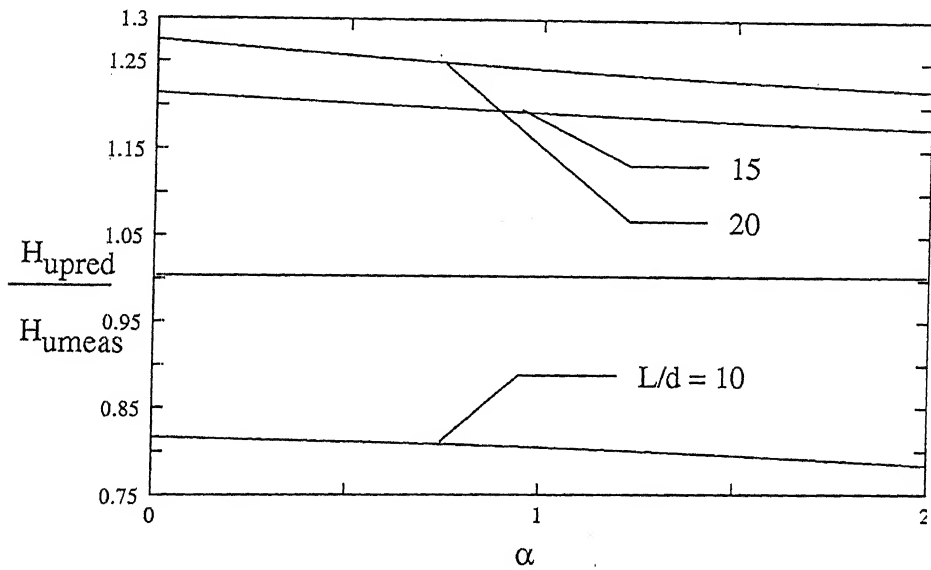


Figure 4.25: Comparison of Test Results for Ultimate Capacity of Double Bulb Under-reamed Pile in Non-homogeneous Soils.

H (kg)	$\rho$ (mm)	$k_{ho}$ (kg/cm <sup>3</sup> )				
		$\alpha = 0.0$	0.50	1.00	1.50	2.00
15	2	1.2	1.070	0.969	0.887	0.818
22	4	0.88	0.785	0.711	0.650	0.600
28	6	0.747	0.666	0.604	0.552	0.509
32	8	0.640	0.571	0.517	0.473	0.436
32.5	10	0.520	0.464	0.420	0.384	0.355
35	12	0.467	0.416	0.377	0.345	0.318

Table 4.4: Variation of Initial Subgrade Modulus with Non-homogeneity Factor for Cylindrical Pile of  $L/d = 10$ .

H (kg)	$\rho$ (mm)	$k_{ho}$ (kg/cm <sup>3</sup> )				
		$\alpha = 0.0$	0.50	1.00	1.50	2.00
25	2	1.330	1.189	1.077	0.986	0.909
40	4	1.067	0.951	0.862	0.789	0.727
53	6	0.942	0.840	0.761	0.696	0.642
65	8	0.867	0.773	0.700	0.641	0.591
70	10	0.747	0.666	0.603	0.552	0.509
80	12	0.711	0.634	0.574	0.526	0.485

Table 4.5: Variation of Initial Subgrade Modulus with Non-homogeneity Factor for Cylindrical Pile of  $L/d=15$ .

H (kg)	$\rho$ (mm)	$k_{ho}$ (kg/cm <sup>3</sup> )				
		$\alpha = 0.0$	0.5	1.0	1.5	2.0
41	2	1.640	1.463	1.325	1.212	1.118
60	4	1.200	1.070	0.969	0.887	0.818
74	6	0.987	0.880	0.797	0.729	0.673
86	8	0.860	0.767	0.695	0.636	0.586
95	10	0.760	0.678	0.614	0.562	0.518
105	12	0.700	0.624	0.565	0.517	0.477

Table 4.6: Variation of Initial Subgrade Modulus with Non-homogeneity Factor for Cylindrical Pile of  $L/d=20$ .

Measured and predicted values of the deformations for single and double bulb under-reamed pile for  $L/d$  ratios 10, 15 and 20 are presented in the tables 4.7 through 4.12. Deformation for single or double bulb under-reamed pile for different loading conditions, are predicted by using the appropriate subgrade moduli at similar or corresponding loads of the cylindrical pile. In all the cases, the predicted deformations are close to the measured values. They are hardly 5 to 15% higher.

H (kg)	$\rho_{meas}$ (mm)	$\rho_{pred}$ (mm)				
		$\alpha = 0.0$	0.5	1.0	1.5	2.0
23.16	2	2.376	2.343	2.321	2.303	2.290
31.58	4	4.417	4.355	4.313	4.286	4.258
40.00	6	6.591	6.502	6.430	6.392	6.357
46.32	8	8.909	8.782	8.699	8.638	8.594
50.53	10	10.961	10.789	10.682	10.607	10.515
58.53	12	13.706	13.280	12.914	12.602	12.327

Table 4.7: Comparison of Test Results for Deformation of Single Bulb Under-reamed Pile of  $L/d=10$  in Non-homogeneous Soils.

H (kg)	$\rho_{meas}$ (mm)	$\rho_{pred}$ (mm)				
		$\alpha = 0.0$	0.5	1.0	1.5	2.0
35.79	2	2.716	2.689	2.625	2.574	2.496
50.53	4	4.905	4.858	4.792	4.715	4.687
65.26	6	6.696	6.634	6.574	6.526	6.485
75.79	8	8.876	8.840	8.747	8.668	8.593
84.21	10	11.169	11.125	11.082	10.927	10.852
90.53	12	12.694	12.667	12.654	12.642	12.576

Table 4.8: Comparison of Test Results for Deformation of Single Bulb Under-reamed Pile of L/d=15 in Non-homogeneous Soils.

H (kg)	$\rho_{meas}$ (mm)	$\rho_{pred}$ (mm)				
		$\alpha = 0.0$	0.5	1.0	1.5	2.0
52.63	2	2.548	2.539	2.528	2.515	2.502
71.580	4	4.626	4.609	4.584	4.557	4.525
88.420	6	6.563	6.527	6.493	6.459	6.414
101.053	8	8.438	8.391	8.349	8.305	8.247
113.684	10	10.705	10.645	10.591	10.535	10.462

Table 4.9: Comparison of Test Results for Deformation of Single Bulb Under-reamed Pile of L/d=20 in Non-homogeneous Soils.

H (kg)	$\rho_{meas}$ (mm)	$\rho_{pred}$ (mm)				
		$\alpha = 0.0$	0.5	1.0	1.5	2.0
21.05	2	2.923	2.868	2.828	2.799	2.773
29.47	4	4.510	4.425	4.362	4.319	4.276
40.00	6	6.685	6.557	6.467	6.410	6.344
44.21	8	8.443	8.283	8.169	8.097	8.013
50.53	10	10.703	10.498	10.356	10.251	10.136
61.05	12	13.225	12.995	12.804	12.663	12.558

Table 4.10: Comparison of Test Results for Deformation of Double Bulb Under-reamed Pile of L/d=10 in Non-homogeneous Soils.

H (kg)	$\rho_{meas}$ (mm)	$\rho_{pred}$ (mm)				
		$\alpha = 0.0$	0.5	1.0	1.5	2.0
40.00	2	2.914	2.886	2.862	2.846	2.837
54.74	4	4.716	4.670	4.632	4.607	4.592
71.58	6	6.824	6.755	6.708	6.669	6.644
80.00	8	8.746	8.656	8.596	8.539	8.506
92.63	10	11.00	10.889	10.813	10.741	10.699

Table 4.11: Comparison of Test Results for Deformation of Double Bulb Under-reamed Pile of L/d=15 in Non-homogeneous Soils.

H (kg)	$\rho_{meas}$ (mm)	$\rho_{pred}$ (mm)				
		$\alpha = 0.0$	0.5	1.0	1.5	2.0
63.16	2	3.079	3.067	3.065	3.058	3.0332
82.105	4	4.905	4.890	4.880	4.876	4.860
100.00	6	6.928	6.906	6.896	6.878	6.864
113.68	8	8.665	8.644	8.633	8.624	8.610
128.42	10	10.733	10.707	10.693	10.684	10.663

Table 4.12: Comparison of Test Results for Deformation of Double Bulb Under-reamed Pile of  $L/d=20$  in Non-homogeneous Soils.

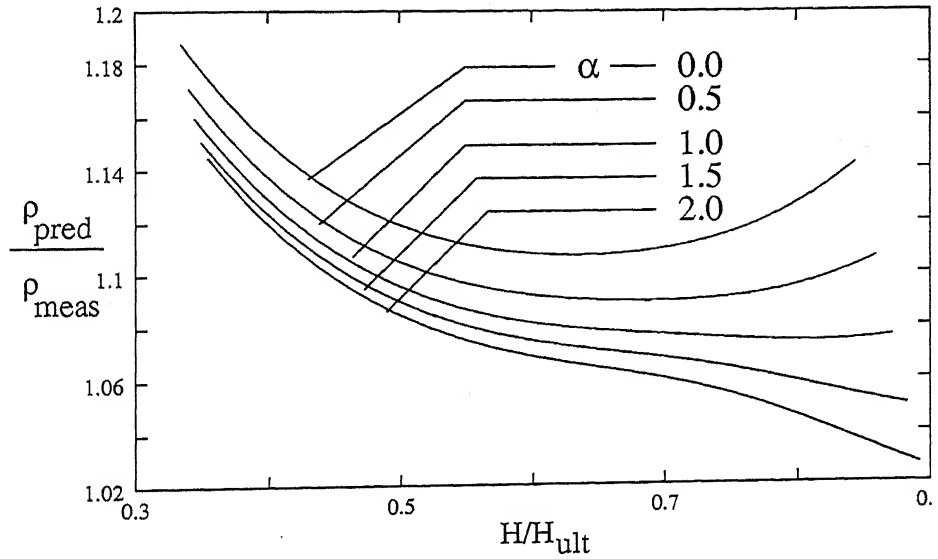


Figure 4.26: Comparison of Test Results for Deformation of Single Bulb Under-reamed Pile of  $L/d=10$  in Non-homogeneous Soils.

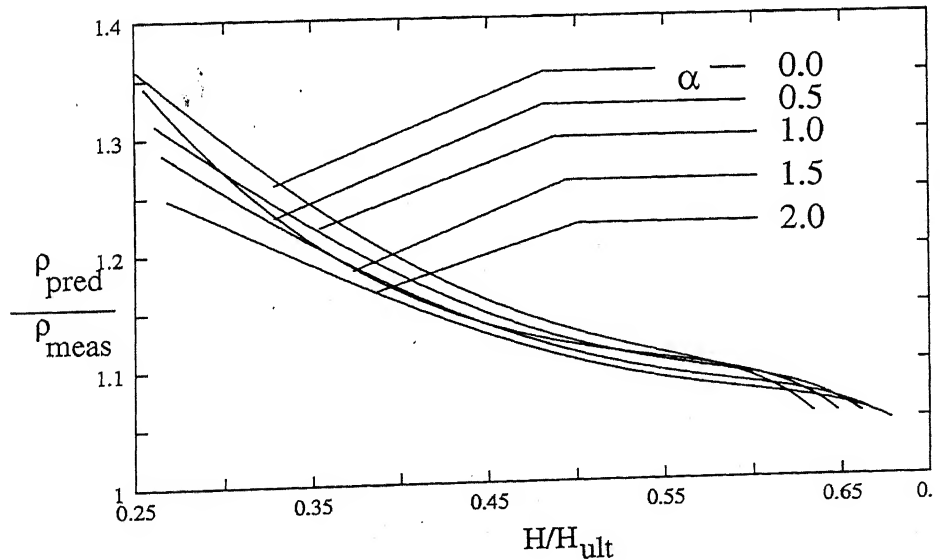


Figure 4.27: Comparison of Test Results for Deformation of Single Bulb Under-reamed Pile of  $L/d=15$  in Non-homogeneous Soils.



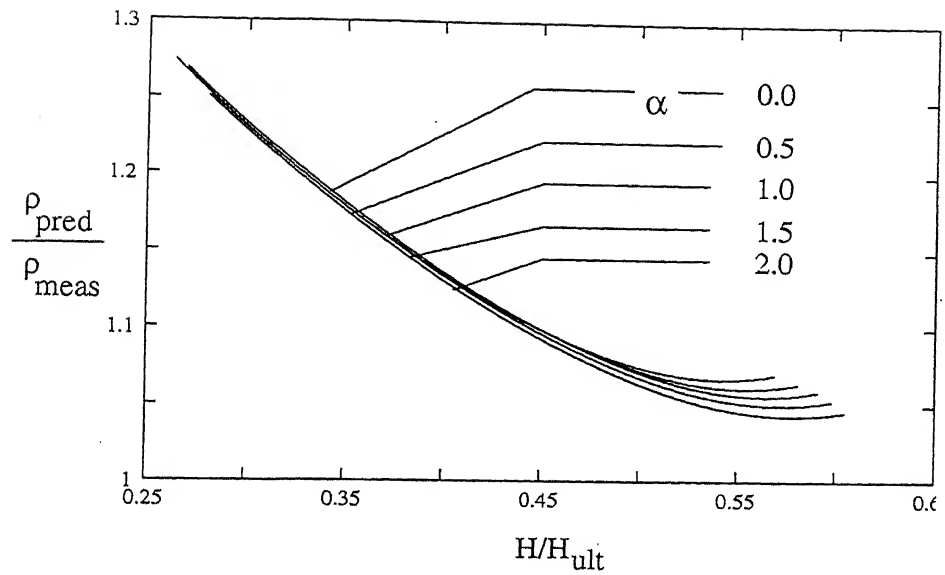


Figure 4.28: Comparison of Test Results for Deformation of Single Bulb Under-reamed Pile of  $L/d=20$  in Non-homogeneous Soils.

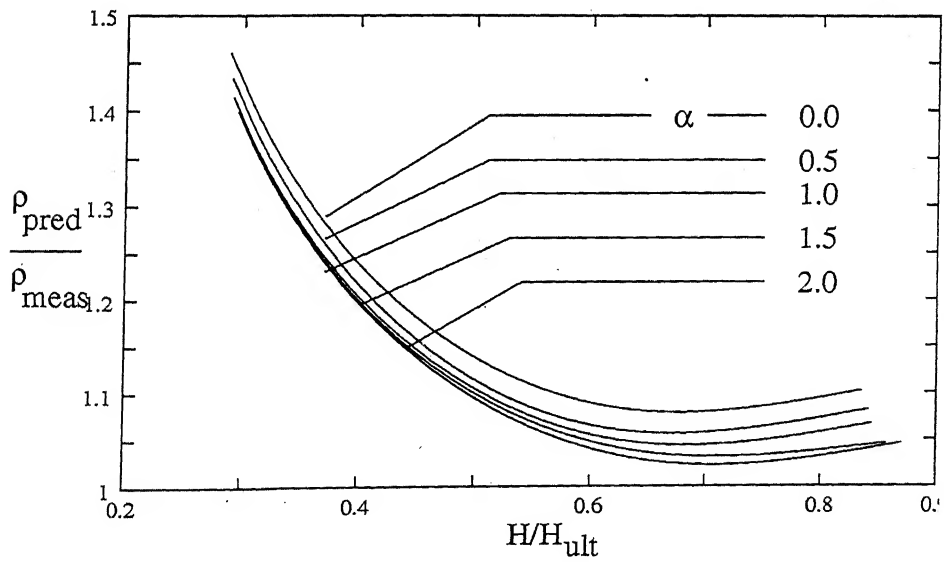


Figure 4.29: Comparison of Test Results for Deformation of Double Bulb Under-reamed Pile of  $L/d =10$  in Non-homogeneous Soils.

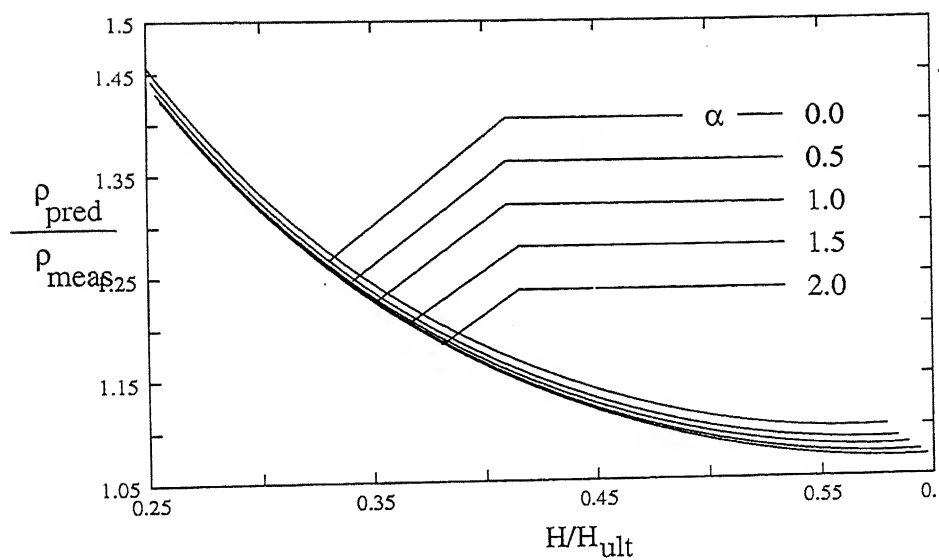


Figure 4.30: Comparison of Test Results for Deformation of Double Bulb Under-reamed Pile of  $L/d=15$  in Non-homogeneous Soils.

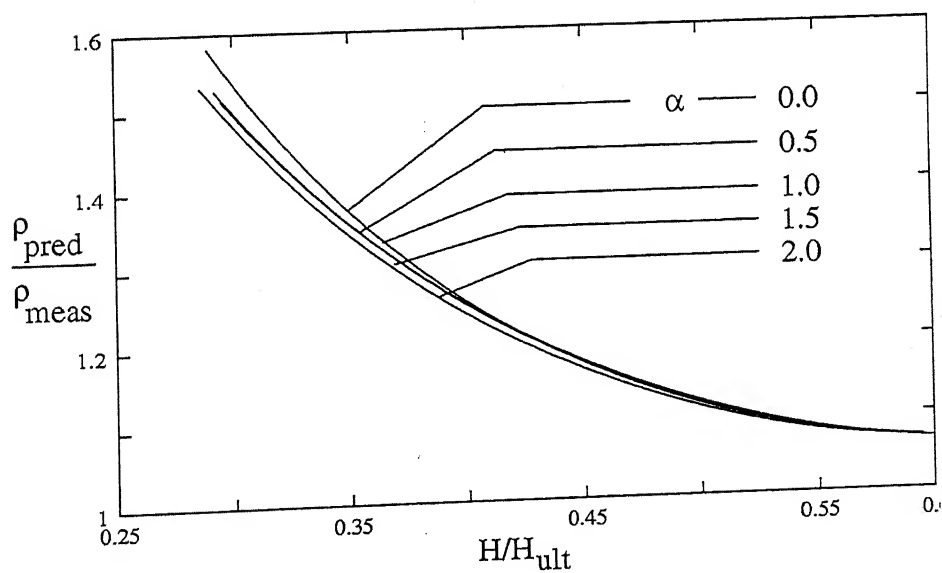


Figure 4.31: Comparison of Test Results for Deformation of Double Bulb Under-reamed Pile of  $L/d=20$  in Non-homogeneous Soils.

# Chapter 5

## Conclusions

Under-reamed piles are frequently used in alluvial soils in the Gangatic plains to transmit mostly compressive and tensile and occasionally lateral loads. Prediction of lateral loads is one of the complex problems for the design of structures subjected to lateral loads. Existing design techniques for under-reamed piles subjected to lateral loads are based on few model tests, without any theoretical analysis. A design method is proposed based on simple deformation mechanisms which relate the lateral soil pressures acting simply on the pile to the pile displacement. In this investigation, under-reamed pile is treated to be rigid and the soil as elastic or plastic medium. The actual shape of the bulb is replaced by an equivalent cylinder having identical projected surface and plan areas. The two soil parameters, undrained shear strength,  $c_u$ , and coefficient of subgrade reaction,  $k_h$ , of the soil are treated as constants in homogeneous soils and to linearly increase with depth in non-homogeneous soils. The response of an under-reamed pile in homogeneous and non-homogeneous soils, to a lateral load is analysed and solutions obtained are discussed separately for single and double bulb under-reamed piles with free and fixed head conditions.

The effects of the parameters such as the coefficient of subgrade reaction ( $k_h$ ) and the undrained shear strength ( $c_u$ ), the length ( $L_b$ ), depth ( $L_1$ ), diameter ( $d_b$ ) and the number of bulbs on the ultimate capacity and the deformation at the top of the pile for free and fixed head conditions are studied.

Position of the bulb at the top has significant effect on both the ultimate lateral resistance and deformation but little effect if located at the bottom and no effect if located in the region of 0.5 to 0.7 times the length of the piles. Both ultimate capacity and deformation of single bulb under-reamed pile are almost the same as that of cylindrical pile for the bulb at 0.5 to 0.7L. It is preferable to place the bulb close to the ground surface than at mid length of the pile as is conventionally done. Significant increase in ultimate lateral resistance and decrease in deformation can be achieved with increase in the size

of the bulb and by providing one more bulb i.e. in case of two bulb under-reamed pile. However no additional benefit accrues in providing more than two bulbs, since one of the bulbs would have to be located in the region (0.5 to 0.7L) in which case no additional increase in the lateral capacity of under-reamed pile is possible.

Ultimate lateral resistance of single bulb under-reamed pile with diameter ratio,  $d_r = 2.5$ , length of the bulb,  $L_b^* = 0.2$  and  $L/d=10$  in homogeneous soils is 1.92 times that of cylindrical pile for the bulb at ground surface. For increasing length of bulb,  $L_b^*$ , from 0.1 to 0.2, the normalised ultimate lateral resistance increases by 28% for diameter and  $L/d$  ratios of 2.5 and 10 respectively. Similarly by increasing the diameter ratio,  $d_r$ , from 1.0 to 2.0 and 2.0 to 3.0, the normalised ultimate lateral resistance increases by 48% and 32% for length of bulb,  $L_b^* = 0.15$  and  $L/d=10$ . Significant increase in the ultimate lateral resistance is discerned for increasing the  $L/d$  ratio upto 15 and no further increase for  $L/d>15$ . The normalised ultimate lateral resistance by modified Broms's approach increases by 38% for the length of the bulb increasing from 0.1 to 0.3 and 31% with diameter ratio increasing from 1.5 to 3.0 for  $L/d=10$  and  $e^* = 0.02$ .

The normalised deformation coefficient decreases by 16% with increase in length of the bulb from 0.1 to 0.2 for  $d_r = 2.5$ ,  $L/d=10$  and  $e^* = 0.02$ . For diameter ratio,  $d_r$ , increasing from 1.5 to 3.0, the normalised deformation coefficient decreases by 34% for  $L_b^* = 0.15$ . Both the normalised ultimate lateral resistance and deformation influence coefficient appear to be independent of eccentricity,  $e^*$ .

Ultimate lateral capacity of double bulb under-reamed pile with zero spacing in homogeneous soils is 31% more than the capacity of single bulb under-reamed pile for  $d_r = 2.5$ ,  $L/d=10$ ,  $L_b^* = 0.2$ ,  $e^* = 0.02$  and  $L_1^* = 0.0$ . For the length of bulb,  $L_b^*$ , increasing from 0.1 to 0.2, the capacity increases by 30% for diameter and  $L/d$  ratios of 2.5 and 10 respectively. No significant increase in the normalised ultimate lateral resistance is observed for the length of bulb,  $L_b^*>0.25$ . Ultimate lateral capacity increases by 68% with the diameter ratio,  $d_r$ , increasing from 1.5 to 3.0 for  $L/d=10$ ,  $L_b^* = 0.1$  and  $S^* = 0.05$ . Significant decrease in the capacity occurs with increase in spacing between the bulbs. The normalised ultimate lateral resistance by modified Broms's approach increases by 24% with length of the bulb increasing from 0.1 to 0.2 and 51% for diameter ratio increasing from 1.5 to 3.0 for  $L/d=10$ ,  $S^* = 0.1$  and  $D^* = 0.0$ .

The normalised deformation coefficient decreases by 16% by providing second bulb with zero spacing for  $d_r = 2.5$ ,  $L_b^*=0.1$  and  $e^* = 0.02$ . Normalised deformation coefficient decreases by 9% with increase in length of the bulb by 100% from 0.1 to 0.2 for  $d_r = 2.5$ ,  $S^* = 0.1$  and  $e^* = 0.02$ . No significant decrease in deformation occurs for length of bulb,  $L_b^*>0.15$ . For diameter ratio,  $d_r$ , increasing from 1.5 to 3.0, the normalised deformation

coefficient decreases by 33% for  $L_b^* = 0.1$  and  $S^* = 0.1$ .

The ultimate lateral capacity of rigid fixed head short single bulb under-reamed pile in homogeneous soil is 33% more to that of cylindrical pile. No significant increase in the capacity occurs with length and diameter of the bulb for smaller  $L/d$  ratios and for  $L/d > 10$ , significant in the capacity.

The normalised ultimate lateral resistance of rigid fixed intermediate length single bulb under-reamed pile increases by 19% with length of the bulb,  $L_b^*$ , increasing from 0.1 to 0.2 for  $d_r = 2.5$ ,  $L/d=10$  and  $M_y^* = 200$ . For the diameter ratio,  $d_r$ , increasing from 1.0 to 2.0 and 2.0 to 3.0, ultimate lateral capacity increases by 27% and 19% for  $L_b^* = 0.15$ ,  $L/d=10$  and  $M_y^* = 200$ .

The non-homogeneity of cohesive soils has significant effect on the ultimate lateral resistance and deformation at working loads for both free and fixed head conditions. Fixed head condition provides higher ultimate lateral capacity and lower ground line deformation than free head condition for both single and double bulb under-reamed pile.

The ultimate lateral resistance of single bulb under-reamed pile in non-homogeneous soils is 2.18 times that of straight shafted pile for  $L/d=10$ ,  $L_b^* = 0.2$ ,  $\alpha = 1.0$  and  $e^* = 0.02$ , whereas it is 1.92 times in homogeneous soils. The normalised ultimate lateral resistance increases by 24% with length of the bulb increasing from 0.1 to 0.2 with  $d_r = 2.5$  and 55% with diameter ratio increasing from 1.5 to 3.0 with  $L_b^* = 0.2$  for  $L/d=10$ ,  $\alpha = 1.0$  and  $e^* = 0.02$ . For the non-homogeneity factor increasing from 0 to 1.0 and 1.0 to 2.0, the ultimate lateral resistance increases by 17% and 10% respectively for  $d_r = 2.5$ ,  $L_b^* = 0.2$ ,  $L/d=10$  and  $e^* = 0.02$ .

The normalised ultimate lateral resistance increases by 19% with length of bulb,  $L_b^*$ , increasing from 0.1 to 0.2 and 41% for diameter ratio,  $d_r$ , increasing from 1.5 to 3.0 for  $L/d=10$ ,  $D^* = 0.0$ ,  $\alpha = 1.0$  and  $e^* = 0.02$ . For the non-homogeneity factor,  $\alpha$ , increasing from 0.0 to 1.0 and 1.0 to 2.0, ultimate lateral resistance increases respectively by 25% and 20% for  $L_b^* = 0.2$ ,  $d_r = 2.5$  and  $D^* = 0.0$ .

The ultimate lateral capacity of double bulb under-reamed pile is 2.78 times that of straight shafted pile for  $L_b^* = 0.2$ ,  $L/d=10$ ,  $d_r = 2.5$  and  $S^* = 0.05$ . Provision of second bulb gives 33% additional strength to single bulb under-reamed pile whereas the increase is only 30% in homogeneous soils. Normalised ultimate lateral resistance increases by 28% with length of bulb increasing from 0.1 to 0.2 and 40% for diameter ratio increasing from 1.5 to 3.0 with  $L_b^* = 0.2$  for  $L/d=10$  and  $S^* = 0.05$ . The normalised ultimate lateral resistance increases by 16% with increase in non-homogeneity factor from 0.0 to

1.0 for the same set of parameters.

For the length and diameter ratio of the bulb increasing from 0.1 to 0.2 and 1.0 to 2.0 respectively in modified Broms's approach, the normalised ultimate resistance increases by 25% and 35% for  $L/d=10$ ,  $S^* = 0.05$ ,  $D^* = 0.0$  and  $e^* = 0.02$ . The normalised ultimate lateral resistance decreases with increase in spacing between the bulbs.

The ultimate lateral capacity of rigid fixed head short single bulb under-reamed pile in non-homogeneous soils with  $\alpha = 1.0$  increases by 40% over the value for piles in homogeneous soils. The lateral capacity increases significantly with increase in length and diameter ratio of the bulb for  $L/d > 10$ .

The normalised ultimate lateral resistance of rigid fixed head intermediate length under-reamed pile increases by 16% and 26% with the length and diameter ratio of the bulb increasing from 0.1 to 0.2 and 1.0 to 2.0 respectively for  $L/d=10$ ,  $L_b^* = 0.2$ ,  $\alpha = 1.0$  and  $M_y^* = 200$ .

The analytical solutions obtained are accurate, and are within the frame work of elastic or plastic soil response and yet simple enough to be of practical use in estimating the ultimate lateral capacity and deformation of under-reamed piles with different size, position and number of bulbs in both homogeneous and non-homogeneous soils. The results from the present study contribute towards better understanding of the effects of soil and bulb parameters on the behavior of under-reamed piles.

# References

- [1] Barber, E. S. (1953). Discussion to paper by S. M. Gleser. *ASTM*, STP 154: 9-99.
- [2] Banerjee, P. K., and Davies, T. G. (1978). "The behavior of axially and laterally loaded single piles embedded in nonhomogeneous soils." *Geotechnique*, Vol. 28, No. 3, 309-326.
- [3] Basudhar, P.K. (1971). "Flexural Behavior of Axially and Laterally Loaded Pile." A Thesis Submitted in Partial Fullfilment of the Requirements for the Degree of Master of Technology, to the Department of Civil Engineering, Indian Institute of Technology Kanpur, India.
- [4] Briaud, J. L., Smith, T. D., and Tucker, L. M. (1985). "A pressure meter method for laterally loaded piles." *Proc. of the Eleventh International Conference on Soil Mech. and Found. Engrg*, Vol. 3, 1353-1356.
- [5] Brinch-Hansen, J. (1948). "The stabilising effect of piles in clay." C. N. Post, Nov (Published by Christiani & Nielsen, Copenhagen, Denmark).
- [6] Broms, B. B. (1964 a). "Lateral resistance of piles in cohesive soils." *J. Soil Mech. and Found. Div.*, ASCE, Vol. 90, SM2, Proc. Paper 3825, 27-63.
- [7] Broms, B. B. (1972). "Stability of flexible structures (piles and pile groups)." *Proc. 5th Eur. Conf. Soil Mech. Fndn Engg. Madrid*, Vol. 2, 239-269.
- [8] Chen, L. T., and Poulos, H. G. (1997). "Piles subjected to lateral soil movements." *J. Geotechnical and Geoenvironmental Engrg.*, ASCE, Vol. 123, No. 9, 802-811.
- [9] Chen, L. T., Poulos, H. G., and Loganathan, N. (1999). "Pile responses caused by tunneling." *J. Geotechnical and Geoenvironmental Engrg.*, ASCE, Vol. 125, No. 3, 207-215.
- [10] Dastidar, A. G. (1956). "Pilot tests on determine the effect of piles in restraining shear failure in clay." Princeton Univ., Princeton, N. J. (unpublished).

- [11] Georgiadis, M., and Butterfield, R. (1982). "Lateral loaded pile behavior." *J. Soil Mech. and Found. Div.*, ASCE, Vol. 108, No. GTI, 155-165.
- [12] Goh, A. T. C., Teh, C. I., and Wong, K. S. (1997). "Analysis of piles subjected to embankment induced lateral soil movements." *J. Geotechnical and Geoenvironmental Engrg.*, ASCE, Vol. 123, No. 9, 792-801.
- [13] Hetenyi, M. (1946). "Beams on elastic foundation." Ann Arbor. Mich. Univ. of Mich. Press.
- [14] Hsiung, Y., and Chen, Y. (1997). "Simplified method for analyzing laterally loaded single piles in clays." *J. Geotechnical and Geoenvironmental Engrg.*, ASCE, Vol. 123, No. 11, 1018-1029.
- [15] Kondner, R. L. (1963). "Hyperbolic stress-strain response. Cohesive soils." *J. Soil Mechanics and Foundation Division*, Proc. ASCE, Vol.89, SM 1, 115-143.
- [16] Krishnan, R., Gazetas, G., and Velez, A. (1983). "Static and dynamic lateral deflexion of piles in non-homogeneous soil stratum." *Geotechnique*, Vol. 33, No. 3, 307-325.
- [17] Kubo, K. (1965). "Experimental study of the behavior of laterally loaded pile." Proc. 6th ICOSMFE, Montreal, Vol. 2, 275-279.
- [18] Loy, L. Y., Madhav, M. R., and Iwao, Y. (1994). "Lateral resistance of piles in non-homogeneous cohesive soils." *Reports of the Faculty of Science and Engrg., Saga University*, Vol. 23, 47-59.
- [19] Madhav, M. R., Rao, N. S. V. K., and Madhavan, K. (1971). "Laterally loaded pile in elasto-plastic soil." *Soils and Foundation., Japanese Society of Soil Mech. and Found. Engrg*, Vol. 11, No. 2, 1-15.
- [20] Matlock, H. (1970). "Correlations for design of laterally loaded piles in soft clay." Proc. 2nd Offshore Tech. Conf., Houston, Vol. 1, 577-594.
- [21] Matlock, H., and Reese, L. C. (1960). "Generalised solutions for laterally loaded pile." *J. Soil Mechanics and Foundaton Division*, ASCE, Vol. 86, SM5, 63-91.
- [22] McKenzie, T. R. (1955). "Strength of dead man anchors in clay." thesis presented to Princeton University, at Princeton, N. J, in partial fullfilment of the requirements for the degree of Master of Science.
- [23] McClelland, B., and Focht, J. A., Jr. (1958). "Soil modulus for laterally loaded piles." *Trans. ASCE*, Vol. 123, 1049-1063.



- [24] McNulty, J. F. (1956). "Thrust loading on piles." *J. Soil Mechanics and Foundation Division*, ASCE, Vol.82. No. 2, Proc. Paper 940.
- [25] Meyerhof, G. G., Mathur, S. K., and Valsangkar, A. J. (1981). "Lateral resistance and deflection of rigid walls and piles in layered soils." *Can. Geotech. J.*, Vol. 18, 159-170.
- [26] Meyerhof, G. G., Sastry, V. V. R. N., and Yalcin, A. S. (1988). "Lateral resistance and deflection of flexible piles." *Can. Geotech. J.*, Vol. 25, 511-522.
- [27] Mohan, D., Jain, G. S., and Jain, M. P. (1967). "Bearing capacity of multiple under-reamed bored piles." Proc. 3rd Asian Conf. S. M. & F. E., Haifa, Vol.1: 103-106.
- [28] Mokwa, L. R., and Duncan, J. M. (2001). "Experimental evaluation of lateral-load resistance of pile caps." *J. Geotechnical and Geoenvironmental Engrg.*, ASCE, Vol. 127, No. 2, 185-192.
- [29] Poulos, H. G. (1971 a). "Behavior of laterally loaded piles: I-single piles." *J. Soil Mechanics and Foundation Division.*, ASCE, Vol. 97, SM No. 5, 711-731.
- [30] Poulos, H. G. (1971 b). "Behavior of laterally loaded piles:II-pile groups." *J. Soil Mechanics and Foundation Division.*, ASCE, Vol. 97, SM No. 5, 733-751.
- [31] Poulos, H. G. (1985). "Ultimate lateral pile capacity in two-layer soil." *Geotech. Engrg*, Vol. 16, 25-37.
- [32] Poulos, H. G., and Davis, E. H. (1980). *Pile foundation analysis and design*. John Wiley & Sons, Inc., New York, N. Y.
- [33] Prakash, C., and Chandra, R. (1983). "Lateral resistance of single underreamed piles in silty sand." *Indian Geotechnical Journal*, 71-77.\*
- [34] Randolph, M. F. (1981). "The response of flexible piles to lateral loading." *Geotechnique* Vol. 31, No. 2, 247-259.
- [35] Randolph, M. F., and Houlsby, G. T. (1984). "The limiting pressure on a circular pile loaded laterally in cohesive soil." *Geotechnique* Vol. 34, No. 4, 613-623.
- [36] Rao, S. N., Ramakrishna, V. G. S. T., and Raju, G. B. (1996). "Behavior of pile supported dolphins in marine clay under lateral loading." *J. Soil Mech. and Found. Div.*, ASCE, Vol. 122, No. 8, 607-612.
- [37] Reese, L. C. (1958). discussion of "Soil modulus for laterally loaded piles." by B. McClelland and J. A. Focht, Jr., Trans. ASCE. Vol. 123, 1071-1074.

- [38] Sharma, D., Jain, M. P., and Prakash, C. (1978). "*Hand book on under-reamed and bored compaction pile foundation.*" CBRI, Roorkee.
- [39] Soneja, M. R., and Garg, K. G. (1980). "Under-reamed piles under lateral loads." *Indian Geotechnical Journal*, Vol. 10, No. 1, 232-244.
- [40] Stewart, D. P., Jewell, R. J., and Randolph, M. F. (1994). "Design of piled bridge abutments on soft clay for loading from lateral soil movements." *Geotechnique* Vol. 44, No. 2, 277-296.
- [41] Terzaghi, K. (1955). "Evaluation of coefficients of subgrade reaction." *Geotech.*, Vol. 5, 297.
- [42] Verruijt, A., and Kooijman, A. P. (1989). "Laterally loaded piles in a layered elastic medium." *Geotechnique* Vol. 39, No. 1, 39-46.
- [43] Wu, D., Broms, B. B., and Choa, V. (1998). "Design of laterally loaded piles in cohesive soils using p-y curves." *Soils and Foundation., Japanese Society of Soil Mech. and Found. Engrg*, Vol. 38, No. 2, 17-26.

134987

134987

### Date Slip

the date last stamped.

[illegible]

A134987